119
Item 19

THE MOUNT HOPE MOLYBDENUM PROSPECT (#2608)
EUREKA COUNTY, NEVADA -
REPORT OF 1980 - 81 EXPLORATION PROGRAMS

by K. Brock Riedell

Exxon Minerals Company
50 Freeport Blvd., Suite #23
Sparks, NV 89431
May 1982

CONTENTS

LIST OF TABLES

LIST OF FIGURES

LIST OF PHOTOS

LIST OF PLATES

SUMMARY

A large, apparently viable open-pit molybdenum reserve occurs in and around the Mount Hope igneous complex, 35 km north-northwest of Eureka, Nevada. The complex intrudes Ordovician chert and argillite of the Vinini Formation and Permian limestone of the Garden Valley Formation. Miogeosynclinal carbonate rocks probably structurally underlie Vinini within several thousand meters depth.

The complex includes both intrusive and extrusive rhyolitic phases, with subordinate quartz monzonite and dacite porphyries. Contrasts in texture and mode of emplacement lead to a division of rhyolitic phases into (1) welded ash-flow tuffs, (2) explosively intruded rhyolite vent breccias, and (3) nonfragmental intrusive quartz porphyries. The latter both predate and postdate the tuffs and vent breccias. The later episode of quartz porphyry intrusion formed a large mass consisting, from the margin inwards, of border phase, main phase, aplitic, and coarse-grained quartz porphyries. Radiometric age determinations are highly discordant, but suggest ages of 49 m.y. for rhyolitic phases, alteration, and molybdenum mineralization; and 30-33 m.y. for late dikes of dacite porphyry. Cauldron subsidence accompanied ash-flow eruption, and the tuffs apparently ponded in two small calderas.

Well zoned alteration and mineralization affected nearly all the complex and a wide aureole in Paleozoic sedimentary rocks. Alteration-mineralization zones, from the margins to core of the deposit, are (1) weak argillic-propylitic; (2) argillic, locally in orbicular aggregates, with strong lead-silver and zinc-manganese anomalies; (3) potassic-phyllic, characterized by anomalous copper, tin, and fluorine; (4) potassic, nearly coextensive with molybdenite ore and containing a zone of anomalous scheelite; (5) high-silica; and (6) biotite. Late sericite-clay alteration overlaps the high-silica and biotite zones.

Mineralization occurs in a stockwork of quartz-molybdenite veinlets and rare molybdenite paint on fractures. Distribution of molybdenite suggests a configuration of multiple ore shells, with two side-by-side mineralized systems that each include two stacked shells. The western molybdenum system is shallow, but has lower molybdenum grade and contains a distinct low-grade apex. The eastern system, although at least 120 m deep in most areas, contains higher grade and more homogeneous mineralization. Highest molybdenum grades occur in a zone of spatial overlapping between the two systems. Molybdenum shells cap and are genetically related to aplitic and coarse-grained quartz porphyries. The entire system has been tilted 10 to 20 degrees easterly. Post-mineral faults attenuated the eastern system and produced zones where drill holes are anomalously barren. Erosion has locally truncated the upper portions of the molybdenum zone, and assays document minor supergene enrichment of molybdenum.

Drilling to date has tested only a portion of the inferred molybdenum shells, and higher grade zones possibly remain undiscovered. The deposit is open to the west, southeast, northeast, and north, and the large size of the altered area suggests additional ore shells may occur in these areas. Mineralized fragments in rhyolite vent breccia confirm the presence of a pulse of molybdenite mineralization distinctly earlier

than those known at present. A significant tonnage of such "pre-eruptive" mineralization, possibly of high grade, could lie concealed, especially beneath the eastern portion of the complex. Finally, gravels east of Mount Hope may conceal significant mineralization.

The Sulphur Springs target is centered about a swarm of quartz porphyry and dacite porphyry dikes cutting Vinini hornfels. Alteration, sulfide mineralization, and copper and zinc anomalies may represent peripheral effects of a molybdenum shell at depth. Rotary hole ESS-1 intercepted a flat molybdenum gradient through a depth of 358 m, however, and suggests that any mineralization is quite deep. Unaltered quartz porphyry of the Garden Pass target is not permissive for molybdenum mineralization within 1200 m of the surface. The Henderson rhyolite is re-interpreted as tuffs derived from Mount Hope, and not a separate center of intrusion and potential mineralization.

RECOMMENDATIONS

Mining Geology program

(1) Grid drilling should expand to cover the entire inferred configuration of molybdenum ore shells. Considerable untested potential remains within the two known systems, especially west of EMH-8 and -22, north of EMH-5, -14, -7, and -21, and southeast of EMH-20.

(2) Test the hypothesis that the better grade mineralization in EMH-57 represents a cone-sheet fracture system by offsetting this hole on an arc drawn through EMH-57 and centered on EMH-1.

(3) Contingent on the results of EMH-23, expand grid drilling east of EMH-13 to delineate potentially shallow eastern system mineralization in the hanging wall of the Mount Hope fault.

Exploration program

(1) Drill at least three holes in the north and northeast portions of the complex in search of outlying ore shells. At least one hole should also test the strong silver anomaly northeast of the summit.

(2) Drill two holes along the east edge of the complex, guided by abundance of veined autoliths in rhyolite vent breccias, in search of potentially high-grade pre-eruptive molybdenite mineralization.

(3) Complete the gravity survey over the pediment east of Mount Hope. Drill at least five rotary holes through the gravels in this area and take spot cores of underlying bedrock. Deeper follow-up coring is warranted if spot cores show peripheral alteration and mineralization, or if tuffs that could conceal pre-eruptive mineralization underlie the gravels.

(4) Complete geologic mapping of the northeast and southeast corners of the claim block in search of remaining outlying targets.

INTRODUCTION

This report summarizes the results of Exxon's exploration of the Mount Hope molybdenum prospect in 1980 and 1981, and my geologic synthesis and re-evaluation in early 1982. It presents our current understanding of the geology of the Mount Hope complex; describes the nature, configuration, controls, and evolution of molybdenite mineralization; and recommends as-yet untested exploration targets. It is not intended to be comprehensive, but rather to update the report of Westra (1980). Because detailed drill evaluation by the Mining Geology group is continuing, no estimates of grade and tonnage are presented. Data from Mining Geology drilling are not included, but some of their findings are briefly noted where these support or modify our concepts.

The acquisition of geologic information through drilling of the property has led to continuing revisions in our classification of igneous phases and alteration types. One of the primary objectives of this report, therefore, is to integrate all existing geologic mapping and drill data into a consistent classification of lithology and alteration. To this end, all available thin sections from surface outcrop and Exploration drilling were examined and described, and some drill core re-examined. In the sections that follow, I propose a revised lithologic classification which more accurately reflects and contrasts the mode of formation of various rock types. Appendix 2 contains summarized logs of all Exploration drill holes in these revised units.

The Reno-based Exploration staff assumed responsibility for the project in July, 1979. Progress since that date has been along four principal thrusts:

(1) Drilling of 19 core holes (Appendix 1 and Plate 2C) has delineated an apparently viable open-pit molybdenite orebody. Continuing re-evaluation of geologic data led to the development of a multi-shell model for the deposit (Plate 2D), which successfully guided placement of higher grade holes in 1981. The Corporation announced the discovery in August 1981, and responsibility for evaluation of the prime target area was transferred to the Mining Geology group.

(2) Continued geologic mapping better defined structure, alteration, and ore potential in the prime target area (Plates 2 and 2A). We extended reconnaissance mapping through most of the claim block (Plate 1) and found additional target areas east of the Mount Hope complex.

(3) Initial evaluation of the outlying Sulphur Springs, Garden Pass, and Henderson target areas (Plate 1A) was completed. A rotary hole tested the upper portion of the Sulphur Springs target.

(4) We acquired additional land to the south and west in early 1981 to cover potential waste and tailings sites in Kobeh Valley, and staked over abandoned competitor claims west of Henderson Summit. We presently control 33,000 acres (Plate 1A) consisting of 1657 unpatented and 15 patented claims.

It would be a gross disservice not to acknowledge the contributions of J. A. Kizis, Jr. and T. D. Irwin to this study. Joe discussed many of these concepts with me at length, first recognized the pyroclastic nature of several of the rock types, and proposed a new origin for orbicular alteration textures. Tom provided experience, numerous suggestions, and a critical ear that helped keep our evaluation on the right track.

REGIONAL GEOLOGIC SETTING

The Mount Hope igneous complex, 35 km north-northwest of Eureka, is one of a small cluster of Tertiary felsic intrusive and extrusive centers cutting Paleozoic sedimentary rocks (Plate 1). Aeromagnetic expression (Mabey, 1966), and the similar suites of igneous rocks in the four areas suggest that they share a common batholithic source at depth. The areas of outcropping felsic rocks are shown on Plate 1A and described in later sections of this report.

The Mount Hope region lies near the leading edge of the Roberts Mountains thrust, which carried eugeosynclinal ("Western assemblage") sedimentary and volcanic rocks eastward over miogeosynclinal ("Eastern assemblage") sedimentary rocks during the Devonian-Mississippian Antler orogeny. Western assemblage argillites, cherts, limestones, sandstones, and conglomerates belonging to the Vinini Formation (Ov) of Ordovician age underlie most of the area. Walker (1962) subdivided the Vinini into three thrust plates, two of which he mapped northwest of Mount Hope. Poor exposure in this area, however, makes it impossible to verify a thrust contact. A hematitic low-angle shear zone separates chert and argillite beds west of September Morn Peak in the Sulphur Springs area, and may represent such a structure within the Vinini section.

Eastern assemblage sedimentary rocks (Pzc) crop out in the northeastern portion of Plate 1 and in several thrust-bounded exposures west of Mount Hope. Walker (1962) and Roberts and others (1967) mapped the Eureka Quartzite, Lone Mountain Dolomite, and Nevada Formation, of Ordovician through Devonian ages, on the east side of the Sulphur Spring Range. The structural outliers to the west consist of Devonian dolomite and limestone of the Nevada and Devils Gate Formations. Roberts and others (1967) considered these exposures to represent windows through the Roberts Mountains thrust. Winterer (1968) suggested they were blocks structurally interlayered with and overlying Vinini, emplaced by early Cretaceous gravity sliding. Our mapping strongly supports the latter hypothesis (See Plate 1).

Permian sedimentary rocks of the "Overlap assemblage" represent detritus eroded off the Antler highlands. The Garden Valley Formation, consisting of sandy limestone, sandstone, shale, and chert-pebble conglomerate, crops out in the Sulphur Spring Range and along the southeastern contact of the Mount Hope complex.

The Roberts Mountains thrust is not exposed in the immediate area. Distribution of Western and Eastern assemblage rocks suggests, however, that the trace is concealed beneath the Garden Valley Formation of the Sulphur Spring Range, or is faulted out by the structure through Mulligan Gap. The upper plate should therefore be fairly thin, with Eastern assemblage rocks underlying Vinini at shallow depth throughout the area. Drilling to depths of 880 m, however, has intercepted no lower plate rocks.

Basalt flows dated at 13.6-18.6 m.y. (Murphy and others, 1978) crop out in the foothills of the Roberts Mountains and in Kobeh Valley. Unconsolidated to poorly consolidated gravel, sand, and silt of Quaternary and possibly late Tertiary age fill valleys formed by Basin-and-

Range block faulting. These deposits may attain thicknesses of 1525 m in Kobeh Valley and up to 2300 m in Diamond Valley (Hydro-Search, Inc., 1982, p. 19).

THE MOUNT HOPE TARGET

ROCK TYPES

Paleozoic sedimentary rocks

The Mount Hope complex intrudes Vinini and Garden Valley Formations of the Western and Overlap assemblages, respectively. Near the complex, Vinini Formation (Ov and Ovl) consists of thin- to medium-bedded shale, siltstone, chert, and conglomerate, with subordinate quartzite and limestone. A thin but persistent sandy limestone unit (Ovl) divides the section into a lower unit (cropping out west of the limestone) of dominantly argillaceous sediments, and an upper unit with common beds of chert and quartzite. The limestone bed appears to thicken eastwardly, and may correlate with calc-silicate rocks in EMH-2, -3, -12, -17, and -20 (Plates 3:B-B' and 4).

Contact metamorphic effects are evident in all lithologies of the Vinini up to 600 m from the contact with the Mount Hope complex. Chert is recrystallized, argillaceous units form quartz-K-feldspar-biotite hornfelses, and calcareous units are replaced by marble or diopside + actinolite hornfelses (Photo 1). Metamorphic zoning within the Vinini argillites is described more fully below.

The basal limestone unit of the Garden Valley Formation (Pg) is preserved in a small asymmetrical syncline along the southeastern contact of the complex. Although locally unrecrystallized, more commonly it forms marble or skarn (Photo 1) containing grossularite, diopside, tremolite, wollastonite, and fluorite, with retrograde clays, chlorite, and carbonates. Missallati (1973) and Westra (1980) described skarn alteration in greater detail.

We now believe that no lower plate sedimentary rocks have been intersected by drilling. Westra (1980) tentatively correlated calc-silicate rocks below 822 m in EMH-3 with Eastern assemblage carbonates. The calc-silicate rocks, however, are petrographically similar to calcareous horizons in more recent holes that appear to lie within the Vinini.

The Mount Hope igneous complex

The Mount Hope complex consists of rhyolitic and subordinate rhyodacitic to dacitic phases emplaced in a subvolcanic to volcanic setting. Missallati (1973) and Westra (1980) previously subdivided and mapped the complex. Continued mapping, core-logging, and petrographic study led to the revised classification of igneous phases detailed in Table 1. Because the rhyolitic units are mineralogically and chemically similar, the new subdivisions are based on differences in mode and environment of formation as reflected by textural variations observable in hand specimen (see far right column of Table 1). Rock nomenclature is after Peterson (1961); the distinction between aphanitic and aplitic (or phaneritic) textures is set at an average size of groundmass grains of 0.08 mm, the approximate resolving limit of a ten-power hand lens. The term aplitic, as used herein, refers to fine sucrosic grain size and not to allotriomorphic-granular texture (as used by Dilles, 1982). Table 2 compares the revised classification with those of Westra (1980) and 1980-81 Explora-

Table 1. IGNEOUS ROCKS OF THE MOUNT HOPE COMPLEX

ROCK UNIT AND ABBREVIATION	OCCURRENCE	PHENOCRYSTS	XENOLITHS AND ROCK FRAGMENTS	GROUNDMASS	DISTINGUISHING FIELD CHARACTERISTICS
Dacite porphyry (Tdp)	Rare dikes	5-10% bipyramidal to rounded quartz, 1-12mm 30-35% oligoclase-andesine, 1-3 mm 10-15% biotite, ≤2mm	---	Quartz, plagioclase >K-feldspar 0.03-0.1mm	Gray-green color; large quartz phenocrysts; lack of K-feldspar
Quartz porphyry breccia (Tbx)	Rare pipes(?) and dike	---	Angular to subrounded fragments of quartz porphyry and border quartz porphyry in a hematitic, silicified rock flour matrix	---	Breccia with rock flour, not igneous matrix
Fine-grained granite (Tgr)	Rare dikes	---	---	50-70% K-feldspar 30-50% quartz 0.1-3mm	Equigranular to crowded porphyritic texture
Coarse-grained quartz porphyry (Tqpc)	Intrusive mass, deep in complex	5-15% bipyramidal to rounded quartz, 2-6mm 5% sanidine laths, 3-8mm 3-10% oligoclase, 2-3mm 3% biotite, ≤2mm	---	Quartz, K-feldspar > plagioclase 0.02-0.4mm	Large phenocrysts; variable aphanitic to phaneritic groundmass
Aplitic quartz porphyry (Tqpa)	Intrusive mass and dikes, deep in complex. Texture commonly obscured by silicification	5-15% bipyramidal to subrounded quartz, 0.5-4mm 8-15% sanidine laths, 1-5mm 0-10% oligoclase, 0.5-2mm 0-3% altered biotite, ≤2mm	---	Quartz, K-feldspar> plagioclase 0.05-0.3mm	Small phenocrysts; fine sugary groundmass (averages ≥0.08mm)
Quartz porphyry (Tqp)	Intrusive mass and dikes	5-15% bipyramidal to rounded quartz, 0.5-4mm 3-15% sanidine laths, 1-5mm 0-10% oligoclase, 0.5-2mm 0-5% biotite, ≤2mm	---	Quartz, K-feldspar > plagioclase 0.01-0.1mm	Small, unbroken phenocrysts; aphanitic groundmass (averages <0.08mm)
Quartz porphyry border phase (Tbqp)	Irregular border zone of Tqp mass; some dikes	5-15% broken to rounded quartz, 0.5-4mm 8-15% broken to lath-shaped sanidine, 0.5-4mm 0-10% oligoclase, 0.5-2mm	≤5% Vinini gray siltstone and brown biotite hornfels	Quartz, K-feldspar> plagioclase 0.005-0.03mm	Intrusive texture; both broken and unbroken phenocrysts; rare Vinini xenoliths; presence of brown hornfels xenoliths
Quartz-eye tuff (Tqt)	Rare remnants of ash-flow sheet	4% rounded quartz, 0.5-3mm 8% sanidine, 1-10mm	---	Quartz, K-feldspar, plagioclase; prominent shard structure	Large phenocrysts, ash-flow textures
Rhyolite vent breccia (Trb)	Ring-dikes along cauldron margins	5-20% broken to (rarely) rounded quartz, 0.5-3mm 2-10% oligoclase, 0.3-2mm 2-5% broken sanidine, 0.5-3mm	2- >50% Vinini gray siltstone and (rarely) biotite hornfels ≤5% early quartz porphyry	Quartz, K-feldspar <0.005-0.02mm; comminuted?	Small, broken phenocrysts; fragmental intrusive texture; commonly ≥10% xenoliths
Mount Hope Tuff (Tht)	Welded crystal, crystal-vitric and crystal-lithic ash-flow tuffs; primarily within calderas	10-25% broken to (rarely) rounded quartz, 0.5-3mm 5-15% oligoclase, 0.5-2mm 3-10% broken sanidine, 0.5-3mm 0-2% biotite	≤10% Vinini gray siltstone ≤5% early quartz porphyry	Quartz, K-feldspar; weak to prominent shard structure and pumice	≥25% small, broken phenocrysts; commonly ≤10% xenoliths. Ash-flow textures: Tht_1, rare pumice Tht_2, variable pumice Tht_3, common to abundant (10-40%) pumice
Early quartz porphyry (Tqpe)	Autoliths in Mount Hope Tuff and rhyolite vent breccia	5-15% subrounded to broken quartz, 0.5-4mm 8-15% sanidine laths, 1-5mm 0-10% oligoclase, 0.5-2mm	---	Quartz, K-feldspar; <0.03-0.15mm	No reliable criteria for distinguishing from Tqp
Biotite quartz monzonite porphyry (Tqmp)	Rare dikes	7-8% andesine laths, 1-5mm 2% bipyramidal to rounded quartz, 0.5-3mm 1-2% K-feldspar laths, 0.5-2mm 3% biotite, 0.5-2mm	---	Quartz, K-feldspar plagioclase 0.1-0.5mm	Gray-green color; phaneritic groundmass

Table 2.

CORRELATION BETWEEN CLASSIFICATIONS OF TERTIARY IGNEOUS ROCKS OF THE MOUNT HOPE COMPLEX

This report	Westra (1980)	1980 drill logs	1981 drill logs
Dacite porphyry (Tdp)	Granodiorite porphyry (Tgp)	-----	-----
Quartz porphyry breccia (Tbx)	Breccia pipe (Tbx)	-----	-----
Fine-grained granite (Tgr)	Biotite granite and aplite (Tgr)	Aplite, granite-aplite, or fine-grained granite	Fine-grained granite (Tgr)
Coarse-grained quartz porphyry (Tqpc)	Biotite granite porphyry (Tgr), contact zone (Tgrbx), and coarse quartz-K-feldspar porphyry (Tqp_3)	Porphyritic granite and coarse quartz-K-feldspar porphyry	Coarse-grained quartz porphyry (Tqpc)
Aplitic quartz porphyry (Tqpa)	Quartz porphyry (2) (Tqp_2)	Aplitic quartz porphyry	Aplitic quartz porphyry (Tqpa)
Quartz porphyry (Tqp)	Quartz porphyry (1) (Tqp_1)	Quartz porphyry	Quartz porphyry (Tqp)
Quartz porphyry border phase (Tbqp)	Quartz porphyry border phase (Tbqp) and intrusive contact breccia (Tbx)	Crowded quartz porphyry	Border quartz porphyry (Tbqp)
Quartz-eye tuff (Tqt)	Quartz porphyry (Tqp)	-----	-----
Rhyolite vent breccia (Trb)	Intrusive rhyolite breccia (Trb), coarse rhyolite breccia (Trbx and Trbxo) and crowded rhyolite-sediment breccia (Trebx)	-----	Rhyolite breccia (Trb)
Mount Hope Tuff (Tht_3)	Flowbanded rhyolite (Trfb), rhyolite crystal-lapilli tuff (Tmrl), medium crystalline rhyolite (Tmr), fine crystalline rhyolite (Tfr), and intrusive rhyolite breccia (Trb)	-----	Flowbanded rhyolite (Trfb)
Mount Hope Tuff (Tht_2 and Tht)	Medium crystalline rhyolite (Tmr), fine crystalline rhyolite (Tfr), and intrusive rhyolite breccia (Trb)	Medium crystalline rhyolite (Tmr) and flowbanded rhyolite (Trfb)	Medium crystalline rhyolite (Tmr) and flowbanded rhyolite (Trfb)
Mount Hope Tuff (Tht_1)	-----	-----	Medium crystalline rhyolite (Tmr), flowbanded rhyolite (Trfb), and rhyolite breccia (Trb)
Early quartz porphyry (Tqpe)	Quartz porphyry (1) (Tqp_1)	-----	-----
Biotite quartz monzonite porphyry (Tqmp)	Biotite quartz latite porphyry (Tbqlp)	-----	-----

tion drill logs. Photos 2 through 16 illustrate the igneous phases in hand specimen and thin section.

Rare dikes of biotite quartz monzonite porphyry (Tqmp) cut Vinini Formation west of the Mount Hope complex, and are cut in turn by dikes of quartz porphyry. Because biotite quartz monzonite porphyry is mineralogically distinct from, and cuts none of the rhyolitic rocks, it is probably the oldest igneous unit.

Contrasts in texture, occurrence, and mode of emplacement lead to division of the rhyolitic rocks into three groups. Welded rhyolite tuffs are distinguished by shard structures and variable amounts of pumice, although alteration commonly obscures such textures. They probably formed as localized ash-flows erupted from small calderas overlying the complex. Rhyolite vent breccias form steeply dipping ring-dikes that were explosively intruded into ring fracture zones bounding the cauldrons following ash-flow eruption. In contrast, nonfragmental textures characterize the various quartz porphyries and suggest gradual, controlled crystallization in a hypabyssal intrusive setting. Quartz porphyries occur both as autoliths in and dikes cutting rhyolite tuffs and vent breccias, and must therefore both predate and postdate the latter rock types. Mineralogical and chemical similarities among the rhyolitic rocks, along with these complex age relationships, suggest that the rhyolite tuffs, rhyolite breccias, and quartz porphyries are all comagmatic. Most likely, a single magma chamber initially crystallized a rind of quartz porphyry under controlled conditions, then explosively vented to form rhyolite ash-flow tuffs and breccias. Subsequently, the magma resealed itself and the remaining melt once again crystallized into nonfragmental quartz porphyries.

The most extensive ash-flow unit, the Mount Hope Tuff (Tht), consists of variably welded tuffs characterized by abundant small, angular phenocrysts and phenoclasts. Included fragments of pumice are texturally similar to the quartz porphyries, averaging 25 percent unbroken quartz and feldspar phenocrysts. Because pumice records magmatic textures at the moment of frothing just prior to eruption, these fragments confirm a genetic link between the Mount Hope Tuff and the quartz porphyries. The tuffs contrast texturally with the porphyries (and pumice fragments) because of (1) fracturing of crystals during ash-flow transport, and (2) elutriation, or dissipation of fine ash out of the top of the eruptive cloud, resulting in increased phenocryst content in the tuffs (Photo 7).

Petrographic study has led to delineation of three ash-flow cooling units within the Mount Hope Tuff. Although not readily discernible in hand specimen, these distinctions are of exploration significance because the more competent better welded horizons locally host significant molybdenite, whereas the weakly welded zones are barren to only weakly mineralized. The lowest cooling unit (Tht_1), characterized by rare pumice, does not crop out and is presently known only from EMH-18. This hole intercepted approximately 300 m of true thickness of the lower unit, but later intrusives cut out the densely welded zone, if present, and the basal contact.

The middle cooling unit (Tht_2) contains variable amounts of pumice fragments, these being more numerous (or conspicuous?) in the densely welded basal portions. It overlies the lower cooling unit in EMH-18,

but lies directly atop Vinini Formation in EMH-5 and -10. These intercepts suggest a thickness of 365-380 m. Rhyolite tuffs northwest of Henderson Summit are tentatively correlated with this cooling unit.

Common to abundant pumice characterizes the entire preserved thickness, at least 150 meters, of the upper cooling unit (Tht_3). It overlies the middle unit directly in EMH-10. The presence of an air-fall tuff bed 88 m above the base of upper cooling unit in EMH-10 suggests that it formed from at least two distinct ash-flows.

Small erosional outliers of a quartz-eye tuff (Tqt) occur 1350-1400 meters south of Mount Hope, 360 m northwest of September Morn Peak, and in a small body at the north end of the Garden Pass stock. These display shard and pumice structures but otherwise resemble quartz porphyry.

Rhyolite vent breccia (Trb) has broken crystals similar to those in the Mount Hope Tuff, but contains fewer phenocrysts and neither shards nor pumice. A very fine-grained, possibly comminuted rhyolitic groundmass suggests explosive emplacement. The vent breccias form ring-dikes that cut all units of Mount Hope Tuff. They are generally distinguishable from the tuffs by their more abundant lithic fragments, but both fragment-poor vent breccias and fragment-rich tuffs occur. Westra (1980) mapped four separate units of "explosion breccia" based on abundance and size of lithic fragments, but the gradational nature of these distinctions led to their abandonment in more recent core-logging.

Intrusive rhyolitic quartz porphyries contain subhedral to euhedral (or rarely broken) quartz, K-feldspar, and plagioclase phenocrysts in groundmasses of allotriomorphic-granular texture and varying grain size. Early quartz porphyry (Tqpe), presently known only from autoliths in Mount Hope Tuff and rhyolite vent breccia, is the only quartz porphyry phase that predates those units. Autoliths of early quartz porphyry are most common in rhyolite vent breccia along the eastern and southeastern edges of the complex, which suggests that a mass of early quartz porphyry may occur at depth in this area, as hypothetically shown on Plates 3:B-B' and 9. No reliable hand-specimen or petrographic criteria distinguish this rock from the quartz porphyries that postdate the eruptive episode.

The four other quartz porphyry phases occupy a large, irregular intrusive mass that cuts both Mount Hope Tuff and rhyolite vent breccia and comprises most of the complex at depth (Plates 3 and 4). From the margins to the core of this mass, the quartz porphyry phases show progressively coarser groundmasses and younger relative ages. Presumably, the various porphyry phases record episodic crystallization of a body of magma from the margin inwards.

The discontinuous rind of the porphyry mass consists of quartz porphyry border phase (Tbqp), distinguished by extremely fine-grained groundmass, commonly broken phenocrysts, and numerous xenoliths of Vinini hornfels. Main-phase quartz porphyry (Tqp) forms a large body of somewhat variable texture. Its groundmass gradually coarsens with depth, but attempts to further subdivide the unit are probably unwarranted. Quartz porphyry also comprises the Garden Pass stock and numerous dikes cutting Vinini Formation.

Distinctly coarser groundmass, with mesoscopically discernible texture ($\geq$ 0.08 mm), distinguishes the aplitic quartz porphyry (Tqpa). It appears to cut overlying quartz porphyry, but relationships are somewhat obscure. Coarse-grained quartz porphyry (Tqpc) is a complex unit with a brecciated border zone, characterized by a fine-grained phaneritic groundmass, and an aphanitic to aplitic interior. The finer-grained core of this intrusive body may be the result of pressure quenching during brecciation of the border zone. Westra (1980) and my 1980 core logs subdivided the coarse-grained quartz porphyry, but such distinctions proved complex, gradational, and probably unnecessary.

Other rhyolitic units are volumetrically insignificant. Fine-grained granite (Tgr) forms rare dikes cutting all quartz porphyry phases. Hydrothermal quartz porphyry breccias occur in float 500 m east-northeast of the summit of Mount Hope, and in dikes too small to be shown on Plates 2, 3, or 4.

Dacite porphyry (Tdp) occurs as dikes on the lower slopes north and east of Mount Hope. It appears to cut rhyolite vent breccia in Phillips drill holes along the east edge of the Mount Hope complex (Plates 6 and 7; Westra, 1980, Plate 2:C-C'). If the rhyolitic units of the complex are indeed cogenetic, then dacite porphyry is probably the youngest intrusive phase present.

CAULDRON STRUCTURES

Reconstructed thicknesses of Mount Hope Tuff strongly suggest that ash-flow eruption resulted in several cycles of cauldron subsidence, producing small calderas. Highly variable and locally steep dips of eutaxitic foliation (Plate 2) suggest subsidence concurrent with eruption. Large slump blocks, intracaldera breccias and moat sediments are not presently recognized, but may have been destroyed by later intrusion of rhyolite vent breccias and quartz porphyries.

The lowest cooling unit of the Mount Hope Tuff (Tht_1) is juxtaposed against Vinini Formation by a ring fracture system, presently occupied by rhyolite vent breccia, just north and west of the summit of Mount Hope. Thicknesses of this unit in EMH-18 imply at least 300 m of subsidence (Plates 3:A-A', 5, 6, and 7). These relationships suggest that the lowest unit filled a caldera approximately 1000 m across, outlined by the discontinuous outcrops of rhyolite vent breccia northwest, north, and northeast of the summit. Because the lowest unit is known only in EMH-18 and does not occur between the middle cooling unit and Vinini Formation in EMH-5 or -10, it probably erupted from, and accumulated almost entirely within this caldera.

Similarly, the semicircular body of rhyolite vent breccia bordering the complex on the east side filled a structure that juxtaposed the middle and upper cooling units (Tht_2 and Tht_3) against Paleozoic sediments to the east and south (Plates 3:B-B', 4:C-C', 6, 7, and 8). This body of vent breccia partially outlines an inferred caldera comprising the entire eastern half of the complex, approximately 1200 m across. Both middle and upper units ponded in, and probably erupted from this eastern caldera. At least 350 m of subsidence is inferred. Because the middle cooling unit appears to have accumulated in the western caldera as well

(Plates 2 and 3:A-A'), its eruption may have initiated renewed collapse of the older western caldera. The middle and possibly upper cooling units escaped over the caldera rims, forming outflow facies preserved northwest of Henderson Summit and in widely scattered patches that probably represent local depressions at the time of eruption.

The Bowser fault (Plate 2; northeastern continuation shown on Plate 1) forms a broad semicircular structure that may be a yet larger cauldron. A crudely defined ring of aeromagnetic highs (Westra, 1980, Plate 3) suggests continuation of this structure under gravels east of its northeastern mapped extent. It contains no significant volume of ponded rhyolite tuffs, and any volcano-tectonic affinity is obscure. Westra (1980, Plate 1) mapped two semicircular features from aerial photographs, but field evidence for such structures is lacking.

ALTERATION AND MINERALIZATION

Zoning

Hydrothermal alteration and mineralization affect nearly all the Mount Hope complex and a wide area of adjacent Paleozoic sedimentary rocks. Surface geochemistry and initial geologic mapping showed well developed zoning of metals and alteration types (Westra, 1980, Plates 1B - 1J). More recent mapping and petrographic study better defined mineralogy and extent of alteration assemblages, especially in Vinini Formation. This study led to a revised classification of alteration zones that correlates assemblages in igneous rocks, assemblages in Vinini, and zoning patterns of geochemistry, sulfide content, and vein density (Figure 1). Plate 2A shows the extent of these revised zones, based on 79 thin sections from outcrop and near the collars of drill holes. Downhole petrographic studies allowed delineation of subsurface alteration in this same classification, as summarized in the sketch logs in Appendix 2 and shown on Plates 3A and 4A.

Photos 17 through 31 illustrate alteration types in chip specimen and thin section. Figure 1 outlines the mineralogic and geochemical effects of each zone, and the discussions that follow summarize their salient and identifying characteristics in igneous rocks and Vinini argillites. Further study is needed to define zoning in calcareous sediments.

Weak argillic-propylitic assemblages characterize the outermost portions of the sulfide system. Dacite porphyry more commonly shows typically propylitic assemblages, perhaps because higher Ca content (Westra, 1980, Table 3) stabilized calcite and epidote. Thermal metamorphism of Vinini argillites produced hornfels that fractures across rather than along bedding, without megascopic mineral changes.

The wide argillic zone is especially well developed in Mount Hope Tuff and rhyolite vent breccia. Clay and minor carbonate completely replace plagioclase, but K-feldspar is stable to weakly dusted by clay-sericite. Preferential weathering of argillized plagioclase in outcrop produces a "bughole" texture that is particularly conspicuous in quartz porphyry (Photo 17). Secondary biotite in Vinini hornfels imparts a distinctive chocolate brown color. Thin veinlets of pyrite and commonly dark clays increase dramatically inward and downward, especially in Mount Hope Tuff; the inner argillic zone contains the highest sulfide

FIGURE 1. Schematic alteration and metal zoning through the Mount Hope deposit. Abbreviations:

bi	-	biotite
carb	-	carbonate
chl	-	chlorite
cl	-	clay
ep	-	epidote
fl	-	fluorite
kf	-	K-feldspar
mt	-	magnetite
plag	-	plagioclase
py	-	pyrite
qz	-	quartz
sc	-	sericite
sulf	-	sulfide

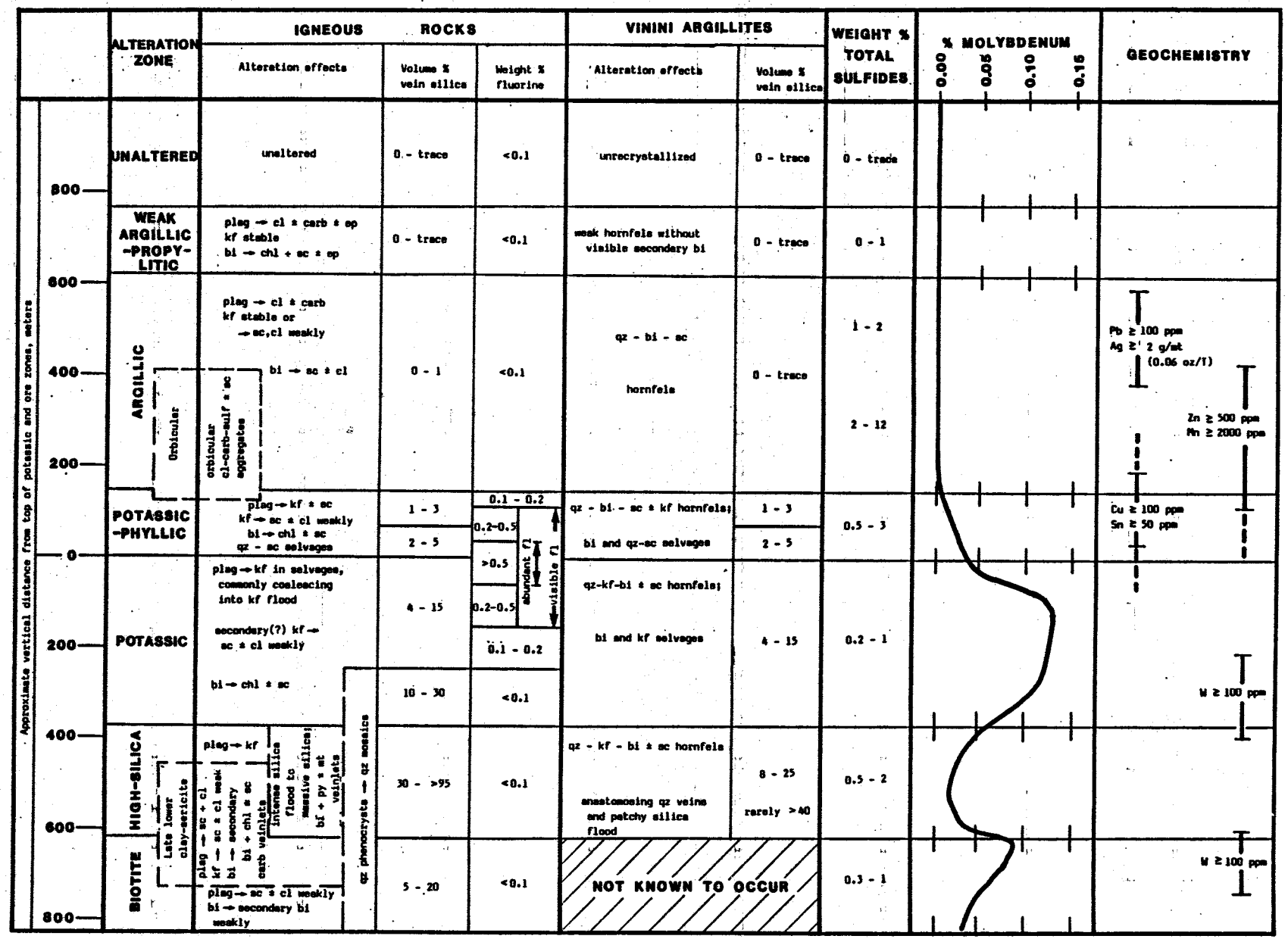
Approximate vertical distance from top of potassic and ore zones, meters
800
600
400
200
0
200
400
600
800
ALTERATION ZONE
IGNEOUS ROCKS
Alteration effects
Volume % vein silica
Weight % fluorine
VININI ARGILLITES
Alteration effects
Volume % vein silica
WEIGHT % TOTAL SULFIDES
% MOLYBDENUM
0.00
0.05
0.10
0.15
GEOCHEMISTRY
UNALTERED
unaltered
0 - trace
<0.1
unrecrystallized
0 - trace
0 - trace
WEAK ARGILLIC -PROPY- LITIC
plag → cl ± carb ± ep
kf stable
bi → chl + ac ± ep
0 - trace
<0.1
weak hornfels without visible secondary bi
0 - trace
0 - 1
ARGILLIC
Orbicular
plag → cl ± carb
kf stable or
→ ac,cl weakly
bi → ac ± cl
orbicular cl-carb-sulf ± ac aggregates
0 - 1
<0.1
qz - bi - ac
hornfels
0 - trace
1 - 2
2 - 12
Pb ≥ 100 ppm
Ag ≥ 2 g/mt (0.06 oz/T)
Zn ≥ 500 ppm
Mn ≥ 2000 ppm
POTASSIC -PHYLLIC
plag → kf ± ac
kf → ac ± cl weakly
bi → chl ± ac
qz - ac selvages
1 - 3
2 - 5
0.1 - 0.2
0.2-0.5
qz - bi - ac ± kf hornfels;
bi and qz-ac selvages
1 - 3
2 - 5
0.5 - 3
Cu ≥ 100 ppm
Sn ≥ 50 ppm
POTASSIC
plag → kf in selvages, commonly coalescing into kf flood
secondary(?) kf → ac ± cl weakly
bi → chl ± ac
4 - 15
>0.5
0.2-0.5
0.1 - 0.2
abundant fl
visible fl
qz-kf-bi ± ac hornfels;
bi and kf selvages
4 - 15
0.2 - 1
W ≥ 100 ppm
HIGH-SILICA
Late lower clay-sericite
plag → kf
plag → ac + cl
kf → ac ± cl weak
bi → secondary bi + chl ± ac
carb veinlets
intense silica flood to massive silica; bf + py ± mt veinlets
qz phenocrysts → qz mosaics
10 - 30
30 - >95
<0.1
qz - kf - bi ± ac hornfels
anastomosing qz veins and patchy silica flood
8 - 25
rarely >40
0.5 - 2
BIOTITE
plag → ac ± cl weakly
bi → secondary bi weakly
5 - 20
<0.1
NOT KNOWN TO OCCUR
0.3 - 1
W ≥ 100 ppm

content (up to 10 weight percent) in the system. Fractures containing sphalerite, galena, or pyrrhotite are common. Rare hairline quartz veinlets, some with molybdenite, cut more competent hosts such as the more densely welded tuffs.

Orbicular aggregates up to 10 cm in diameter, containing clays, carbonates, minor sericite, and sulfides, are common in the inner argillic zone (Photos 21 and 22). They are best developed in rhyolite vent breccias, but also occur in Mount Hope Tuff and rarely in quartz porphyry border phase (Plate 2A). Orbicles are generally zoned, with cores rich in pyrite, pyrrhotite, and (or) sphalerite, and rims comprised of carbonates and clays with subordinate sulfides. Stronger orbicular alteration destroys primary rock texture, but relict quartz phenocrysts are preserved in rims of aggregates.

Orbicular alteration textures occur in rock volumes that lack quartz veinlets, and therefore suggest that host rocks were too porous and incompetent to fracture. Alteration therefore was controlled by point sources rather than channelways, and outward growth from such loci produced the orbicular habit. The exact nature of the point sources is somewhat obscure. Because both lithic and pumice fragments may lie immediately adjacent to an alteration aggregate and be unaffected or only partly replaced, they are unlikely loci. Pyrite of solfataric origin is a more plausible seed, because orbicular alteration is concentrated along the ring fracture system of the eastern caldera, where solfataric activity would have concentrated late in the eruptive cycle.

Molybdenum values are quite low (< 20 ppm) throughout the argillic zone. Lead, silver, zinc, and manganese are strongly anomalous, however, and may locally occur in economic concentrations. Mount Hope Tuff contains at least sixty meters of greater than 0.2% zinc in EMH-3, -5, and -10. EMH-3 intercepted 320 m of 0.5% zinc and 76 m of 13.4 g/mt (0.39 oz/T silver. Where these metal haloes intersected limestones of the Garden Valley Formation, the high-grade replacement deposits exploited by the Mount Hope Mine formed.

Initial surface geochemistry (Westra, 1980, Plate 1J) delineated a strong silver anomaly within the argillic zone, northeast of the summit of Mount Hope. Additional sampling of this area on a 61-meter (200-foot) grid defined a zone 300 m east-west containing at least 10 g/mt (0.3 oz/T). EMH-18 tested the western end fo this zone but failed to intercept values in excess of 7 g/mt (0.2 oz/T) in 15-meter composite samples.

A discontinuous potassic-phyllic zone is best developed in quartz porphyries and Vinini hornfels. In the former, hydrothermal sanidine partially to completely replaces plagioclase and weakly floods the groundmass, changing the color of the rock from light gray to "ceramic" white. Pale green sericite in turn weakly replaces primary and hydrothermal K-feldspar, and locally (as in EMH-9) occurs more pervasively in the groundmass. Vinini argillites form quartz-biotite-sericite hornfels with minor K-feldspar of probable metamorphic origin. Up to five percent quartz ± fluorite ± molybdenite veinlets cut porphyry and hornfels, and are commonly lined with gray to green-gray selvages of fine-grained quartz and sericite. In Vinini, the veinlets commonly contain sanidine as well as quartz and fluorite; and dark brown biotite-rich haloes surround the

quartz-sericite selvages (Photo 23) and occur along earlier veinlets. Throughout the potassic-phyllic zone, quartz veinlets commonly occur in nearly vertical sheeted sets (Photos 17 and 24) that appear to form radial and annular patterns centered about an area near drill hole EMH-1. Sulfide content is relatively low, and therefore this is not a classic quartz-sericite-pyrite zone.

Abrupt downhole increase in molybdenum content marks the potassic-phyllic zone and produces the steep molybdenum gradients above ore. No more than 150 to 200 m separate the 0.01% and 0.1% Mo contours in most drill holes. Chalcopyrite-bearing veinlets are also common in this zone, and chalcocite enrichment in favorable settings produced intercepts of at least 50 m with +0.1% copper (EMH-7, -9, and -20). The highest fluorine values commonly straddle the transition between potassic-phyllic and underlying potassic alteration, producing the "fluorine spike" just above ore. In porphyry, this occurs as fine- to rare coarse-grained fluorite in veinlets and fractures of various ages, only a small fraction of which is megascopically discernible. Logging of visible purple and green fluorite, however, accurately predicts location of the +0.2% F zone (Figure 1) and is a useful guide to ore just below. Vinini hornfels contains up to 0.5% fluorine without visible fluorite, suggesting that fluorine occurs as solid solution in biotite.

A potassic zone comprises the exposed core of the deposit, and widens considerably with depth, especially to the east. K_2O contents of 7 to greater than 10 percent characterize potassic-altered quartz porphyries. Hydrothermal sanidine replaces magmatic plagioclase and floods the groundmass, although such replacement is incomplete in the western and northwestern portions of the potassic zone (e.g. EMH-21 and -22; Photo 25). Green to yellow sericite and clay replace relict (and some K-feldspathized?) plagioclase. Recrystallization of Vinini argillites produces a quartz - K-feldspar - biotite ± sericite hornfels cut by dark brown biotite and pale tan-gray K-feldspar selvages along veinlets. Quartz ± fluorite ± sanidine ± molybdenite veinlets form a random stockwork, with individual veinlets at both high and low angles. Sanidine is common in veinlets cutting Vinini, but in porphyries K-feldspar occurs only where a veinlet cuts sanidine phenocrysts. This hydrothermal feldspar commonly forms overgrowths in crystallographic and optical continuity with the adjacent phenocryst, giving the illusion that the sanidine phenocryst "cuts off" the veinlet (Photo 26). Quartz forms similar overgrowths in veinlets adjacent to quartz phenocrysts.

Dilles (1982, p. 6) suggested that numerous quartz veinlets formed due to replacement rather than open-space filling. Well formed, parallel walls of veinlets and dilation of earlier features suggest, however, that filling of fractures was the dominant mechanism in nearly all cases.

Potassic alteration is approximately coextensive with the surface molybdenum anomaly (Plates 2A and 2B), and with ore-grade molybdenite mineralization at depth (Plates 3A, 3B, 4A, and 4B). Anomalous tungsten is common in the deeper portion of the potassic zone, with intercepts 50 to 100 m long commonly averaging 100 to 200 ppm tungsten. The strongest tungsten intercept is in Vinini biotite and calc-silicate hornfelses of EMH-12, with 215 m of 420 ppm W. Hazen Research, Inc. (1981, p. 12,

35-50) reported that the tungsten occurs as grains of scheelite 0.01-0.10 mm across included in phenocrysts and disseminated in rock groundmasses. Sulfide content of the potassic zone is quite low, and outcrops contain only sparse limonites.

A gradual increase in barren granular hydrothermal silica marks the deeper portions of the molybdenum and potassic zones. In igneous rocks, the underlying high-silica zone is defined as rocks containing at least 30 volume percent vein quartz. In the western portion of the deposit, two such zones occur and are separated by a deeper potassic zone (Plates 3A:A-A', 4A). High-silica alteration consists of dense barren quartz stockwork and irregular patches containing mosaic quartz and minor carbonate (Photo 18). Locally, massive silica completely obliterates igneous texture. Silica flooding is slightly coarser grained than quartz stockwork veinlets, and lacks fluorite. High-silica alteration in Vinini hornfels is poorly developed and difficult to recognize. Vein quartz increases only slightly, but veinlets are less regular and nebulous patches of silica flood are more common than in the overlying potassic zone (Photos 18 and 28). The high-silica zones at Mount Hope are similar to pervasive silica zones underlying ore at Climax, Henderson, Mount Emmons, and Pine Grove (Wallace and others, 1968; Mutschler and others, 1981, p. 883; M. W. Ganster, pers. commun., 1979).

Petrographic study suggests that silica flooding in igneous rocks began with suturing of strained quartz phenocrysts, forming mosaics that grew outwards and coalesced into patches of granular silica (Photo 29). Igneous relects in high-silica alteration, therefore, generally appear depleted in quartz phenocrysts.

A slight increase in pyrite content accompanies the transition between the potassic and high-silica zones. Magnetite, absent from higher levels of the system, averages up to 0.5 weight percent in veinlets with quartz, dark green biotite, and pyrite. Traces of arsenopyrite and primary hematite also occur. Some drill holes contain anomalous base metals in these deep levels, but such concentrations are rate.

A significant increase in sericite and clay after relict feldspars occurs 50 to 100 meters below the top of the high-silica zone (only the deepest silica zone in the western half of the deposit), and overlaps into the underlying biotite zone. This increase in clay-sericite may be analogous to paragenetically late lower argillization at Henderson (MacKenzie, 1970, p. 139-142).

A biotite zone, developed especially in coarse-grained quartz porphyry, underlies the deep high-silica zones. Megascopically recognizeable mafic sites distinguish this zone, and consist of aggregates of secondary biotite with retrograde chlorite and sericite. Primary biotite and oligoclase become more abundant with depth. Widely spaced high-angle quartz-calcite veins are common. A thin zone of low-grade molybdenum and tungsten mineralization generally occurs near the top of the biotite zone.

Local variations from these highly generalized patterns of alteration-mineralization zoning of course exist. Lithology exhibits strong control on alteration types, and therefore dikes of potassic-altered quartz porphyry locally cut argillized Mount Hope Tuff (e.g. drill hole

UPMH-2, 126 m depth). Metal haloes are stronger in Mount Hope Tuff than in other lithologies. Finally, alteration and geochemical zones that evolved late in the evolution of the system, such as the fluorine halo, are typically flatter in shape than earlier zones, such as potassic alteration or molybdenum (cf. Bright and White, unpubl. ms.). This pattern may account for the changing positions of some metal zones relative to molybdenum mineralization in the periphery as compared with more central portions of the deposit.

Nature and habit of molybdenum mineralization

As in other bulk-tonnage molybdenum deposits, mineralization at Mount Hope occurs in a stockwork of fractures and veinlets. Disseminated molybdenite, although present, is very rare. The bulk of mineralization occurs in four types of veinlets, described below and illustrated in Photo 32. Hazen Research, Inc. (1981, p. 15-32) studied mineralogy and texture of ore mineralization in detail, and the following descriptions integrate some of their findings:

(1) "Typical" quartz-molybdenite veinlets (comprise 75% of ore) - range from 0.5 to 5 mm thick and generally contain grains of molybdenite averaging 1 mm in long dimension

(2) "Gaudy" quartz-molybdenite veinlets (10% of ore) - veins 5-20 mm thick, lined with rich clusters of molybdenite grains averaging 0.08 mm across; most common in Vinini hornfels

(3) "Blue quartz" veins (10% of ore) - 3 to 10 mm thick, with a bluish-gray hue imparted by sparse grains of molybdenite averaging 0.05 mm across; most common deeper in the system

(4) Molybdenite "paint" (5% of ore) - thin films of molybdenite, commonly smeared and slickensided, on late fractures that are devoid of quartz

Vein paragenesis

Age relationships between veinlet types at Mount Hope are quite complex and only a generalized sequence is known. The following relationships are well established by core-logging and petrographic study:

(1) Quartz-molybdenite veinlets cut barren quartz - fluorite ± K-feldspar veinlets, and are in turn cut by thicker blue quartz veins (Photo 33).

(2) Silica flood commonly cuts quartz-molybdenite ± fluorite veinlets (Photo 34), in some instances assimilating remnants of mineralization as "ghost molybdenite".

(3) Quartz - sericite - pyrite ± fluorite veinlets cut quartz - K-feldspar - molybdenite veinlets (Photo 35).

(4) Clay-, carbonate-, and pyrite-bearing fractures without quartz cut all quartz-bearing veinlets.

These relationships suggest the following sequence of veinlet types, which is generally similar to that proposed by Westra (1980, p. 29):

(1) early barren quartz ± fluorite ± K-feldspar veinlets

(2) quartz - fluorite - molybdenite ± K-feldspar veinlets

(3) quartz - molybdenite ± fluorite veinlets

(4) blue quartz veins

(5) granular silica flood

(6) quartz - sericite ± pyrite ± fluorite veinlets (shallower) and quartz - pyrite ± magnetite ± biotite veinlets (deeper)

(7) molybdenite paint

(8) late fractures lined with pyrite, clays, and (or) carbonates

These relationships appear to record a transition from earlier, thin, molybdenite-rich quartz veins through progressively thicker veinlets with sparse molybdenite (blue quartz veins) into barren accumulations of silica. Evidently, hydrothermal fluids became depleted in molybdenum in time, possibly due to influx of meteoric water.

Configuration and genesis of the molybdenite body

Significant molybdenum mineralization at Mount Hope occurs nearly entirely in Vinini hornfels and the various quartz porphyry phases, mostly in the zone of potassic alteration. Early drilling suggested that the deposit consisted of a single teacup-shaped molybdenum ore shell (Westra, 1980, p. 33). Additional drilling showed a far more complex pattern of mineralization (Plates 3B and 4B) that suggests the presence of multiple ore shells. Widely separated intercepts of better grade in EMH-5, -7, -11, -19, and -20 may be the product of stacked molybdenum ore shells, separated vertically by 300-400 m of lower grade rock (Plates 3B and 4B). Stacked high-silica zones in EMH-1 (Plate 3A:A-A', 4A:C-C') support this configuration.

Significant molybdenum mineralization occurs over an area of at least 1500 m in a north 60° west direction, by 750 m north-south. Because ore shells in known Climax-type systems average 670 to 1100 m in diameter (White and others, 1981, p. 274), the Mount Hope deposit is evidently abnormally large in the horizontal dimension to be the product of a single shell. An alternative configuration was therefore proposed, with two partially overlapping systems lying side-by-side along an axis trending north 60° west (Plate 2D). Each of these systems consists in turn of at least two stacked shells, with the shallower shells of generally higher grade. The lower grade western system is approximately 1050 m north-south by 750 m east-west and has a low-grade apex 300 m in diameter. EMH-1 pierced the center of the system, but averaged less than 0.03% Mo through the projected interval of the shallower molybdenum shell (Plate 3B:A-A' and 4B:C-C'). The eastern system, 1000 m east-west by 800 m north-south, is centered between EMH-9 and -13. Although deeper than the western system, this body contains higher grade and more regular molybdenum mineralization, except where cut and attenuated by post-

mineral structures.

The following evidence supports the presence of two side-by-side molybdenite systems:

(1) Molybdenum contours on level plans (Plates 6A-9A) and east-west cross sections (Plate 4B:D-D') suggest the presence of side-by-side domes of mineralization.

(2) A contour map showing elevations of the top of the high-silica zone (Figure 2) defines two domes that are coaxial with the proposed molybdenum shells. Although silica flooding postdates molybdenite mineralization, high-silica zones at Climax (Wallace and others, 1968, p. 625) and Mount Emmons (M. W. Ganster, pers. commun., 1979) are coaxial with, and closely mimic the shape of the immediately overlying ore shells

(3) The multi-shell model predicts that spatial overlapping of ore shells should produce a zone of significantly higher grade mineralization over the "saddle" between the domes of high-silica in Figure 2. EMH-2, -11, -12, and -14 all penetrate this area, and all intercept at least 100 m of 0.15 - 0.20% Mo (Plates 4B and 7B). Moreover, the intensity of quartz veining appears to be greater in these intercepts than in those holes outside the inferred overlap zone, as would be predicted.

(4) There are contrasts in nature of mineralization between the two systems, with the eastern system containing generally thicker veinlets that are richer in molybdenite than the western system.

(5) The multi-shell configuration explains the marked asymmetry of surface alteration zones (Plate 2A). The potassic core and surrounding potassic-phyllic zone clearly outline the shallow western system. The anomalously wide argillic zone and potassic-phyllic outlier to the east reflect the deeper eastern system.

(6) Although the deposit as a whole is a very heterogeneous body of mineralization, the multi-shell model delineates zones of remarkably consistent grade (Plate 2D). After these consistencies became evident in mid-1981, we were able to predict the outcome of drill holes with marked success.

Recent drilling by the Mining Geology group has confirmed patterns of molybdenum distribution and shell configuration shown on Plate 2D. A notable exception, however, was a high-grade intercept from EMH-57, located on the western flank of the western system 260 m southwest of EMH-22. Common thick, high-angle veins with coarse molybdenite (M. R. Mapa, pers. commun., 1982) suggest that this hole could have intersected a mineralized cone-sheet fracture system, such as those that control high-grade mineralization at Urad (Wallace and others, 1978) and Mount Emmons

FIGURE 2. Plan showing elevation of the top of the high-silica alteration zone. Contour interval 100 meters.

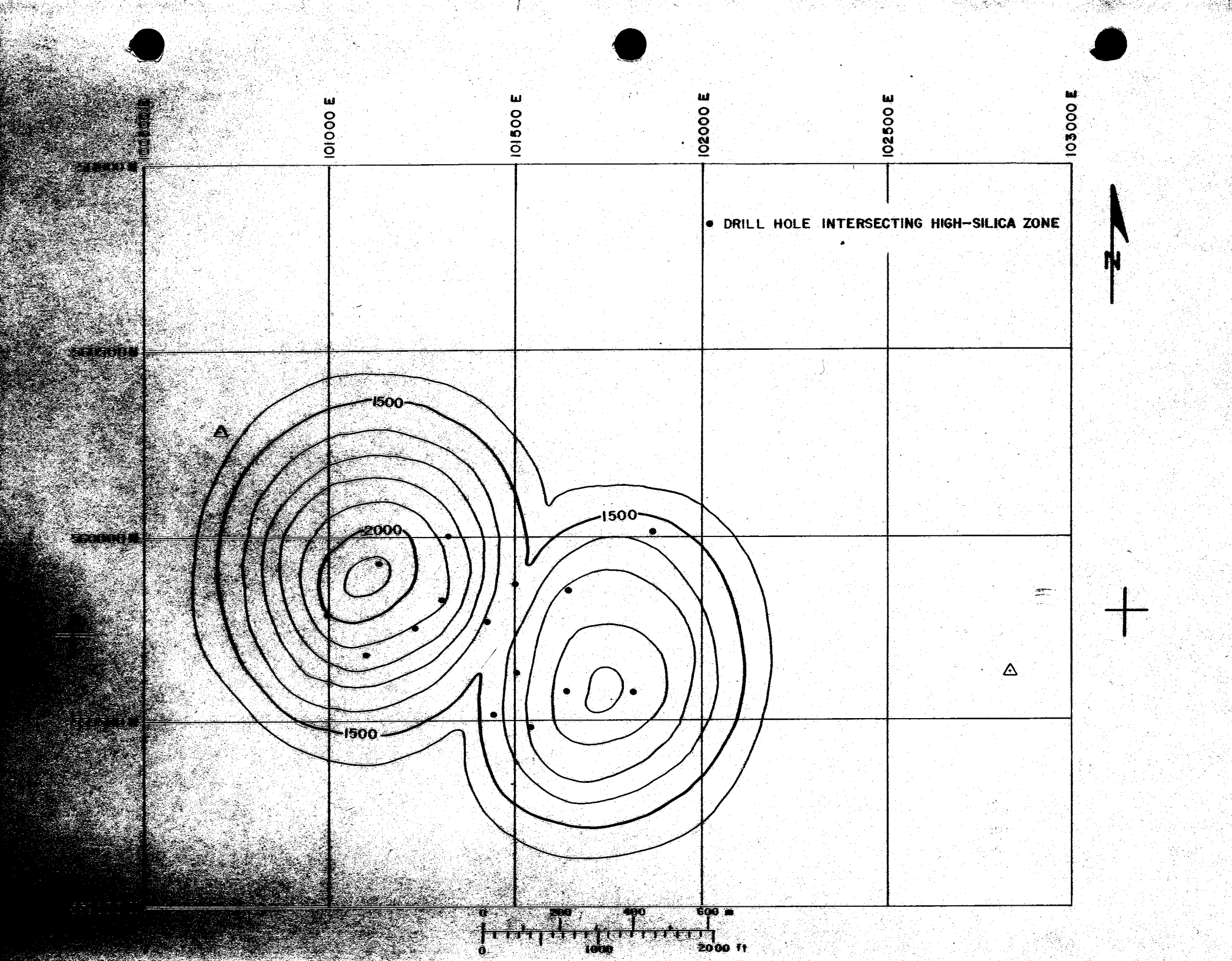
101000 E
101500 E
102000 E
102500 E
103000 E
DRILL HOLE INTERSECTING HIGH-SILICA ZONE
N
1500
2000
1500
1500
0
200
400
600 m
0
1000
2000 ft

(M. W. Ganster, pers. commun., 1979). Such a structure would presumably follow an arc around the center of the associated molybdenum shell. The anomalous higher grade zone in EMH-10, consisting primarily of molybdenite in late fractures related to the Ravine fault system, may be a similar mineralized structure (Plate 9A).

Studies at Climax, Henderson, and Mount Emmons (White and others, 1981) establish genetic links between intrusions of rhyolite porphyry magma and overlying molybdenum oreshells. Spatial, temporal, and textural evidence suggests similar relationships between mineralization and intrusion at Mount Hope. The shallower molybdenum shells lie 150 to 500 m symmetrically above the upper contact of aplitic quartz porphyry (Plates 3B and 4B). The underlying but probably related zones of high-silica alteration commonly straddle the upper contact of this same intrusive phase (Plates 3A and 4A). Deeper zones of molybdenite mineralization cap coarse-grained quartz porphyry 0 to 200 m above its upper contact. Thus, the shallow and deep shells appear to be spatially related with cupolas of aplitic and coarse-grained quartz porphyries, respectively. Coarse-grained quartz porphyry cuts molybdenite-bearing veinlets and silica flooding (Photo 36) related to the shallower systems, but is in turn cut by mineralization of the deeper shells. Molybdenum mineralization must therefore both predate and postdate intrusion of coarse-grained quartz porphyry; this concurs with spatial relationships just described.

Micrographic intergrowths of quartz and K-feldspar commonly occur in the groundmass of the uppermost 60 m of aplitic quartz porphyry (Photo 37). Rare crenulate quartz layers, separated by quenched porphyry groundmass, occur in the same horizon (Photo 38). White and others (1981, p. 295-296) described similar textures from the ore-forming Primos porphyry at Henderson and suggested that they record the accumulation of a mineralizing aqueous phase. Crenulate quartz bands form from cyclic variations in P_{H_2O} and P_{HF}; fluid overpressures result in crystallization of quartz alone until rock failure leads to P_{H_2O} decrease and crystallization of quenched porphyry. The presence of micrographic and crenulate textures in aplitic quartz porphyry supports spatial and temporal evidence that this intrusive phase was the principal mineralizer at Mount Hope.

The two-system, four-shell model outlined above explains all mineralization of significance encountered in Exploration drilling to date. Locally, however, rhyolite vent breccia contains autoliths of early quartz porphyry cut by sheeted or stockwork quartz veins (Photo 39). These fragments carry molybdenite mineralization in Phillips drill holes east of EPMH-15 (Westra, 1980, p. 31). Because the vent breccias cut this mineralization, it is temporally distinct from molybdenite bodies associated with aplitic and coarse-grained quartz porphyries, and is therefore termed "pre-eruptive". Perhaps this mineralization was genetically associated with the early quartz porphyry, was partially destroyed during explosive venting and cauldron subsidence, but is preserved as mineralized autoliths in rhyolite vent breccia.

In summary, spatial, temporal, and textural relationships link molybdenum mineralization with three of the five intrusive quartz porphyry phases of the complex. Because all five phases are mineralogically and chemically similar, the lack of mineralization related to quartz

porphyry and quartz porphyry border phase is clearly anomalous. The eruptive cycle preceding these phases undoubtedly liberated large amounts of volatiles and metals into the atmosphere, and thus quartz porphyry and border phase were products of a "wasted" hydrothermal system. Micrographic textures occur in K-feldspar phenocrysts in these intrusive phases (Photo 40) but not in their groundmasses. Apparently fluids accumulated during crystallization of phenocrysts near the top of the magma reservoir that was to become the Mount Hope complex. The lack of micrographic intergrowths in groundmasses of main and border phase quartz porphyry records subsequent loss of these fluids, presumably due to venting. Later aplitic and coarse-grained quartz porphyry phases produced mineralization because the system had had sufficient time to once again evolve significant magmatic-hydrothermal fluids.

Relative ages between the four inferred shells of mineralization are imperfectly known. Age relationships of coarse-grained quartz porphyry cited above show that deeper shells postdate shallower shells. Interfering alteration-mineralization patterns in drill holes just west and east of the overlap zone should establish relative ages between the two shells. EMH-16 (just west of the overlap zone) intercepted a shallower molybdenum zone correlated with the western system, underlain by better grade mineralization similar to that of the eastern system. This deeper mineralization cuts the high-silica zone underlying and postdating the shallow western molybdenum shell (Plate 9A). The shallower eastern oreshell therefore appears to postdate the shallow western shell. No evidence bearing on relative ages of the deeper systems is available.

Distribution of tungsten

Patterns of tungsten mineralization appear less regular than those of molybdenum. The distribution of 100 ppm tungsten, however, suggests four shells of mineralization (Plate 4C) analogous to those for better-grade molybdenum. Tungsten zones are thinner than, and may not directly overlap corresponding molybdenum shells. The shallower tungsten zones commonly occur just below the shallow molybdenum shells, in the lower potassic and upper high-silica zones (Figure 1). The apex of the western system is barren of tungsten as well as of molybdenum (Plate 4C:C-C'). Although data is sparse, the deeper zones of tungsten mineralization are better grade and more nearly coextensive with corresponding molybdenum shells. The Climax deposit displays a similar pattern of increasing tungsten-to-molybdenum ratio with progressively deeper and later pulses of mineralization (Wallace and others, 1968, p. 636).

The position of tungsten with respect to molybdenum mineralization at Mount Hope is somewhat anomalous. In most Climax-type deposits, tungsten zones are well above molybdenite ore shells (Westra and Keith, 1981, p. 856); rarely tungsten is coextensive with molybdenum (Climax lower orebody; Wallace and others, 1968, p. 631). It is possible that the shallower tungsten shells correspond to the deeper zones of molybdenum and therefore occupy a peripheral position as in most other deposits. If so, the deeper tungsten zones would suggest that undiscovered molybdenum shells may lie at still greater depth. Weak alteration and mineralization in deep holes near the center of the system (e.g. EMH-2 and -5), however, argue against this alternate configuration.

Oxidation and supergene alteration-mineralization

Oxidized rock, with goethite, jarosite, hematite, and copper oxides, ranges from 12 m thick in EMH-11 to 365 m thick in EMH-18. Deeper oxidation occurs under topographically high areas and along structures. Rare molybdenite and ferrimolybdite occur in oxidized drill core and locally (near and north of EMH-8) in surface outcrop. In general, however, oxidation appears to have leached molybdenum. The oxide zones in EMH-8 and -12 average less than one-fifth the molybdenum content of immediately underlying sulfide mineralization. EMH-6, -8, -12, -16, -17, and -19 intercepted grades of at least 0.03% molybdenum just below oxidation. Apparently, erosion truncated the top of the western portion of the deposit (Plates 3A:A-A' and 4A:C-C'), and unusually complete leaching of molybdenum produced a surprisingly weak surface anomaly (Plate 2B; Westra, 1980, p. 32).

Anomalously high assays near the base of oxidation in EMH-8, -12, and -17 suggest that transported molybdenum was redeposited to form a zone of weak supergene enrichment. The supergene molybdenum may be adsorbed onto iron oxides, or may occur as discrete molybdic oxide species. Enrichment of molybdenum has also been suggested for the Nevada Moly deposit (G. MacDonald, oral commun., 1981) and at the Copper Flat (Hillsboro, N. M.) porphyry copper system (Dunn, 1982, p. 321). Where erosion truncated the copper halo of the Mount Hope system, a thin chalcocite enrichment blanket formed near the base of the oxide zone.

POST-MINERAL STRUCTURE

Several fault zones are traceable between drill holes in the subsurface (Appendix 2; Plates 2-9). Textural evidence in drill core and offsets in alteration and mineralization zones (Plates 2A-9A, 3B, and 4B) suggest significant post-mineral normal offset along these structures. Locally, strong pyrite and molybdenite appear localized in these zones and therefore suggest some pre-mineral history. For descriptive purposes, faults are classified into two sets: (1) high-angle structures trending west-northwest, and (2) moderate- to high-angle ringlike structures. The latter set appears to truncate the former. Drilling has intercepted innumerable additional zones of crushed, broken, and sheared rock, but these are not traceable between holes with any reliability.

Bisoni, Tia, and South faults

West-northwest-trending high-angle faults cut the southwestern edge of the complex and Vinini Formation to the south. The Bisoni and Tia faults dip 60 to 70 degrees northerly (Plate 3:A-A'). The curved trace of the Bisoni fault on Plate 4:C-C' is an illusion imparted by projection of drill holes onto a section line nearly paralleling the strike of the fault plane. The Mount Hope fault truncates these structures on the east, and displaced segments east of the Mount Hope fault have not been located. Abrupt increases in molybdenum below the Bisoni fault in EMH-2 and below the Tia fault in EMH-11 suggest post-mineral normal movement. Magnitude of dip-slip is uncertain, but is probably less than 100 m.

Drilling has not penetrated the South fault, and therefore its attitude is unknown. It appears to truncate the sulfide zone to the south (Plate 2A). This truncation and an apparent right-lateral displacement in the east-dipping limy marker horizon of the Vinini (Plate 2) suggest relative downward motion of the block to the south.

Mount Hope, Lorraine, and Ravine faults

Because eight Exploration drill holes penetrated the Mount Hope fault, the subsurface configuration of at least portions of this structure are well known. It is a listric fault, with easterly dips of 55 degrees near the surface and 30 to 35 degrees at depth (Plate 3:B-B'; the flatter traces on Plate 4 are apparent dips). In plan, it appears to be distinctly spoon-shaped (Plates 5-9). Such a shape would constrain movement to along the trough of the fault surface, a north 65° east direction. The truncation of the potassic-phyllic zone along the fault (Plate 2A), and abrupt increases in molybdenum grade below the fault zone in EMH-5, -9, and -14 (Plates 3B:B-B' and 4B) suggest normal movement. Eastward relative movement of the hanging wall concealed better grade mineralization of the eastern system beneath peripheral argillic alteration. As a result, very weak surface molybdenum geochemistry occurs over the eastern system, except on the south (upthrown) side of the Mount Hope fault trace.

The Mount Hope fault displaced the apex of the eastern system east-northeasterly, producing a relatively blank area intercepted by EMH-13, but presumably juxtaposing mineralization in both hanging wall and footwall northeast of EMH-13 (Plate 3B:B-B'). Such stacking of mineralization could explain the isolated intercept between 460 and 550 m depth in EPMH-15; it represents the eastern edge of hanging wall mineralization. Plate 2D shows the inferred extent of the blank area due to movement on the Mount Hope fault as a crescent-shaped zone near the center of the eastern system.

Drill hole control is inadequate to allow precise estimates of displacement on the Mount Hope fault. Offsets in contacts range from 90 to over 200 m, and omissions of geochemical zoning patterns across the fault in EMH-9 and -13 suggest dip-slip of 135 to 220 m. Displacement of the apex of the eastern system to the east of EMH-13, as in Plate 3B:B-B', requires 240 m of dip-slip.

Recent drilling by the Mining Geology group has verified the presence of the relatively blank zone surrounding EMH-13 shown on Plate 2D. Their geologists, however, consider the Mount Hope fault as mapped herein to consist of two separate structures trending north-northeast and west-northwest (S. C. Moore, pers. commun., 1982). It is possible that the trace diverges from that mapped on Plate 2 at approximately 559800N - 103450E and extends southerly to south-southeasterly under a prominent gully. If so, the west-northwest-trending strand of the fault as shown on Plate 2 could represent the north-dipping Tia (or Bisoni?) fault offset by normal movement on the north-northeast-trending strand. Two lines of evidence argue against such an interpretation:

(1) The proposed north-northeast-trending strand projects through the collar of EMH-17, yet drill core here was notably competent and unbroken.

(2) The Mount Hope fault appears to truncate the surface molybdenum anomaly north of 559500N, but the hypothesized southerly continuation of the strand trending north-northeasterly has no affect on distribution of molybdenum south of this line. Anomalies in this area, however, may be transported.

EMH-13 and Mining Geology drill hole EMH-48 pierce the Lorraine fault. It appears to dip southwesterly at a moderate angle and cannot be traced into the footwall of the Mount Hope fault (Plate 3:B-B' and 4:D-D'). It may be an antithetic normal structure to the Mount Hope fault.

The listric Ravine fault is traceable through the footwall of the Mount Hope fault in drill holes EMH-3, -5, -10, and -14. The linear segment of its trace (Plate 2) shows it to be nearly vertical above an elevation of 2350 m. With depth, it flattens to a moderate angle (Plate 4:C-C') and appears to break into several spoon-shaped strands (Plates 8 and 9). Deep oxidation along the structure appears to truncate the molybdenum zone between EMH-16 and EMH-7 on Plate 5A. At the 2073 m elevation (Plate 6A) the fault cuts off the zone of 0.12% molybdenum between EMH-2 and -14. The fault attenuates the better grade in EMH-5, producing the anomalously low-grade intercept in this hole (Plates 2D, 4B:C-C', and 7A). In EMH-10, a wide zone of crushed and sheared rock marks the fault zone. Paragenetically late molybdenite fills these fractures and produces the anomalous zone of higher grade mineralization lying north of the inferred eastern shell (Plates 8A and 9A).

Post-mineral tilting

Westra (1980, p. 33) suggested that the Mount Hope system had been tilted approximately 20 degrees easterly. More recent drilling substantiates slight post-mineral tilting to the east or northeast (see especially Plate 3:B-B'). Map patterns of cooling units within Mount Hope Tuff suggest that the volcanic sequence dips gently northeastward. These observations are in accord with gentle eastward dips of Miocene basalts in the Roberts Mountains (Murphy and others, 1978) and the regional tendency of mountain ranges to be bounded on the west by Basin-and-Range faults and on the east by broad pediments. The gravel-covered pediment east of Mount Hope, and the northwest-trending Basin-and-Range fault on the west edge of the Sulphur Springs target area (Plates 1 and 1A) confirm this pattern locally. Local and regional evidence, therefore, suggests that Basin-and-Range block faulting tilted the Mount Hope area between 10 and 20 degrees eastward to northeastward subsequent to mineralization.

EVOLUTION AND AGE OF THE MOUNT HOPE COMPLEX

The Mount Hope complex and deposit evolved through a complex series of Tertiary igneous and hydrothermal events, as outlined below and in Figures 3a-3h:

(1) Intrusion of dikes of biotite quartz monzonite porphyry into country rocks of the Vinini Formation (Ov).

(2: Figure 3a) Intrusion of a rhyolite porphyry magma to shallow depths. Crystallization of the border zone of this magma as early quartz porphyry (Tqpe). Formation of a body of pre-eruptive molybdenum mineralization related to this intrusion, as evidenced by mineralized autholiths in later rhyolite breccia.

(3: Figure 3b) Eruption of the lower cooling unit of the Mount Hope Tuff (Tht_1) from a vent over the western portion of the magma chamber. Collapse of the western caldera, in which the ash-flows ponded. No significant outflow facies resulted from this eruption.

(4: Figure 3c) Eruption of the middle and upper cooling units of the Mount Hope Tuff (Tht_2 and Tht_3) from the eastern portion of the chamber; collapse of the eastern caldera. Eruption of Tht_2 probably resulted in renewed collapse of the western caldera, as it appears to have ponded in this structure. Either or both of these ash-flow units formed outflow facies north of Henderson Summit and possibly under gravels east of Mount Hope. Emplacement of ring-dikes of rhyolite vent breccia (Trb) into cauldron margins. These events may have descroyed a significant volume of pre-eruptive mineralization. Quartz-eye tuff (Tqt) is of uncertain age but is probably related to this episode.

(5) Cessation of eruptive phase of activity, accompanied by solfatoric alteration-mineralization concentrated along ring fracture systems.

(6: Figure 3d) Intrusion and crystallization of quartz porphyry (Tqp and Tbqp). No significant molybdenum mineralization resulted, presumably due to catastrophic volatile loss during immediately preceding eruptive events.

(7: Figure 3e) Intrusion of the western mass of aplitic quartz porphyry (Tqpa). By this time, magmatic convection and vapor exsolution had once again produced significant volumes of hydrothermal fluid; formation of the shallow western molybdenum shell. Cone-sheet fractures related to the magma cupola may have concentrated better grade mineralization.

(8: Figure 3f) Intrusion of the eastern mass of aplitic quartz porphyry. Formation of the shallow eastern molybdenum shell, which locally overlapped and augmented western system mineralization.

(9: Figure 3g) Intrusion of coarse-grained quartz porphyry; formation of deep zones of molybdenite mineralization. Intrusion of fine-grained granite.

FIGURES 3a - 3h. Series of palinspastically restored east-west cross-sections illustrating the evolution of the Mount Hope complex and deposit. Rock units as on Plate 2. See text for discussion.

low-grade
molybdenum mineralization

medium-grade
molybdenum mineralization

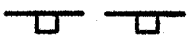

high-grade
molybdenum mineralization

magma

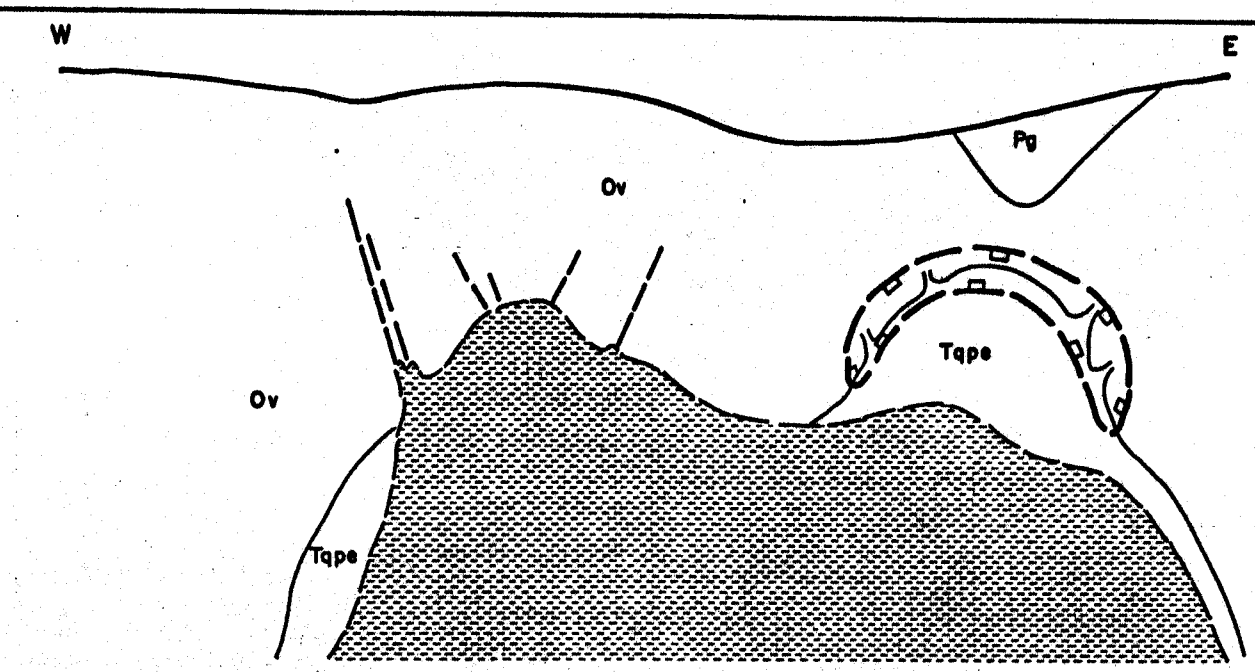

FIGURE 3a.

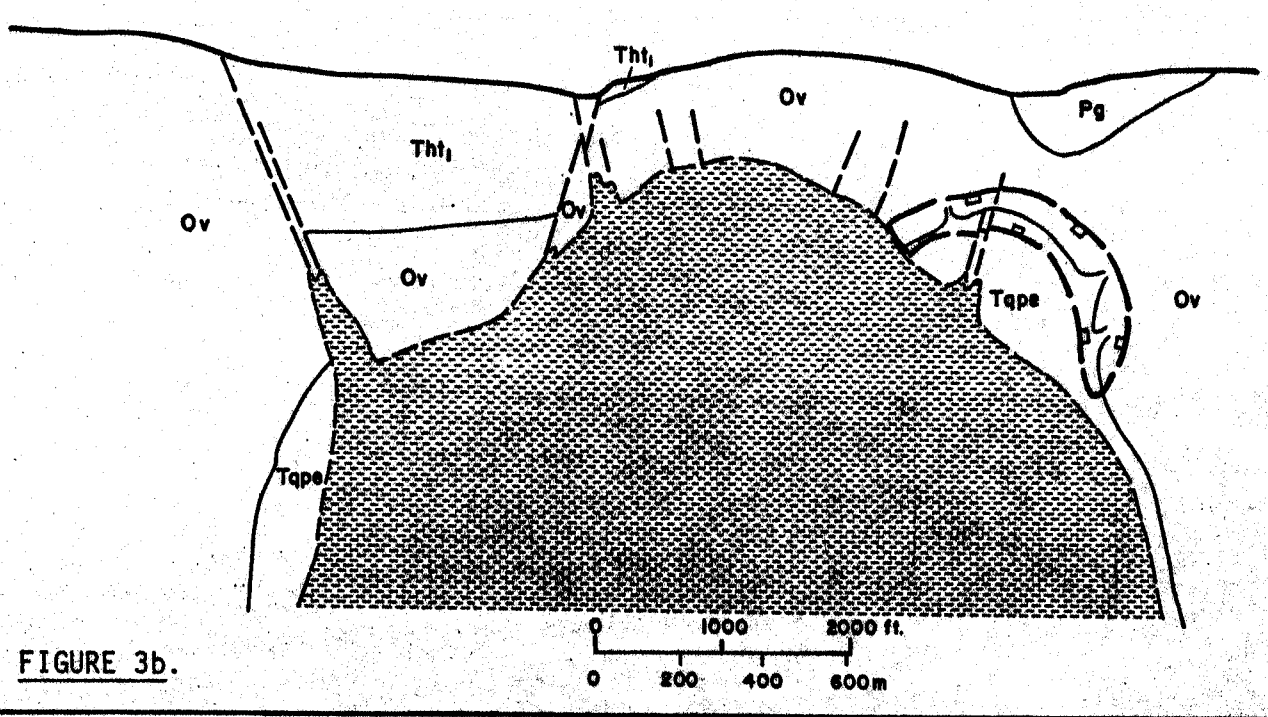

FIGURE 3b.

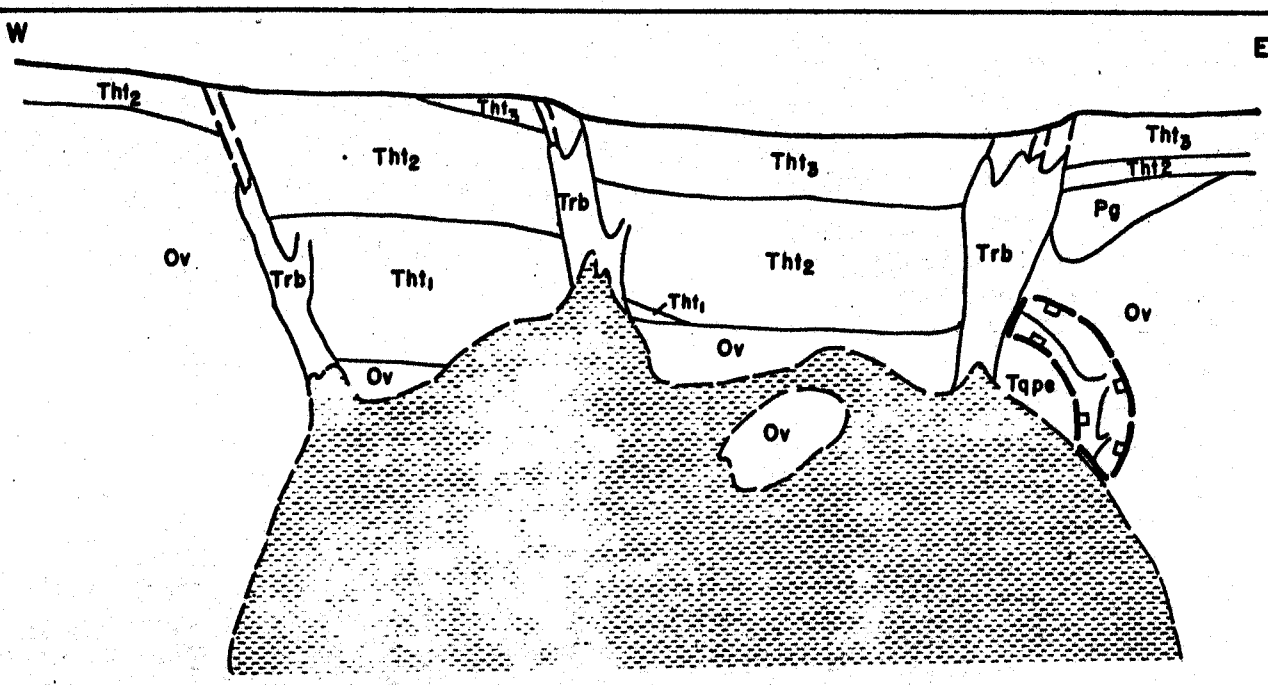

FIGURE 3c.

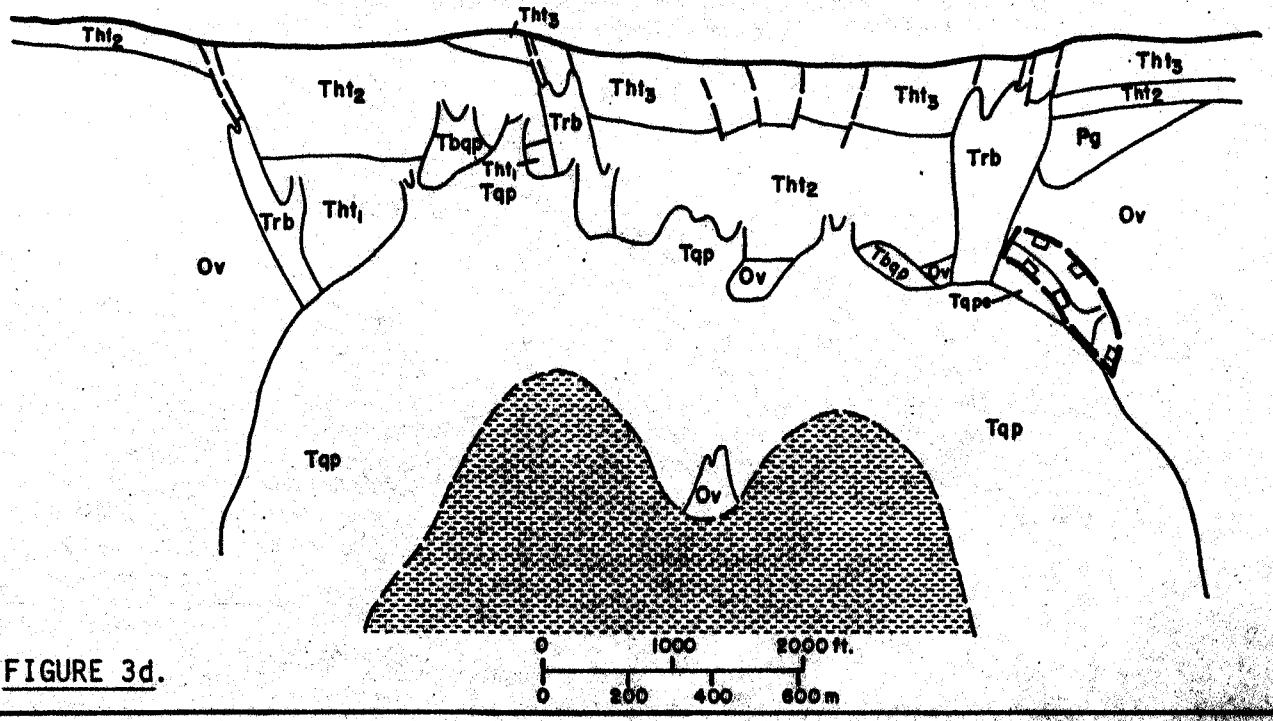

FIGURE 3d.

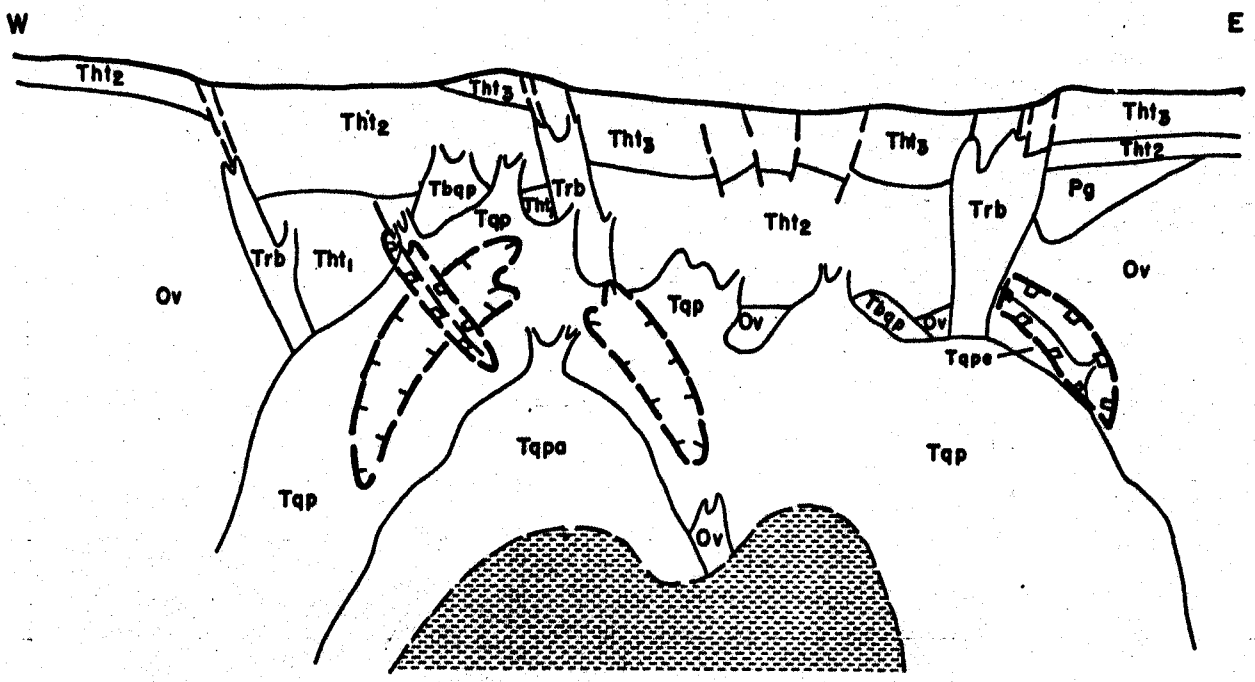

FIGURE 3e.

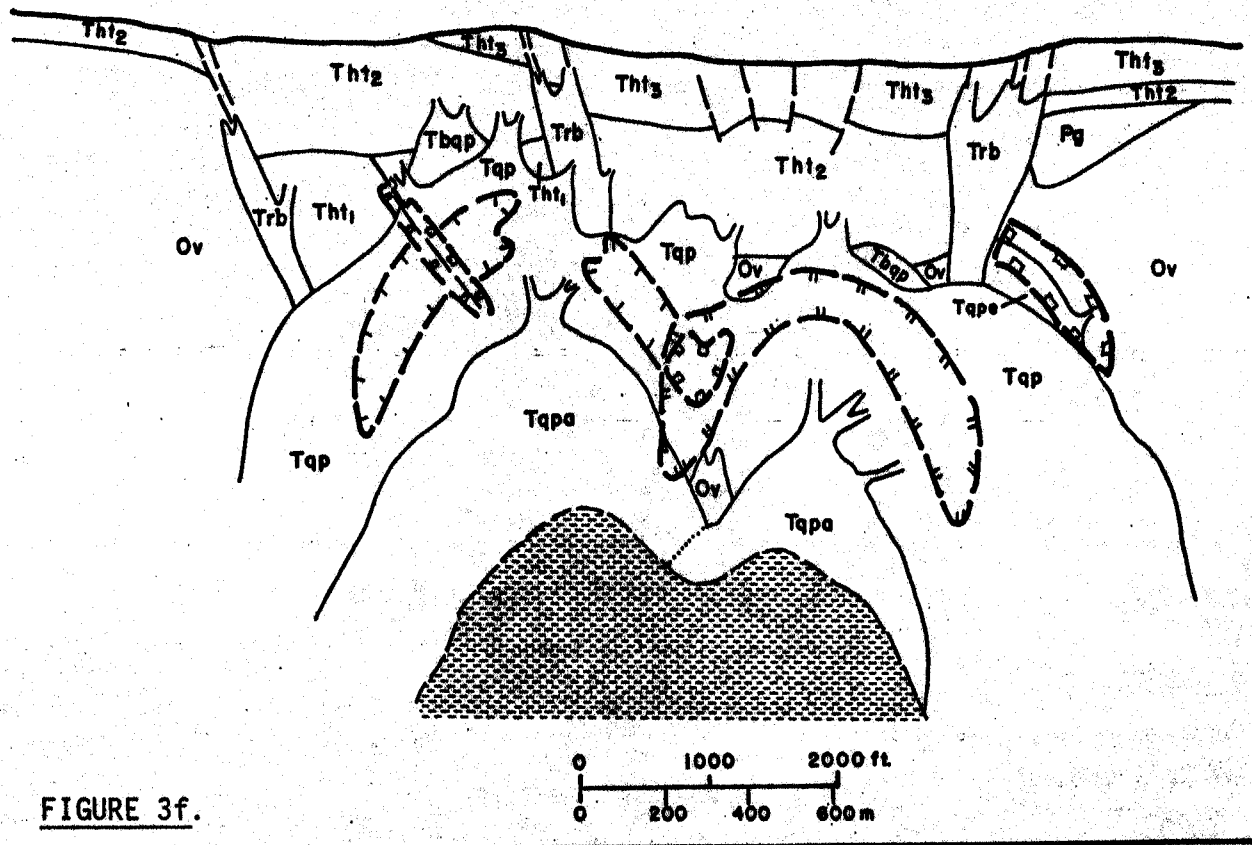

FIGURE 3f.

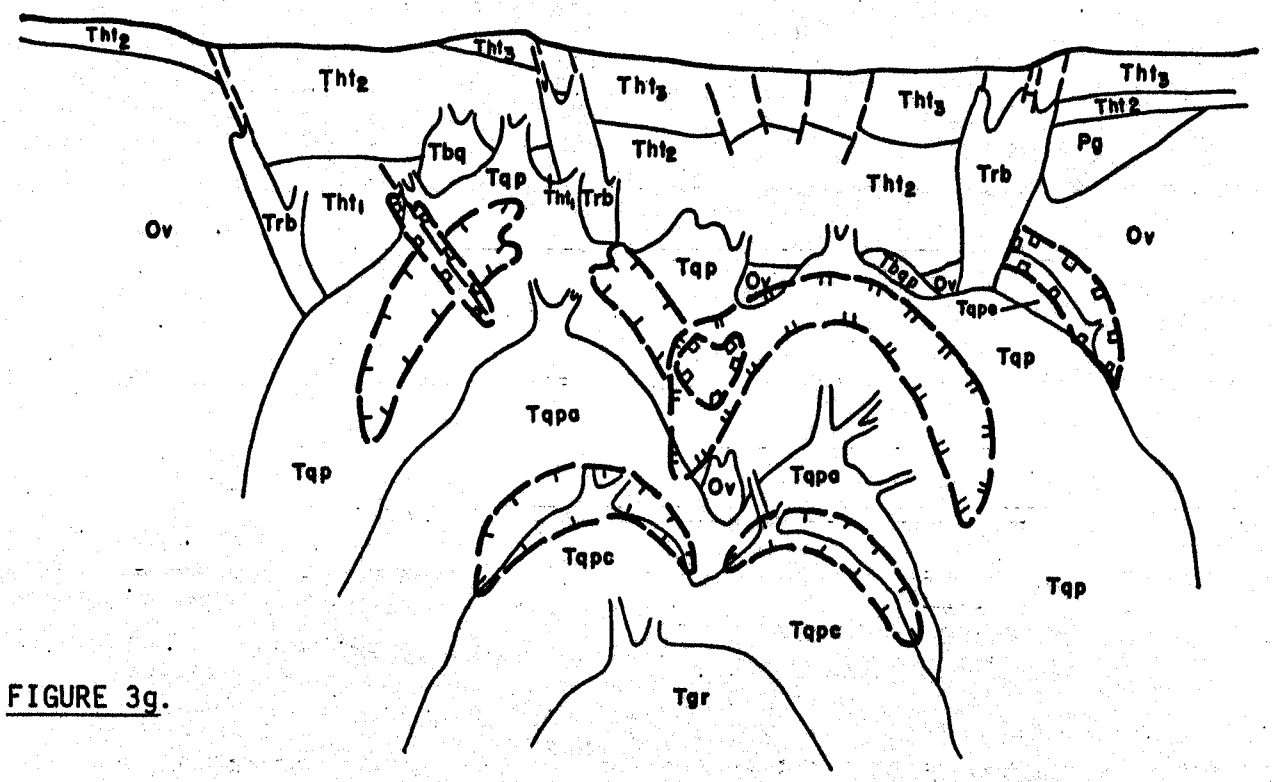

FIGURE 3g.

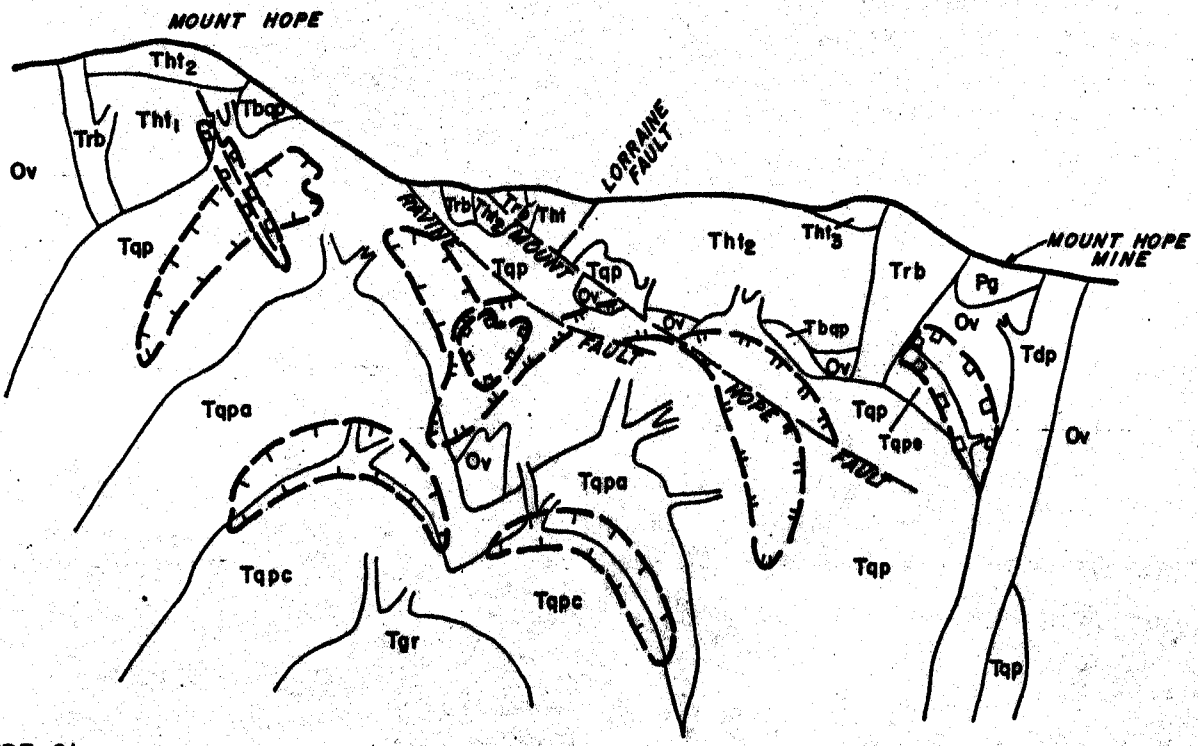

FIGURE 3h.

(10: Figure 3h) Intrusion of dacite porphyry. Although postmineral in age, its emplacement into a sulfide system at hypabyssal levels would probably have caused circulation of meteoric water, resulting in propylitic alteration and zinc mineralization of the dacite. Deposit tilted 10-20 degrees eastwardly or northeastwardly during Basin-and-Range faulting. Postmineral movement on the Mount Hope and Ravine faults, possibly also associated with Basin-and-Range deformation, fragmented and attenuated the eastern system. Erosion to present topography.

The unravelling of the igneous and hydrothermal evolution of the complex allows estimation of the depth of formation of the Mount Hope deposit. Because mineralized quartz porphyries intrude cogenetic volcanic rocks and are somewhat finer grained than those in other Climax-type systems (cf. White and others, 1981, p. 290-294), a relatively shallow level of formation is likely. Figures 3e and 3f suggest that known molybdenite mineralization may have formed at depths of only 400-500 m (or more depending on the unknown thickness of Mount Hope Tuff lost during subsequent erosion). Pre-eruptive mineralization could have occurred at yet shallower depths. This is less than the range of 600 to >4500 m inferred by Westra and Keith (1981, p. 855), White and others (1981, p. 286-287) and Mutschler and others (1981, p. 885-887) for depths of formation of other known Climax-type deposits. The Mount Hope system, therefore, may well have evolved under less cover than other major Climax-type molybdenum systems.

The exact age of these igneous and hydrothermal events remains elusive. Previous radiometric age determinations from the complex by Silberman and McKee (1971) and Edwards and McLaughlin (1972) ranged from 29.9 to 49 m.y. (Table 3). Because of this uncertainty, we submitted two core samples to Krueger Geochron Laboratories for additional K-Ar dates. We intended to date late intrusive events with the sample from EMH-5 (among the freshest rocks drilled to date), and to date major alteration and mineralization with the K-feldspar-flooded quartz porphyry in EMH-3. Our results, integrated with published determinations in Table 3, show marked discordancy and contradict well established relative age relationships. The 49.1-m.y. feldspar date from EMH-5 is considered the most reliable of the new determinations, and compares favorably with the 49-m.y. date on the unaltered Garden Pass quartz porphyry. Therefore, the rhyolitic rocks of the Mount Hope complex, and the molybdenum deposit, may actually be 49 m.y. in age, but yield apparently younger dates due to resetting by later thermal events. The radiometric ages of 29.9-32.6 m.y. for dacite porphyry are in accord with its younger relative age. Dacite porphyry may therefore have initiated thermal resetting of many of the ages for the rhyolitic rocks, but cannot account for a determination as young as 26.0 m.y. Moreover, an age of 49 m.y. for the Mount Hope complex would place it in a major magmatic hiatus in the Great Basin (S. B. Keith, pers. comun., 1982). We plan fission-track determinations in an attempt to resolve these inconsistencies.

POTENTIAL FOR FUTURE EXPLORATION

The multi-shell model of molybdenum distribution (Plate 2D) has been shown to be a powerful tool to locate mineralization and predict grades of molybdenite in different portions of the system. Comparison

Table 3. RADIOMETRIC AGE DETERMINATIONS FROM THE MOUNT HOPE COMPLEX

ROCK UNIT	LOCATION	ALTERATION ZONE	MATERIAL DATED	METHOD	AGE	SOURCE
Dacite porphyry	2300m NE of Mt. Hope Mine	unaltered	biotite	K-Ar	32.6±1.5	Edwards and McLaughlin (1972)
				Rb-Sr	29.9±6	
Coarse-grained quartz porphyry	Drill hole EMH-5, 820-823m depth	biotite	biotite, with minor chlorite	K-Ar	31.7±1.3	Exxon sample; analyses by Krueger Geochem Labs
			K-feldspar	K-Ar	49.1±2.1	
Quartz porphyry	Garden Pass stock, 3650m N of summit Mt. Hope	unaltered	biotite	K-Ar	49±2	Edwards and McLaughlin (1972)
	Drill hole EMH-3, 527-530m depth	potassic	primary and hydrothermal K-feldspar	K-Ar	26.0±1.0	Exxon sample; analysis by Krueger Geochem Labs
Rhyolite vent breccia(?)	~ 75m NW of Mt. Hope Mine	argillic	whole rock	K-Ar	39.8±1	Edwards and McLaughlin (1972)
Rhyolite vent breccia or Mt. Hope Tuff(?)	NE portion of Mt. Hope complex	argillic	biotite	K-Ar	35.6±0.7	Silberman and McKee (1971)

of Plates 2C and 2D suggests, however, that considerable potential remains even within the molybdenum systems inferred to date. Present Exploration (and most Mining Geology) drilling has focused on the overlap zone and adjacent portions of both shells. Expansion of this pattern is essential and should be guided by the inferred shall configuration. A particularly attractive untested target is east-northeast of EMH-13, where mineralization may be juxtaposed on both hanging wall and footwall of the Mount Hope Fault (Plate 3B:B-B'). EMH-23 (Plate 2C) will test this area. EMH-57 showed potential for higher grade mineralization west of previous drilling. This may represent structurally controlled mineralization in a cone-sheet fracture system, a possibility shown schematically in Figures 3e-3h.

Deeper portions of the system are incompletely explored. The two deep molybdenum shells are presently inferred between widely spaced drill holes, and additional drilling is needed to define grade distribution if planned open-pit mining includes this mineralization. Relict magmatic biotite and plagioclase in coarse-grained quartz porphyry deep in EMH-2 and -5 suggest weakening of alteration with depth, and that still deeper molybdenum shells are unlikely.

Present drilling has by no means defined the limits of mineralization in the Mount Hope deposit. EMH-4 and -18 probably limit the deposit to the southwest and northwest, but the system is open to the west, southeast, northeast, and north. The wide zone of argillization in the northeastern portion of the complex (Plate 2A) seems too distant from known mineralization of the eastern system to be related to it, and may therefore suggest a separate center of mineralization north or northeast of EMH-10. Structurally controlled molybdenite from 517 to 578 m in EMH-10 may be a cone-sheet fracture system tapping a larger, deeper body of mineralization to the northeast (Plate 9A).

The known molybdenum resource at Mount Hope is genetically related to aplitic and coarse-grained quartz porphyries that postdate the period of ash-flow eruption and caldera collapse. Mineralized autoliths in Mount Hope Tuff and rhyolite vent breccia confirm the presence of pre-eruptive molybdenite mineralization, presumably associated with early quartz porphyry. Several arguments suggest that such mineralization could be significantly higher grade than the post-eruptive mineralization drilled to date:

(1) Westra and Keith (1981, p. 865-866) suggested an empirical relationship between potassium and molybdenum enrichment that can be used to estimate potential grade of stockwork molybdenum deposits. The data of Westra (1980, Tables 3 and 5) demonstrate that at least 2.5% K_2O was introduced during potassic alteration at Mount Hope. Such levels of potassium enrichment predict grades in excess of 0.3% molybdenum if fluids were molybdenum-saturated. As previously suggested, catastrophic loss of volatiles and molybdenum during venting left the quartz porphyry incapable of producing mineralization. Molybdenite associated with later aplitic and coarse-grained quartz porphyries averages less than one-half the predicted grade. All post-eruptive mineralization is therefore underfit relative to levels of potassium enrichment, presumably due to release of volatiles and metals during venting. Pre-eruptive mineral-

ization, however, predated such volatile loss and may contain the higher molybdenum grades predicted by Westra and Keith's (1981) model.

(2) Shallow depths of formation inferred for pre-eruptive mineralization in the preceding section suggest that thermal gradients were steep. Consequently, deposition of molybdenite due to drops in temperature (Westra and Keith, 1981, p. 866) would be concentrated in a restricted volume of rock.

Exploration for pre-eruptive mineralization is hindered because its alteration effects would be limited to Paleozoic sediments and pre-eruptive intrusive rocks. The large expanse of Mount Hope Tuff, for example, could conceal such a body. The abundance of veined and mineralized fragments in rhyolite vent breccia north of the Mount Hope Mine suggests this area as the site of a pre-eruptive body, as hypothetically shown on Plates 3B:B-B', 8A, and 9A. Figures 3a-3h illustrate that such a body may have been largely destroyed by later igneous events (analogous to the Urad orebody at Red Mountain, Colorado; Wallace and others, 1978), but a significant portion may still lie under Mount Hope Tuff or west-dipping vent breccias.

Because alteration and mineralization are not limited to the east, potential may exist under gravels in this direction. Gulf Minerals drill hole GMH-1 (Plate 1A) tested an I. P. anomaly on the pediment and intercepted argillized rhyolite porphyry cutting (or overlying?) Vinini chert and limestone, all containing pyrite and pyrrhotite. If the Bowser fault is indeed a cauldron ring structure and extends eastward under gravels, it may have localized additional post-eruptive centers of intrusion and mineralization. A program of rotary drilling and spot coring is recommended to test for concealed mineralization peripheral to any molybdenum centers under the pediment.

In summary, present and planned drilling has by no means tested the extent of the Mount Hope system. Continued exploratory drilling is absolutely essential to prevent the "zone of neglect" that surrounds all too many ore deposits.

THE SULPHUR SPRINGS TARGET

The Sulphur Springs molybdenum target is 4 km east of Mount Hope (Plates 1 and 1A). Shear-controlled copper oxides near the summit of September Morn Peak attracted early prospectors to the area. Bear Creek and Phelps Dodge ran geochemical and geophysical surveys over the area in the late 1960's. Apco Oil drilled at least one rotary hole to ≤425 m in 1971-73. Gulf Minerals staked September Morn Peak and the pediment east of Mount Hope, and drilled three rotary holes in 1974-76 (Plate 1A). GMH-2 (T.D. 283 m) and GMH-3 (T.D. 290 m; at same site as ESS-1) tested the upper portion of the Sulphur Springs target. Exxon's evaluation included geologic mapping, grid geochemistry, and one rotary drill hole.

Vinini Formation underlies much of the area, and consists of chert- and argillite-dominated members separated by a west-dipping thrust fault. Garden Valley Formation unconformably overlies Vinini to the east. The Roberts Mountains thrust and Eastern assemblage carbonate rocks presumably underlie Vinini within reasonable depths.

Rhyolitic to dacitic igneous rocks are identical to those of the Mount Hope complex. A swarm of quartz porphyry and dacite porphyry dikes cut Vinini throughout the area. Rocks similar to quartz-eye and Mount Hope tuffs crop out 550 m northwest of September Morn Peak. It is uncertain whether these represent a local vent or outflow from the Mount Hope center.

A system of high angle faults cuts all rhyolitic phases. September Morn Peak occupies an upthrown block bounded by such structures on the north and west. A Basin-and-Range fault bounds the area on the west and southwest and localizes dikes of dacite porphyry.

A distinct center of surface alteration and mineralization surrounds September Morn Peak. Argillite recrystallized to a gray, fine-grained hornfels in a zone about 500 m in diameter surrounding the summit. Strong goethite, jarosite, and fracture-controlled copper oxides mark this area. Clay replaces plagioclase in intrusive rocks within the sulfide zone. Strongly anomalous copper (60-5600 ppm) and zinc (80-2400 ppm) are coextensive with surface alteration. A central molybdenum anomaly (4-14 ppm) occurs on the upper western slopes of September Morn Peak.

Gulf drill holes GMH-2 and -3 tested only the near-surface base metal potential. Both holes encountered 0.5 to 5 percent pyrite in veinlets. GMH-3 cut argillized dikes of dacite porphyry and rhyolite breccias, and bottomed in pale brown biotitic hornfels. The upper 150 m of GMH-3 intercepted strong zinc and copper mineralization. No data on molybdenum or other elements are available.

Widespread, intense, and well zones alteration and geochemistry on the surface, coupled with gradients in GMH-3 and a setting similar to the Mount Hope system supported a molybdenum stockwork target within 500-600 m depths under September Morn Peak. Near-surface copper and zinc anomalies were considered as peripheral metal haloes, and the strong hornfels as suggesting an igneous mass at depth. A combined rotary-core drill hole at the site of GMH-3 was proposed to test the deeper molybdenum target.

Rotary hole ESS-1 was drilled and cased to 358 m depth in May, 1980. It cut Vinini chert and hornfels with increasing recrystallization below 200 m. Strongly anomalous copper (+200 ppm) and zinc (+600 ppm) occur in the upper 160 m (see histograms, Appendix 2), but molybdenum and fluorine are low and show no gradients.

Because of the inconclusive geochemistry of the rotary portion of ESS-1, we have yet to re-enter it. The source of the strong hornfels, surface alteration, and copper-zinc mineralization, therefore, remains unexplained. The lack of gradients in either fluorine or molybdenum up to 200 m below the copper halo, however, downgrades the target considerably. If a molybdenum system is present, it will probably be at least 600-700 m deep.

THE GARDEN PASS AND HENDERSON TARGETS

The Garden Pass and Henderson targets lie 4 km north and northwest, respectively, from Mount Hope. The Garden Pass plug consists of homogeneous quartz porphyry, with fresh biotite and only weakly sericitized plagioclase. The rock contains several percent garnet throughout, which appears to be accessory and not hydrothermal. A small area of volcanic rock, possibly quartz-eye tuff, is preserved at the north end of the plug. Contact effects in adjacent Vinini Formation are minimal. Fluorine reaches values of 0.22%, but metals are near background throughout the plug.

The lack of alteration and weak geochemistry preclude significant molybdenum mineralization within 1200 meters of the surface. Trace element geochemistry (Westra, 1980, Table 5) suggests that the Garden Pass magma had high potential for Climax-type mineralization, but did not evolve a hydrothermal fluid.

The Henderson rhyolite was first mapped as a plug, but subsequent field and petrographic re-examination showed it to be a blanket of Mount Hope Tuff overlying Vinini and Nevada Formations. Irregular autoliths of early quartz porphyry are common. Outcrop pattern of the tuffs suggests that they are outflow facies from the Mount Hope center, although some may be derived from local vents. The tuffs are nearly fresh, and limonites and geochemistry are weak. Thus, little potential exists for an intrusive body with molybdenite mineralization under the tuffs.

The Gull disseminated gold prospect (#994) occurs in the northern portion of the klippe of Nevada Formation just southwest of the Henderson rhyolite (Tingley, 1968). Gold-anomalous jasperoids attracted Lyle Campbell to the area, who staked it in 1967 under the premise that the carbonates represented a window through the Roberts Mountains thrust. Subsequent drilling by Union Pacific, however, disclosed the true structural relationships and intercepted no economic gold mineralization.

REFERENCES CITED

Bright, M. J., and White, W. H., ms., Hydrothermal alteration and primary trace element dispersion associatiated with the Henderson molybdenum deposit, Colorado: unpubl. ms., 53 p.

Dilles, J. H., 1982, A petrologic report on rock samples from the Mount Hope porphyry molybdenum deposit, Nevada: unpubl. report for Exxon Minerals Company, 75 p.

Dunn, P. G., 1982, Geology of the Copper Flat porphyry copper deposit, Hillsboro, Sierra County, New Mexico, in, Titley, S. R., ed., Advances in Geology of the Porphyry Copper Deposits: Tucson, Univ. Ariz. Press, p. 313-325.

Edwards, G., and McLaughlin, W. A., 1972, Shell list no. 1 - K-Ar and Rb-Sr age determinations of California, Nevada, and Utah rocks and minerals: Isochron/West, no. 3, p. 1-7.

Hazen Research, Inc., 1981, Mount Hope project - mineralogical investigation of molybdenum ore samples: unpubl. report for Exxon Minerals Company, 62 p.

Hydro-Search, Inc., 1982, Mount Hope project - Phase I hydrology: unpubl. report for Exxon Minerals Company, 2 vols.

Mabey, D. R., 1966, Regional gravity and magnetic anomalies in part of Eureka County, Nevada: Mining Geophysics, vol. 1, p. 77-84.

MacKenzie, W. B., 1970, Hydrothermal alteration associated with the Urad and Henderson molybdenite deposits, Clear Creek County, Colorado: unpubl. Ph.D. thesis, Univ. Michigan, 208 p.

Missallati, A. A., 1973, Geology and ore deposits of the Mount Hope mining district, Eureka County, Nevada: unpubl. Ph.D. thesis, Stanford Univ., 160 p.

Murphy, M. A., McKee, E. H., Winterer, E. L., Matti, J. C., and Dunham, J. B., 1978, Preliminary geologic map of the Roberts Creek Mountain quadrangle, Nevada: U. S. Geol. Survey open-file map 78-376.

Mutschler, F. E., Wright, E. G., Ludington, S., and Abbott, J. T., 1981, Granite molybdenum systems: Econ. Geol., v. 76, p. 874-897.

Peterson, D. W., 1961, Descriptive modal classification of igneous rocks: Geotimes, v. 5, no. 6, p. 30-36.

Roberts, R. J., Montgomery, K. M., and Lehner, R. E., 1967, Geology and mineral resources of Eureka County, Nevada: Nev. Bur. Mines Bull. 64, 152 p.

Silberman, M. L., and McKee, E. H., 1971, K-Ar ages of granitic plutons in north-central Nevada: Isochron/West, no. 1, p. 15-32.

Tingley, J. V., 1968, Final report - Gull prospect, Mount Hope mining district, Eureka County, Nevada: unpubl. report, Union Pacific Railroad Company, Natural Resources Division, 15 p.

Walker, L. G., 1962, Geology of Mount Hope area, Garden Valley quadrangle, Nevada: unpubl. M. A. thesis, Univ. Calif. Los Angeles, 31 p.

Wallace, S. R., MacKenzie, W. B., Blair, R. G., and Muncaster, N. K., 1978, Geology of the Urad and Henderson molybdenite deposits, Clear Creek County, Colorado, with a section on a comparison of these deposits with those at Climax, Colorado: Econ. Geol., vol. 73, p. 325-368.

Wallace, S. R., Muncaster, N. K., Jonson, D. C., MacKenzie, W. B., Bookstrom, A. A., and Surface, V. E., 1968, Multiple intrusion and mineralization at Climax, Colorado, in Ridge, J. D., ed., Ore Deposits of the United States, 1933-1967: New York, Amer. Inst. Mining Metall. Petrol. Eng., p. 605-641.

Westra, G., 1980, The Mount Hope molybdenum prospect (project 2608), Eureka County, Nevada - a progress report: unpubl. report, Exxon Minerals Company, 55 p.

Westra, G., and Keith, S. B., classification and genesis of stockwork molybdenum deposits: Econ. Geol., vol. 76, p. 844-873.

White, W. H., Bookstrom, A. A., Kamilli, R. J., Ganster, M. W., Smith, R. P., Ranta, D. E., and Steininger, R. C., 1981, Character and origin of Climax-type molybdenum deposits: Econ. Geol. 75th Anniv. Vol., p. 270-316.

Winterer, E. L., 1968, Tectonic erosion of the Roberts Mountains, Nevada: J. Geol., vol. 76, p. 347-357.

APPENDIX 1.
1980-81 EXPLORATION DRILLING PROGRAMS

Drilling history

Westra (1980) described Exxon's 1978-79 drilling program at Mount Hope. From March 1980 through September 1981, Exploration completed 14,086 m (46,213 ft) of core drilling on the Mount Hope target and 358 m (1175 ft) of rotary drilling in the Sulphur Springs area (Table 4). Drilling by the Mining Geology group began in August 1981 and has continued without interruption to the present time.

The 1980 Exploration program was planned to search for molybdenum mineralization of grade adequate for bulk underground mining. At that time, we envisioned a molybdenum shell centered near EMH-3, possibly a second shell to the west, and a possible tabular zone of better grade along the southwestern contact of the stock (Westra, 1980, p. 33-34). EMH-5 was located to search for a potential high-grade overlap zone or cone-sheet fracture system, and EMH-6 to test the tabular contact-related zone. Although neither hole intercepted high-grade mineralization, the shallow intercept in EMH-6 first led us to consider an open-pit target. We located EMH-7 and -8 to further test open-pit potential. Both intercepted shallow but low-grade mineralization, with significant molybdenite beginning at 15 m depth in EMH-8.

We then re-evaluated geochemical data from the eastern portion of the deposit, and concluded that the principal molybdenum shell was centered south of EMH-5 and not near EMH-3. EMH-9 tested this area, and, as predicted, encountered better grade mineralization just below the Mount Hope fault. We deepened EMH-4, but failed to find significant mineralization. Finally, we drilled rotary hole ESS-1 into the upper portions of the Sulphur Springs target.

As of the end of the 1980 program, we had encountered a significant tonnage of potentially open-pittable mineralization. After evaluating the data from drilling, we proposed a shell configuration essentially as described herein, with two systems centered near EMH-1 and -9. The possibility of a tabular contact-related zone, however, could not be disproven.

The objectives of the 1981 drilling program were (1) delineation of higher grade mineralization within open-pittable depth; and (2) testing of peripheral areas of the complex. The multi-shell model predicted a high-grade zone of overlap near EMH-2, which EMH-11, -12, and -14 all successfully tested. EMH-16, -17, and -20 intersected mineralization of moderate grade surrounding the overlap zone, and EMH-20 opened up a large area of potential to the southeast. EMH-19, -21, and -22 intercepted lower grade mineralization typical of the western system. EMH-13 was located to extend the open-pit reserve to the east, but encountered the low-grade zone produced by displacement of the eastern system along the Mount Hope fault.

EMH-10 and -18 explored outlying areas. EMH-10 tested the extent of mineralization northeast of EMH-3, and narrowly missed the flank of the eastern system. The structurally controlled mineralization in this hole, however, suggests significant potential still lies to the northeast. EMH-18 tested a hypothesized northern center of mineralization

Table 4. MOUNT HOPE EXPLORATION DRILLING PROGRAMS, 1978-81

Target area	Dates	Drill holes	Amount Drilled meters	feet
MOUNT HOPE	October 1978 - August 1979	EMH-1 through -3 EMH-4 (in part) EPMH-15	3,520	11,548
	March - September 1980	EMH-4 (in part) EMH-5 through -9	3,277	10,750
	March - September 1981	EMH-10 through -14 EMH-16 through -22	7,289	23,915
Total Mount Hope Target	1978-81	EMH-1 through -22	14,086	46,213
SULPHUR SPRINGS	May 1980	ESS-1	358	1,175
TOTAL-PROJECT 2608	1978 - 1981	23 holes	14,444	47,388

suggested by anomalously extensive alteration and sulfides north of EMH-1. EMH-18 appears to have narrowly missed the western system, and found no evidence of the hypothesized northern center.

Sample preparation procedures

In 1978-79, Exxon personnel split all drill core and shipped an entire half-split for analysis. In 1980, we installed a jaw crusher on site and began crushing the split core to approximately 1/2 inch, from which we shipped a one-quarter split. Reproducibility of multiple splits of this 1/2-inch product, however, was unsatisfactory. After thoroughly reviewing our procedures, we concluded that crushing to only 1/2-inch was inadequate to assure homogeneity prior to splitting out a sample for assay. We therefore shipped all the coarse rejects we had prepared on site to Rocky Mountain Geochemical Corporation in Salt Lake City, who crushed this material to -1/8 inch prior to splitting. For all remaining 1980 drilling, we crushed the core to 1/2 inch, and shipped the entire product to Rocky Mountain for fine crushing prior to sampling. This procedure improved reproducibility significantly, and final assays include only analyses of samples prepared in this manner.

Because of the difficulties experienced in 1980, we carefully evaluated our procedure before the 1981 program, and confirmed its validity with Jim Cardwell of Rocky Mountain Geochemical Corporation. We crushed the split core on site to -1/8 inch, using both jaw and roll-type crushers, and then split out one-eighth of the product for shipment. Rocky Mountain then ground the sample to 100 mesh with a Braun pulverizer, split out 150-175 g, and ground this to 200 to 300 mesh with a ring pulverizer. (Finer grinding was found to liberate molybdenite more completely.) The sample was digested in perchloric acid and analyzed with atomic absorption.

We incorporated three types of checks into our 1981 procedures. Internal standard pulps were prepared covering a range from 0.033% to 0.240% molybdenum, and we submitted one or more with each sample batch to check for procedural or calibration errors at the analytical labs. A second one-eighth split was prepared from approximately every tenth sample, and this was submitted without disclosing its identity. Finally, all intercepts of potential ore grade were re-analyzed in their entirety by CMS in Salt Lake City. CMS employs a colorimetric technique for molybbenum, which we feel is more accurate than atomic absorption in the range above 0.1% molybdenum. These checks confirmed the validity of our procedures, the homogeneity of samples, and the care and precision of the labs. Rare discrepancies between labs occurred, but subsequent reanalysis by both labs invariably corrected the discrepancy. Assays reported from 1981 drilling are averages of both Rocky Mountain and CMS analyses, except that values found to be in error were omitted.

APPENDIX 2.
REVISED SKETCH LOGS AND GEOCHEMICAL HISTOGRAMS, EXPLORATION DRILL HOLES

Asterisks indicate known changes from previous lithologic logs. Only actual re-interpretations of lithology are so designated; revisions in nomenclature (as shown on Table 2) are not designated with asterisks.

EMH-1 559,926.5N - 101,138.6E elev. 2334.2m (758.0 ft)

LITHOLOGY

0-287m	0-940 ft	Tqp; cut by dikes of Tqpa at 3, 15, and 168m
287-791	940-2594	Tqpa*; minor autoliths of Tqp
791-874	2594-2867	Tqpc*; cut by dikes of Tgr at 820 and 823m

STRUCTURE

119-125m	390-410 ft	Bisoni fault zone

ALTERATION

0-203m	0-666 ft	Potassic
203-~297	666-~975	High-silica
297-745	975-2445	Potassic
745-874	2445-2867	High-silica

INTERCEPTS

0-168m	0-550 ft	168m (550 ft) of 0.07% Cu
351-689	1150-2260	338m (1110 ft) of 0.061% Mo
533-625	1750-2050	92m (300 ft) of 0.108% Mo
594-686	1950-2250	92m (300 ft) of 173 ppm W

EMH-2 559,767.8N - 101,428.9E elev. 2217m (7274.4 ft)

LITHOLOGY

0-6m	0-20 ft	overburden
6-~ 85	20-~ 280	Trb
85-111	280-363	Ov
111-359	363-1179	Tqp
359-369	1179-1211	Ov
369-469	1211-1539	Tqp; xenolith of Ov at 387-389m
469-490	1539-1609	Ov
490-549	1609-1800	Tqp; xenolith of Ov at 497-499m
549-572	1800-1878	Ovl
572-686	1878-2252	Tqp; cut by dike of Tqpc 664-668m
686-713	2252-2339	Tqpa
713-727	2339-2386	Ovl
727-760	2386-2492	Tqpa
760-833	2492-2734	Tqpc

STRUCTURE

72-80m	237-262 ft	Bisoni fault zone
602-625	1974-2052	Tia fault zone(?)

ALTERATION

6-~ 85m	20-~ 280 ft	Argillic
85-111	280-363	Potassic-phyllic
111-625	363-2052	Potassic
625-727	2052-2386	High-silica
727-833	2386-2734	Biotite

INTERCEPTS

2-122m	6-400 ft	120m (394 ft) of 0.23% Zn
76-823	250-2700	747m (2450 ft) of 0.100% Mo
107-549	350-1800	442m (1450 ft) of 0.128% Mo
229-290	750-950	61m (200 ft) of 0.186% Mo
396-533	1300-1750	137m (450 ft) of 161 ppm W

EMH-3 560,011.0N - 101,874.1E elev. 2271.6m (7452.9 ft)

LITHOLOGY

0-3m	0-10 ft	overburden
3-314	10-1029	Tht_2; cut by Tqp dikes at 150 and 280m
314-351	1029-1151	Tqp
351-361	1151-1184	Ov
361-373	1184-1225	Tqp
373-390	1225-1281	Tht_2(d)
390-456	1281-1495	Tbqp
456-686	1495-2250	Tqp
686-708	2250-2323	Ov
708-822	2323-2698	Tqp; xenoliths of Ov at 710-711 and 720-721m
822-880	2698-2888	Ovl*

STRUCTURE

329-351m	1080-1151 ft	Mount Hope fault zone
404-421	1325-1380	Ravine fault zone

ALTERATION

3-361m	10-1184 ft	Argillic
361-390	1184-1281	Potassic-phyllic
390- ~ 744	1281- ~ 2440	Potassic
744-880	2440-2888	High-silica

INTERCEPTS

76-396m	250-1300 ft	320m (1050) of 0.50% Zn
168-244	550-800	76m (250 ft) of 0.039 oz/T Ag
442-671	1450-2200	229m (750 ft) of 0.097% Mo
448-521	1470-1710	73m (240 ft) of 0.121% Mo

EMH-4 559,525.7N - 101,131.6E elev. 2246.4m (7370.0 ft)

LITHOLOGY

0-5m	0-15 ft	overburden
5-34	15-113	Ovl
34-646	113-2121	Ov; cut by Tqp dikes at 102, 175, and 199-202m

ALTERATION

5- ~ 213m	15- ~ 700 ft	Potassic-phyllic
213-646	700-2121	Potassic

INTERCEPTS

5-46m	15-150 ft	41m (135 ft) of 0.04% Cu
213-610	700-2000	397m (1300 ft) of 0.043% Mo
533-579	1750-1900	46 m (150 ft) of 0.057% Mo
549-610	1800-2000	61m (200 ft) of 155 ppm W

EMH-5 559,852.3N - 101,645.1E elev. 2210.4m (7251.9 ft)

LITHOLOGY

0-1m	0-2 ft	overburden
1-205	2-674	Tht_2
205-232	674-761	Ov; but by Tbdp dike at 208-209m, and by Tqp dike at 218-223m
292-699	761-2294	Tqp; cut by Tgr dikes at 394-395, 600, 603, 607, 624-626, 630-633, and 635-639m
699-730	2294-2394	Tqpa
730-874	2394-2866	Tqpc

STRUCTURE

186-210m	610-690 ft	Mount Hope fault zone
213-256	700-840	Ravine fault zone

ALTERATION

1- ~158m	2- ~520 ft	Argillic
158- ~229	520- ~750	Potassic-phyllic
229-454	750-1490	Potassic
454-707	1490-2320	High-silica
707-874	2320-2866	Biotite

INTERCEPTS

1-61m	2-200 ft	60m (198 ft) of 0.74% Zn
183-874	600-2866	691m (2266 ft) of 0.071% Mo
229-381	750-1250	152m (500 ft) of 0.085% Mo
762-838	2500-2750	76m (250 ft) of 0.095% Mo
640-686	2100-2250	46m (150 ft) of 162 ppm W

EMH-6 559,749.5N - 101,234.1E elev. 2271.2m (7451.3 ft)

LITHOLOGY

0-1m	0-3 ft	overburden
1- ~ 98	3- ~ 320	Tbqp
98-197	320-647	Tqp
197-244	647-799	Tbqp
244-276	799-906	Tqp
276-355	906-1166	Ov; cut by Tqp dike at 289m
355-380	1166-1248	Tqp
380-423	1248-1387	Ov; cut by Tqp dike at 421-422m
423- ~ 546	1387- ~ 1790	Tqp*
546-603	1790-1979	Tqpa
603- ~ 680	1979- ~ 2230	Tqp
680-744	2230-2442	Tqpa; cut by Tgr dike at 732-733m

STRUCTURE

271-287m	890-940 ft	Tia fault zone

ALTERATION

1-443m	3-1455 ft	Potassic
443-685	1455-2246	High-silica
685-744	2246-2442	Biotite

INTERCEPTS

30-107m	100-350 ft	76m (250 ft) of 0.07% Cu
61-671	200-2200	610m (2000 ft) of 0.067% Mo
152-472	500-1550	320m (1050 ft) of 0.081% Mo
323-369	1060-1210	46m (150 ft) of 0.121% Mo
381-442	1250-1450	61m (200 ft) of 166 ppm W

EMH-7 559,997.6N - 101,322.0E elev. 2263.7m (7426.9 ft)

LITHOLOGY

0-5m	0-16 ft	overburden
5- ~189	16- ~620	Tqp; cut by dikes of Tqpa at 119 and 183m; minor autoliths of of Tbqp
189- ~259	620- ~850	Tbqp*
259- ~402	850- ~1320	Tqp
402-606	1320-1988	Tqpa*; cut by dikes of Tgr at 532, 534-536, and 539m

STRUCTURE

500-514m	1640-1685 ft	Bisoni fault zone(?)

ALTERATION

5-392m	16-1285 ft	Potassic
392-524	1285-1720	High-silica
524-541	1720-1775	Potassic
541-606	1775-1988	High-silica

INTERCEPTS

46-122m	150-400 ft	76m (250 ft) of 0.17% Cu
107-606	350-1988	499m (1638 ft) of 0.052% Mo
290-351	950-1150	61m (200 ft) of 0.074% Mo
472-579	1550-1900	107m (350 ft) of 159 ppm W

EMH-8 559,790.8N - 101,005.0E elev. 2339.9m (7676.9 ft)

LITHOLOGY

0-148m	0-485 ft	Ov; cut by Tqp dike at 31-33m and by Tbqp dike at 80-93m
148-211	485-691	Tbqp
211-258	691-847	Ov
258- ~277	847- ~910	Tbqp*
277- ~421	910- ~1380	Tqp
421-557	1380-1826	Tqpa*
557-582	1826-1909	Tqpc
582-593	1909-1944	Tqpa

ALTERATION

0-312m	0-1025 ft	Potassic
312-427	1025-1400	High-silica
427-526	1400-1725	Potassic
526-557	1725-1826	High-silica
557-593	1826-1944	Biotite

INTERCEPTS

15-274m	50-900 ft	259m (850 ft) of 0.061% Mo and 103 ppm W
15-76	50-250	61m (200 ft) of 0.071% Mo

EMH-9 559,582.6N - 101,641.4E elev. 2186.7m (7174.2 ft)

LITHOLOGY

0-4m	0-12 ft	overburden
4-13	12-44	$Tht_2(d)$
13-387	44-1270	Tqp; minor xenoliths of Ov

STRUCTURE

158-192m	520-630 ft	Mount Hope fault zone

ALTERATION

4-61m	12-200 ft	Argillic
61-165	200-540	Potassic-phyllic
165-346	540-1135	Potassic
346-387	1135-1270	High-silica

INTERCEPTS

61-168m	200-550 ft	107m (350 ft) of 0.13% Cu and 0.13% Zn
152-381	500-1250	229m (750 ft) of 0.086% Mo
168-229	550-750	61m (200 ft) of 0.126% Mo

EMH-10 560,250.4N - 101,970.7E elev. 2253.8m (7394.3 ft)

LITHOLOGY

0-2m	0-7 ft	overburden
2- ~43	7- ~140	Tht_3
43- ~158	140- ~520	Tht_3(d)
158-442	520-1451	Tht_2
442-483	1451-1584	Tbqp; cut by dike of Tqpa at 472-478m
483-534	1584-1752	Tht_2; cut by dikes of Tbqp at 493-502 and 514-526m
534-552	1752-1811	Ov; cut by dike of Tbqp at 538-541m, and by Tqp dikes at 543-546 and 550m
552-576	1811-1890	Tqpa*
576-815	1890-2674	Ov; cut by Tgr dikes at 805 and 808m

STRUCTURE

326-341m	1070-1120 ft	Mount Hope fault zone(?)
482-591	1580-1940	Ravine fault zone (probably split into several splays at depth)

ALTERATION

2-514m	7-1687 ft	Argillic
514-815	1687-2674	Potassic-phyllic

INTERCEPTS

258-425m	845-1395 ft	167m (550 ft) of 0.29% Zn
517-578	1695-1895	61m (200 ft) of 0.095% Mo
547-575	1795-1885	28m (90 ft) of 0.161% Mo

EMH-11 559,633.7N - 101,509.0E elev. 2189.4m (7183.1 ft)

LITHOLOGY

0-3m	0-11 ft	Ov
3-17	11-57	Trb
17-28	57-93	Tqp
28-90	93-294	Ov; but by Tbqp dike at 64-71m
90-175	294-575	Tqp; xenolith of Ov at 112-115m
175-207	575-679	Ov; cut by Tqp dike at 204m
207-515	679-1689	Tqp; xenolith of Ov at 446-461m
515-656	1689-2151	Ov; cut by Tqp dikes at 528-542, 550-556, and 588-602m; cut by Tqpc dikes at 578-581, 602-619, 650, 651, 652, and 654m
656-717	2151-2351	Tqp; cut by numerous Tqpc dikes (e.g., 667-668, 671-672, and 697m)

STRUCTURE

61-67m	200-220 ft	Mount Hope fault zone(?)
110-119	360-390	Tia fault zone

ALTERATION

3- ~43m	11- ~140 ft	Argillic
43-116	140-380	Potassic-phyllic
116- ~579	380- ~1900	Potassic
579-717	1900-2351	High-silica

INTERCEPTS

3-101m	11-331 ft	98m (320 ft) of 0.07% Cu
116-710	381-2331	594m (1950 ft) of 0.113% Mo
192-269	631-881	77m (250 ft) of 0.188% Mo

EMH-12 559,636.9N - 101,388.1E elev. 2205.4m (7235.7 ft)

LITHOLOGY

0-4m	0-12 ft	overburden
4-16	12-53	Ov; cut by dike of Tgr* at 11-12m
16-25	53-83	Tqp
25-28	83-93	Ov
28-185	93-607	Tbqp
185-472	607-1547	Ov
472-531	1547-1741	Ovl*

STRUCTURE

50-69m	165-225 ft	Tia fault zone

ALTERATION

4-27m	12-90 ft	Potassic-phyllic
27-531	90-1741	Potassic

INTERCEPTS

4-72m	12-235 ft	68m (223 ft) of 0.05% Cu
59-531	195-1741	472m (1546 ft) of 0.122% Mo
184-300	605-985	116m (380 ft) of 0.163% Mo
376-531	1235-1741	215m (706 ft) of 0.042% W

EMH-13 559,579.2N - 101,817.2E elev. 2149.2m (7051.2 ft)

LITHOLOGY

0-3m	0-11 ft	overburden
3-7	11-22	Trb
7-19	22-62	Tqp
19-66	62-217	Ov; cut by Tqp dikes at 31-35 and 52-55m, and by Trb dikes at 35-41 and 44-50m
66-79	217-259	Tqp
79-265	259-869	Ov; cut by Tqp dikes at 98-102 and 203-204m, by Tqpa* dike at 139-143m, and by Tbqp* dike at 179-180m
265-295m	869-967 ft	Tqp
295-342	967-1123	Tqpa
342- ~384	1123- ~1260	Tqp
384-466	1260-1529	Tqpa*

STRUCTURE

49-56m	160-185 ft	Lorraine fault zone
223-265	730-870	Mount Hope fault zone

ALTERATION

3-53m	11-175 ft	Argillic
53-137	175-450	Potassic-phyllic
137-283	450-930	Potassic
283-466	930-1529	High-silica

INTERCEPTS

61-152m	200-500 ft	91m (300 ft) of 0.26% Zn
363-466	1190-1529	103m (339 ft) of 0.083% Mo

EMH-14 559,867.9N - 101,503.5E elev. 2227.4m (7307.6 ft)

LITHOLOGY

0-5m	0-16 ft	overburden
5-157	16-515	Tht_2; cut by Tqp dike at 123-133m
157-490	515-1607	Tqp; autolith of Tbqp* at 171-175m
490-522	1607-1714	Ov, cut by Tqp dike at 491m
522-534	1714-1753	Tqp
534-552	1753-1810	Ov; cut by Tqp dike at 545-547m
552-651	1810-2135	Tqp; xenolith of Ov at 574-579m; xenolith of Tbqp at 579-585m
651-672	2135-2204	Tqpa

STRUCTURE

113-162m	370-530 ft	Mount Hope fault zone
213-226	700-740	Ravine fault zone
408-418	1340-1370	Bisoni fault zone(?)

ALTERATION

5-131m	16-430 ft	Argillic
131-157	430-515	Potassic-phyllic
157-651	515-1810	Potassic
651-672	1810-2204	High-silica

INTERCEPTS

91-168m	300-550 ft	77m (250 ft) of 0.14% Zn
137-564	450-1850	427m (1400 ft) of 0.116% Mo
213-305	700-1000	92m (300 ft) of 0.151% Mo
488-549	1600-1800	61m (200 ft) of 199 ppm W

EPMH-15 559,673.0N - 102,263.1E elev. 2182.2m (7159.3 ft)

0-12m	0-41 ft	overburden
12-45	41-149	Tht_3* (limits of densely welded zone uncertain because of sparse thin section control)
45-63	149-207	Trb
63-172	207-564	Tht_2*
172-185	564-607	Trb
185- ~372	607- ~1220	Tht_2*
372-393	1220-1290	Tht_2(d)
393- ~411	1290- ~1350	Tbqp
411-959	1350-3146	Tqp

STRUCTURE

577-579m	1892-1900 ft	Mount Hope fault zone(?)

ALTERATION

14-393m	41-1290 ft	Argillic
393-959	1290-3146	Potassic

INTERCEPTS

335-396m	1100-1300 ft	61m (200 ft) of 0.11% Cu
488-959	1600-3146	471m (1546 ft) of 0.088% Mo
655-959	2150-3146	304m (996 ft) of 0.108% Mo

EMH-16 559,824.7N - 101,370.5E elev. 2253.0m (7391.7 ft)

LITHOLOGY

0-5m	0-17 ft	overburden
5-299	17-980	Tqp
299-317	980-1039	Ov
317-655	1039-2150	Tqp; cut by Tqpa* dike at 385m; minor Ov xenoliths
655-748	2150-2455	Tqpa; but by Tqpc dike at 726-727m

STRUCTURE

76-81m	250-265 ft	Bisoni fault zone
668-686	2190-2250	Tia fault zone(?)

ALTERATION

5-329m	17-1080 ft	Potassic
320-527	1080-1730*	High-silica
527-597	1730-1960*	Potassic (local silica flooding)
597-748	1960-2455	High-silica

INTERCEPTS

46-107m	150-350 ft	61m (200 ft) of 0.05% Cu
61-610	200-2000	549m (1800 ft) of 0.094% Mo
283-381	930-1250	98m (320 ft) of 0.119% Mo
442-549	1450-1800	107m (350 ft) of 209 ppm W

EMH-17 559,522.6N - 101,446.7E elev. 2180.3m (7153.1 ft)

LITHOLOGY

0-3m	0-11 ft	overburden
3- ~596	11- ~1955	Ov; cut by Tqp dikes at 52-56, 99, 211-213, 225-227, 234-236, 239-241, 242, 244, 292-294, and 320m; cut by Tgr dikes at 377, 378, and 381m
596-702	1955-2305	Ovl; cut by Tqpc dikes at 631-632, 654-655, and 665-670m; cut by Tqpa dikes at 691-695 and 698m

ALTERATION

3- ~ 98m	11- ~ 320 ft	Potassic-phyllic
98- ~ 597	320- ~ 1960	Potassic
597- ~ 683	1960- ~ 2240	High-silica
683-702	2240-2305	Potassic

INTERCEPTS

137-640m	450-2100 ft	503m (1650 ft) of 0.098% Mo
381-472	1250-1550	91m (300 ft) of 0.133% Mo

EMH-18 560,563.0N - 101,017.2E elev. 2505.9m (8221.5 ft)

LITHOLOGY

0-39m	0-128	Tht_2
39- ~82	128- ~270	Tht_2(d)
82-269	270-884	Tht_1; cut by Trb dikes at 117and 161 167m; xenolith of Ov at 259-260m
269-274	884-898	Tbqp*
274-287	898-943	Trb
287-356	943-1167	Tqp; xenolith of Tbqp at 305-310m
356-392	1167-1285	Tht_1
392-404	1285-1325	Tbqp
404-693	1325-2275	Tqp

STRUCTURE

0-177m	0-580 ft	Ravine fault zone

ALTERATION

0-287m	0-943 ft	Argillic
287-693	943-2275	Potassic-phyllic

INTERCEPTS

335-427m	1100-1400 ft	92m (300 ft) of 0.04% Cu
351-693	1150-2275	342m (1125 ft) of 0.023% Mo
655-693	2150-2275	38m (125 ft) of 0.039% Mo

EMH-19 559,680.8N - 101,104.1E elev. 2277.5m (7472.2 ft)

0-6m	0-19 ft	overburden
6-443	19-1452	Ov; cut by Tbqp dikes at 64-65, 67, and 68-69m; cut by Tqp dikes at 354-357 and 424m
443- ~469	1452- ~1540	Tqp
469-579	1540-1901	Tqpa; cut by Tqpc dike at 548m
579-616	1901-2021	Tqpc*

STRUCTURE

6-30m	19-100 ft	Tia fault zone

ALTERATION

6-456m	19-1495 ft	Potassic
456-530	1495-1740	High-silica
530-579	1740-1901	Potassic
579-616	1901-2021	Biotite

INTERCEPTS

61-610m	200-2000 ft	549m (1800 ft) of 0.048% Mo
76-198	250-650	122m (400 ft) of 0.060% Mo
518-610	1700-2000	92m (300 ft) of 0.077% Mo
518-616	1700-2021	98m (321 ft) of 211 ppm W

EMH-20 559,485.6N - 101,547.1E elev. 2161.6m (7091.9 ft)

LITHOLOGY

0-10m	0-34 ft	overburden
10-544	34-1785	Ov; cut by Tqp dikes at 31-32, 65-70, 156, and 370-375m; cut by Tgr dikes at 340, 341-342, and 342m; cut by Tqpa dikes at 362-364, 366, 368, and 375-386m
544-636	1785-2088	Ovl; cut by Tqpa dike at 588-591m; cut by Tgr dike at 625m

ALTERATION

10-104m	34-430 ft	Potassic-phyllic
104-381	340-1250	Potassic
381-636	1250-2088	High-silica

INTERCEPTS

46-107m	150-350 ft	61m (200 ft) of 0.14% Cu
122-366	400-1200	244m (800 ft) of 0.117% Mo
314-363	1030-1190	49m (160 ft) of 0.172% Mo
442-518	1450-1700	76m (250 ft) of 155 ppm W

EMH-21 560,174.2N - 101,117.4E elev. 2348.5m (7705.0 ft)

LITHOLOGY

0-10m	0-33 ft	overburden
10-329	33-1080	Tqp; cut by Tqpa* dikes at ~80-98, 127, 184, 213, and 234m (locations of Tqpa noted in thin section, not core; may be more extensive)

STRUCTURE

10-73m	33-240 ft	Ravine fault zone

ALTERATION

10-329m	33-1080 ft	Potassic

INTERCEPTS

152-229m	500-750 ft	77m (250 ft) of 0.06% Cu
198-305	650-1000	107m (350 ft) of 0.036% Mo

EMH-22 560,100.2N - 100,940.8E elev. 2424.3m (7953.6 ft)

LITHOLOGY

0-363m	0-1192 ft	Tqp; cut by Tqpa dikes at 236 and 313m

ALTERATION

0-363m	0-1192 ft	Potassic

INTERCEPTS

61-363	200-1192 ft	302m (992 ft) of 0.043% Mo
61-122	200-400	61m (200 ft) of 0.066% Mo

ESS-1 560,686N - 105,183E elev. 2031 m (6663 ft)

LITHOLOGY

0-2m	0-8 ft	overburden
2-358	8-1175	Ov

ALTERATION

2- ~ 200 m	8- ~ 650 ft	Weak hornfels (weak argillic-propylitic?)
200-358	650-1175	Biotite hornfels (argillic?)

INTERCEPTS

2-107 m	8-350 ft	105 m (342 ft) of 0.1% Cu
46-107	150-350	61 m (200 ft) of 0.1% Zn

APPENDIX 3.
SPECIFIC GRAVITY OF MOUNT HOPE ORE

Determinations of specific gravity by Jolly balance were made at the conclusion of the 1980 drilling program. Densities of representative samples were measured from every 200 feet (61 m) of better-grade mineralization:

Quartz porphries	(35 analyses)	2.59 g/cm^3
Vinini hornfels	(5 analyses)	2.76
Mount Hope Tuff	(1 analysis)	2.12
Average	(41 analyses)	2.60 g/cm^3

APPENDIX 4.
METHOD OF VISUALLY ESTIMATING MOLYBDENUM CONTENT OF DRILL CORE

Over the course of the 1980 and 1981 seasons, we evolved a useful empirical method for estimating molybdenum grade of drill core. Because the method involves simply counting mineralized veinlets, it is readily learned and quite reproducible between geologists. Grade is determined by summing contributions of each mineralized veinlet intercepted in five feet (1.524 m) of drill core:

Hairline or poorly mineralized veinlets	25 ppm Mo
Average veinlets (0.5-2.0 mm thick)	50 ppm Mo
Thick or unusually rich veinlets	100 ppm Mo
Gaudy veins (> 10 mm thick and well mineralized) ...	200 ppm Mo

Veinlets at low angle to the core axis are counted a second time if their intercepted length exceeds three core diameters.

PHOTOS 1 - 40

PHOTO 1. Chip specimens illustrating Paleozoic sedimentary rock types.

Ov: Vinini Formation, chocolate brown quartz-K-feldspar-biotite hornfels. EMH-17, 397m depth.

Ovl: Vinini Formation, calc-silicate hornfels of limy marker bed. EMH-17. 673m.

Pg: Garden Valley Formation, wollastonite-bearing marble. Surface sample from outcrop at the Lorraine workings.

PHOTO 2: Chip specimens illustrating igneous rock types.

Tqmp: Biotite quartz monzonite porphyry. Surface sample, 800m west of Mount Hope summit.

Tqpe: Autolith of early quartz porphyry (circled) in Mount Hope Tuff. EMH-14, 24m. See also photo 39.

Tht_1: Lower cooling unit of Mount Hope Tuff. EMH-18, 200m.

Tht_2: Middle cooling unit of Mount Hope Tuff. EMH-10, 306m.

Tht_3: Upper cooling unit of Mount Hope Tuff. Note common white lenses of partially collapsed pumice. EMH-10, 25m.

Trb: Rhyolite vent breccia containing xenoliths of gray Vinini siltstone. EMH-18, 166m.

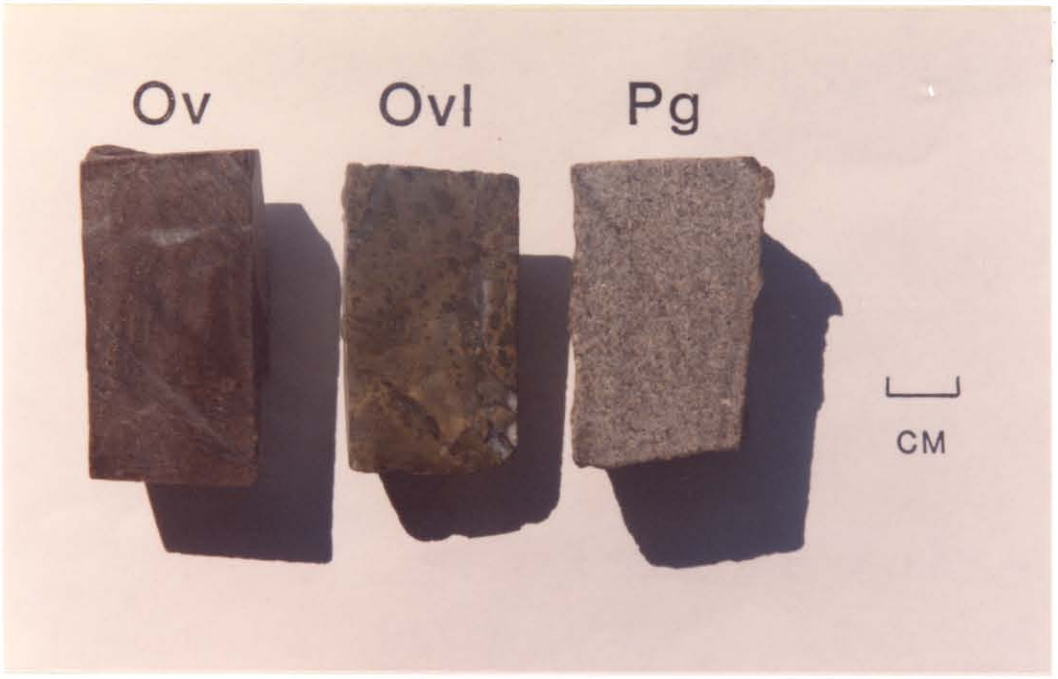

(1)

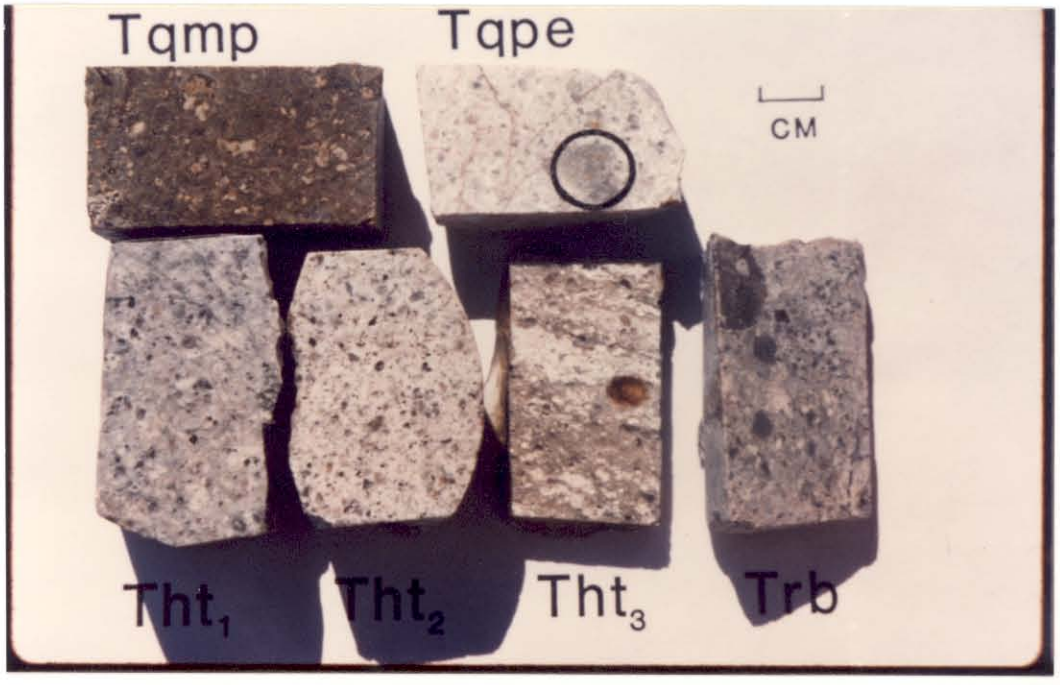

(2)

PHOTO 3. Chip samples illustrating igneous rock types.

Tqt: Quartz-eye tuff. Surface sample, 305m south-southwest of drill hole A-1.

Tbqp: Quartz porphyry border phase. EMH-6, 16m.

Tqp: Quartz porphyry. EMH-22, 313m.

Tqpa: Aplitic quartz porphyry. Pale green sericitic alteration accentuates very fine granularity of groundmass. Texture partially obscured by gray silica flooding. EMH-6, 744m.

PHOTO 4. Chip samples illustrating igneous rock types.

Tqpc: Coarse-grained quartz porphyry. EMH-5, 733m.

Tgr: Fine-grained granite. EMH-6, 732m.

Tbx: Quartz porphyry breccia. Surface sample, 245m east-southeast of EMH-18.

Tdp: Dacite porphyry. Surface sample, 700m northeast of EMH-10.

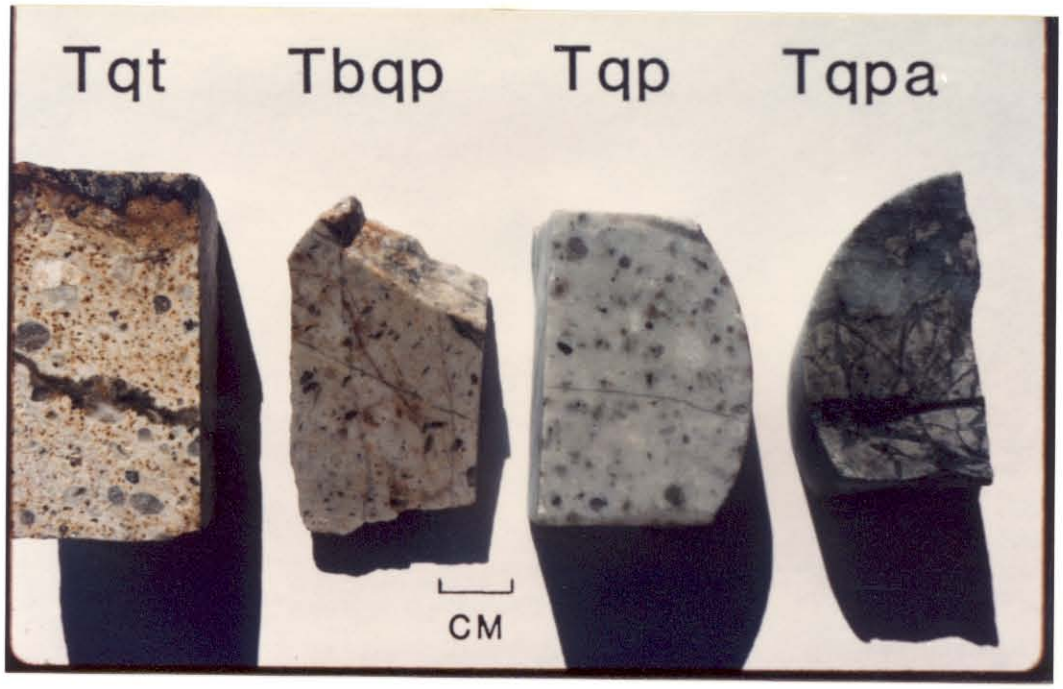

(3)

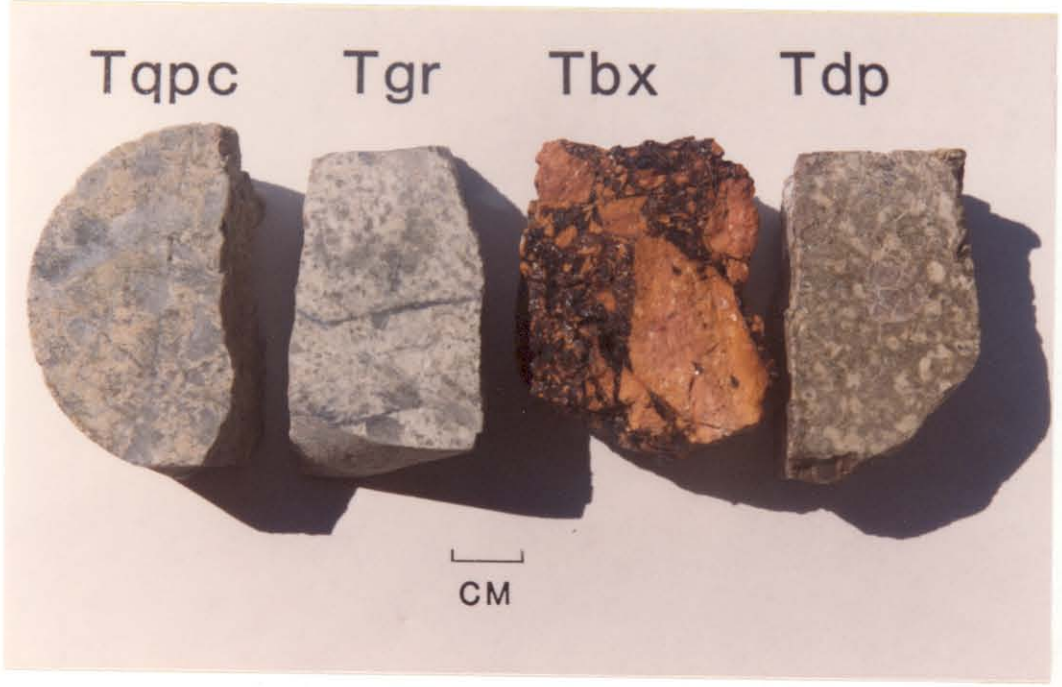

(4)

PHOTO 5. Photomicrograph of biotite quartz monzonite porphyry. Phenocrysts of andesine (lower right), quartz (left center), K-feldspar (upper right), and biotite (top center and upper left) in a fine-grained groundmass. Surface sample, 800m west-southwest of Mount Hope summit. Crossed nicols.

PHOTO 6. Photomicrograph of autolith of early quartz porphyry (right three-fifths of photo) in Mount Hope Tuff. Porphyry contains subhedral to broken K-feldspar and quartz phenocrysts. EMH-18, 244m. K-feldspar stained yellow. Crossed nicols.

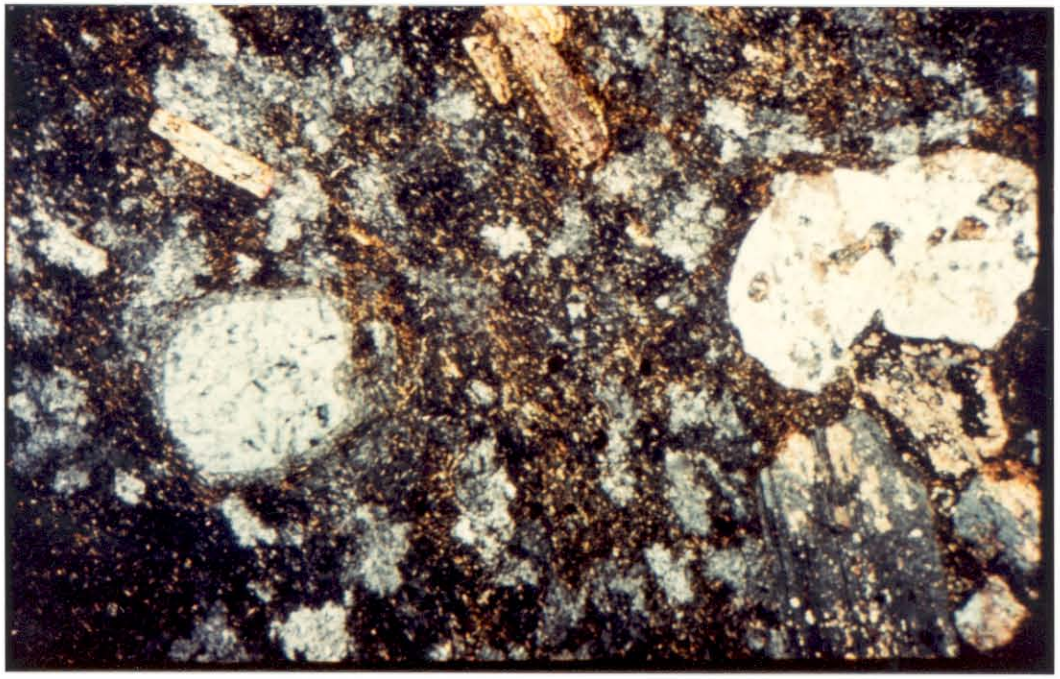

(5)

0.5 mm

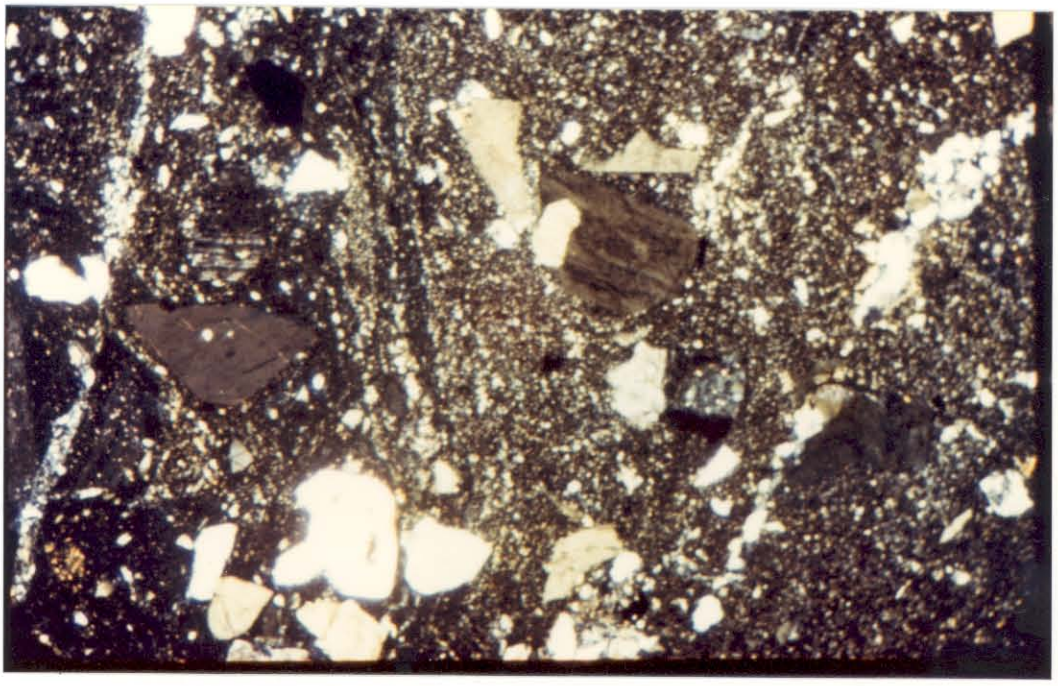

(6)

0.5 mm

PHOTO 7. Photomicrograph of Mount Hope Tuff; partially welded zone of the middle cooling unit. Note angular quartz and altered feldspar phenocrysts. Dark area at lower right is a partially collapsed pumice fragment. Note that density of phenocrysts is far greater in groundmass than in pumice. EMH-10, 243m. Crossed nicols.

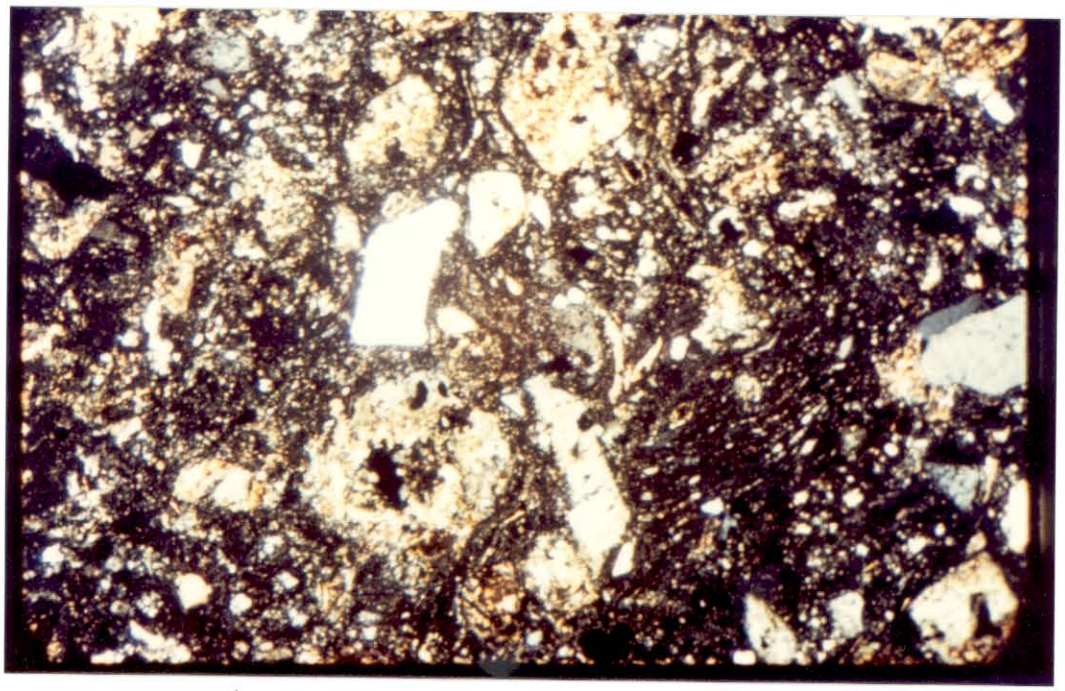

(7)

0.5 mm

PHOTO 8. Photomicrograph of Mount Hope Tuff; partially welded zone of upper cooling unit. Irregular light-colored areas are pumice fragments, here replaced by sericite and clay. Note both broken and rounded quartz phenocrysts. EMH-10, 10m. Crossed nicols.

PHOTO 9. Photomicrograph of Mount Hope Tuff; densely welded zone of upper cooling unit. Pumice fragments (dark areas containing patches of sericite) are collapsed and stretched around phenocrysts. Axial ratios of pumice fragments commonly greater than 8:1. EMH-10, 151m. Crossed nicols.

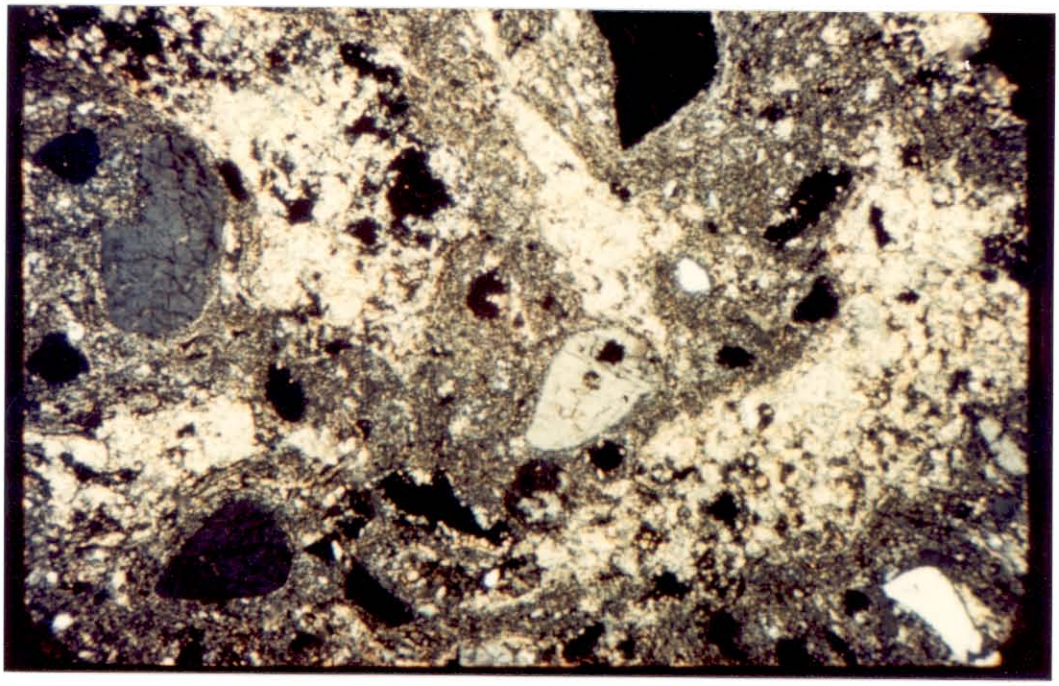

(8)

0.5 mm

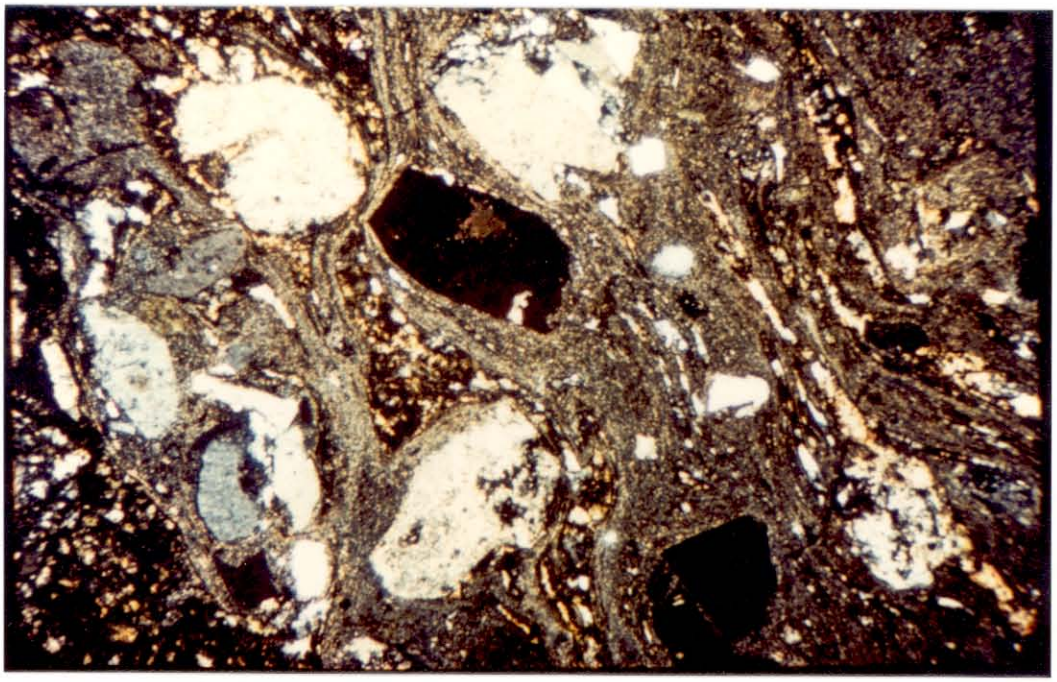

(9)

0.5 mm

PHOTO 10. Photomicrograph of rhyolite vent breccia. Xenoliths of Vinini siltstone at right. Note broken quartz and plagioclase phenocrysts and very fine-grained groundmass without shard structure. EMH-18, 166m. Crossed nicols.

PHOTO 11: Photomicrograph of quartz-eye tuff. Rounded quartz phenocrysts in a groundmass containing lensoid pumice fragments and shards. Surface sample, 305m south-southwest of drill hole A-1. Crossed nicols.

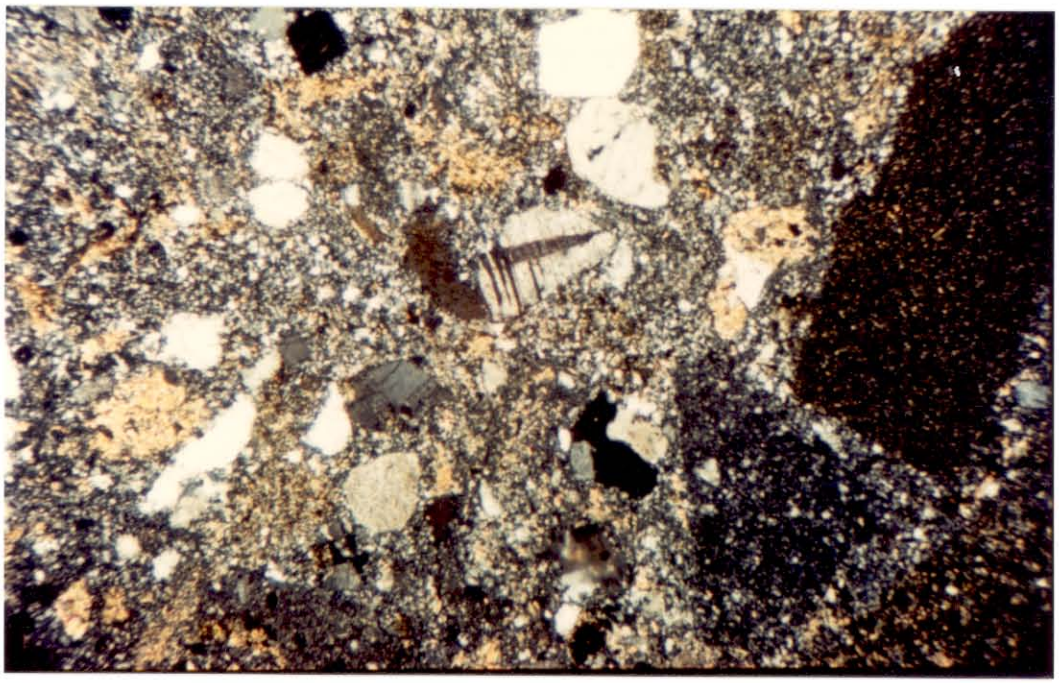

(10)

0.5 mm

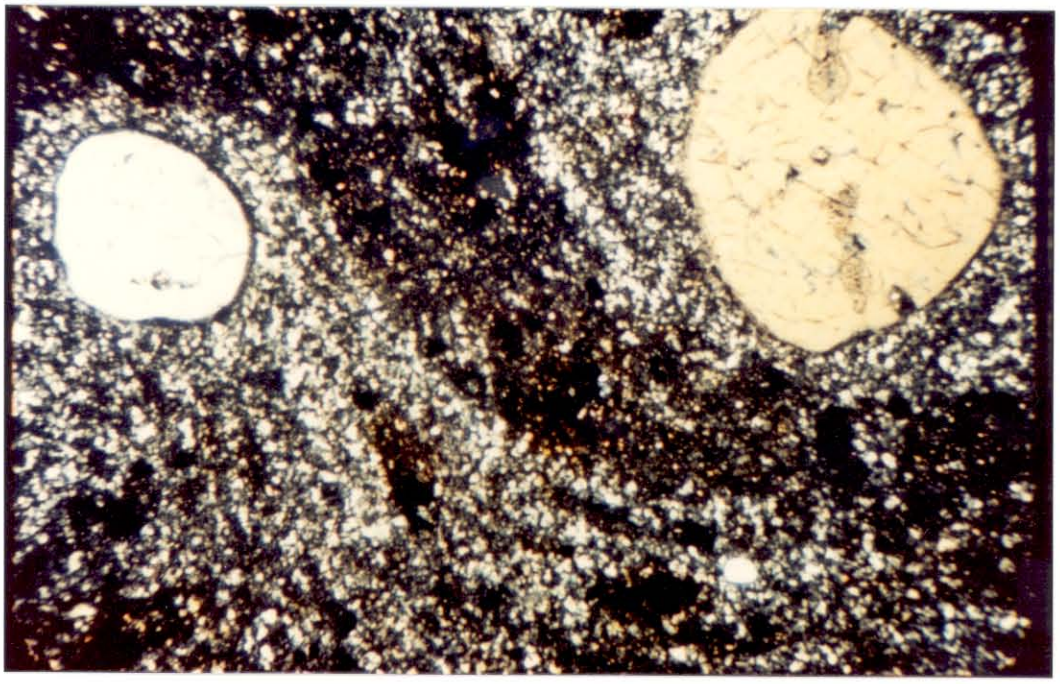

(11)

0.5 mm

PHOTO 12. Photomicrograph of quartz porphyry border phase. Subhedral to broken quartz and K-feldspar phenocrysts, with a xenolith of Vinini biotite hornfels (bottom) in a very fine aphanitic groundmass. EMH-8, 169m. Crossed nicols.

PHOTO 13. Photomicrograph showing contact between quartz porphyry (right and center; groundmass grains $\leqslant$0.05mm) and aplitic quartz porphyry (lower left; groundmass grains 0.08-0.2mm). K-feldspar stained yellow. EMH-7, 183m. Crossed nicols.

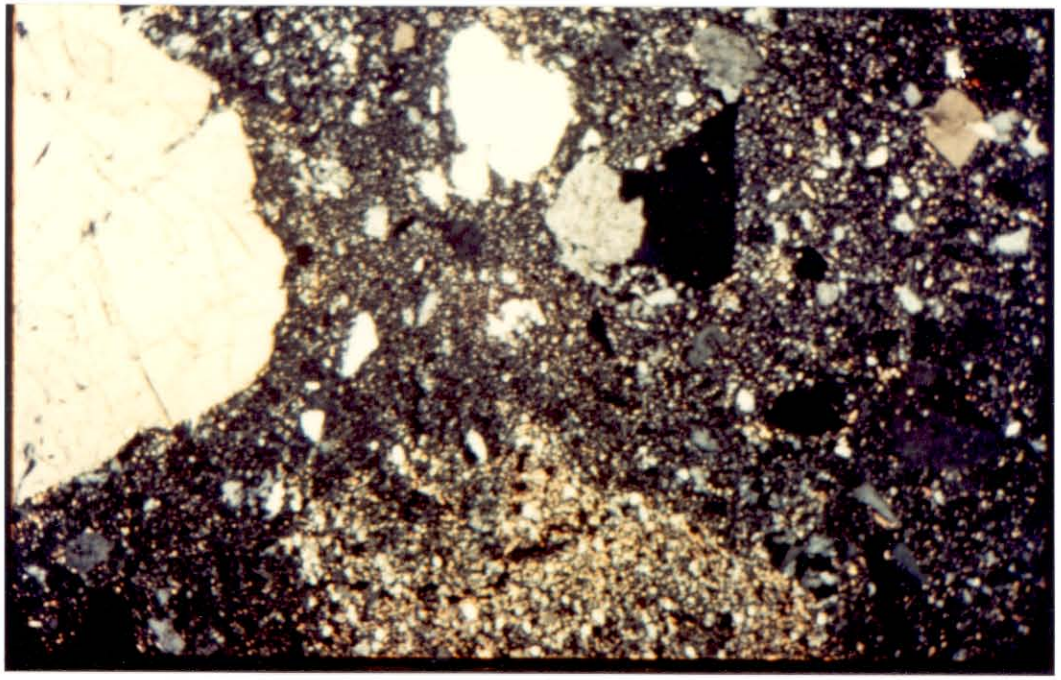

(12)

0.5 mm

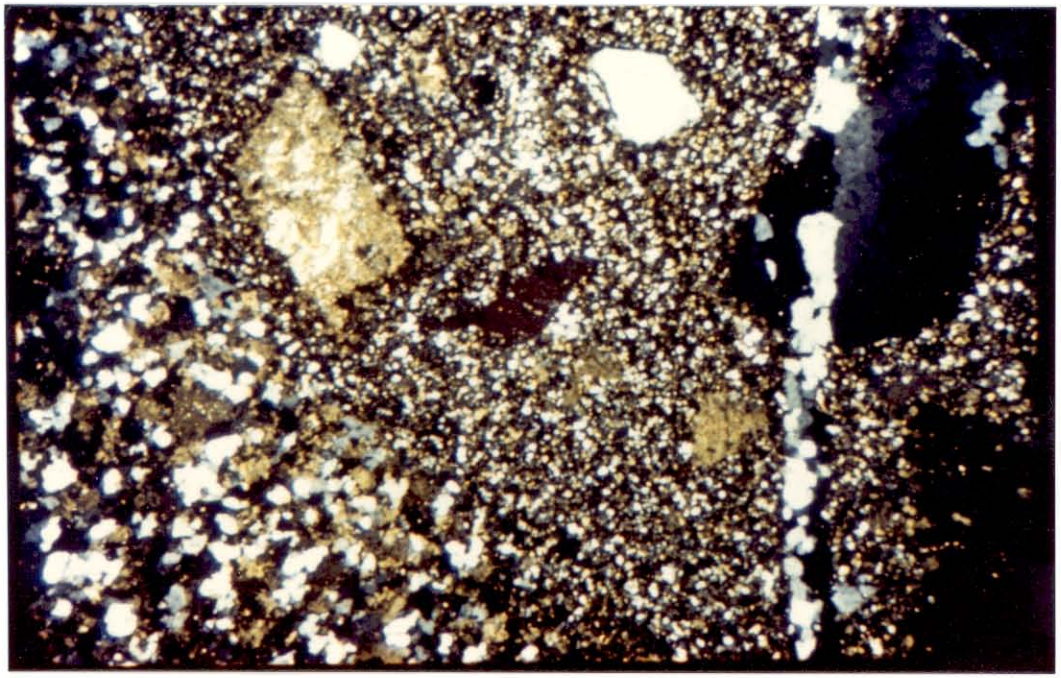

(13)

0.5 mm

PHOTO 14. Photomicrograph of coarse-grained quartz porphyry. Phenocrysts of quartz (top center and lower left), altered biotite (bottom center) and argillized plagioclase (right) in a fine-grained aplitic groundmass. EMH-5, 794m. Crossed nicols.

PHOTO 15. Photomicrograph of fine-grained granite showing "crowded" porphyritic texture of quartz and K-feldspar grains. K-feldspar stained yellow. EMH-5, 394m. Crossed nicols.

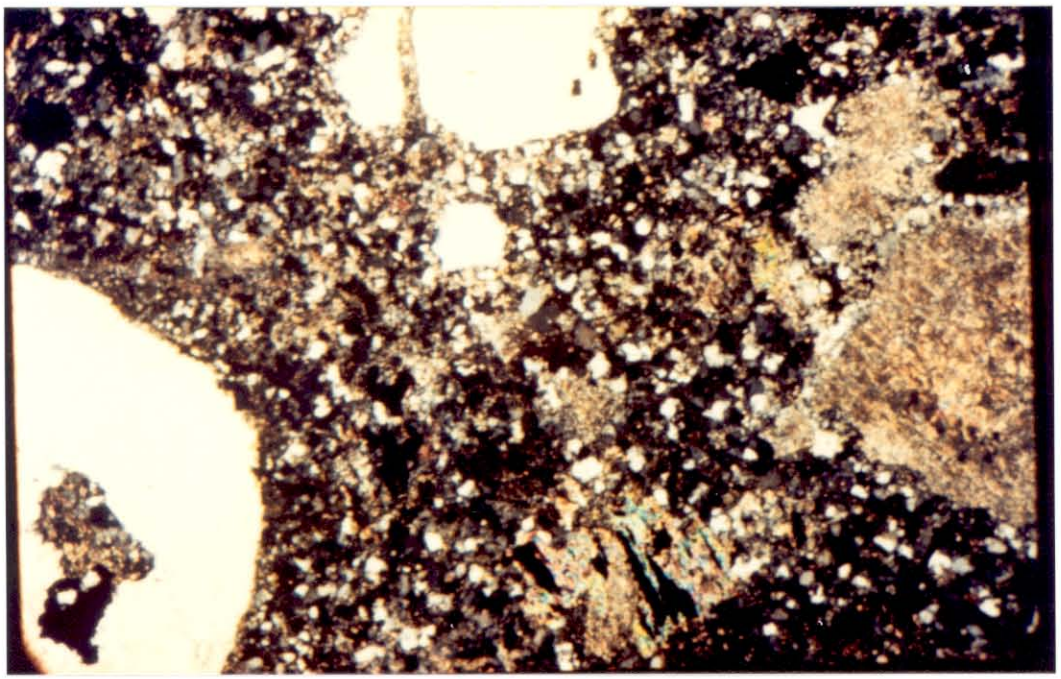

(14)

0.5 mm

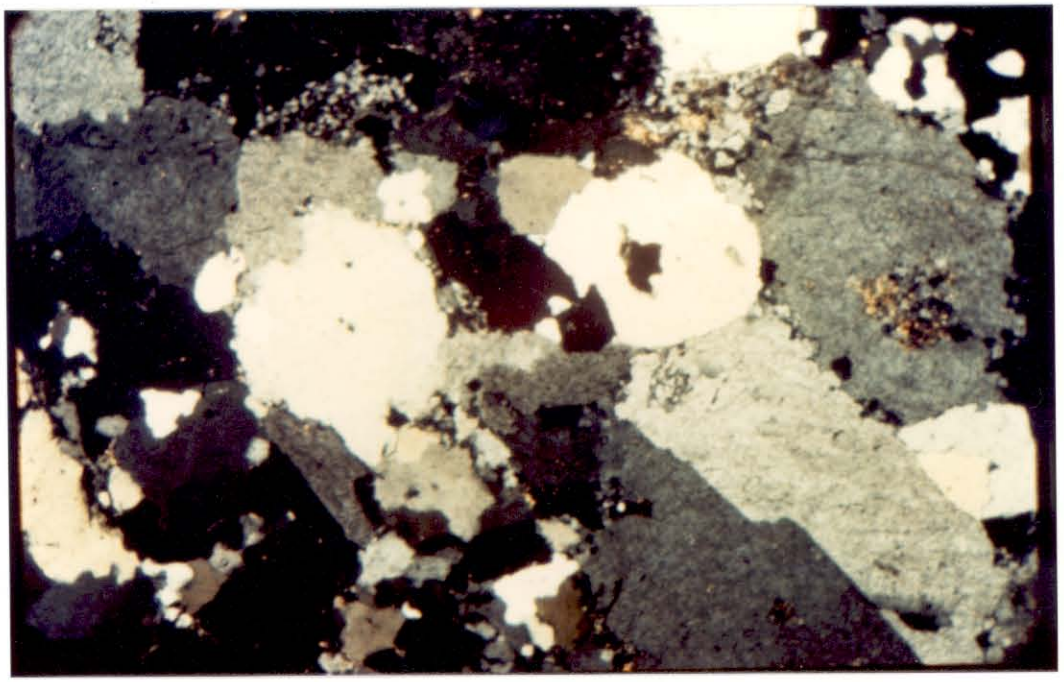

(15)

0.5 mm

PHOTO 16. Photomicrograph of dacite porphyry. Large quartz (lower left), oligoclase-andesine (upper left) and biotite (upper right) phenocrysts in an aphanitic to fine aplitic groundmass. Surface sample, 1700m northwest of September Morn Peak. Crossed nicols.

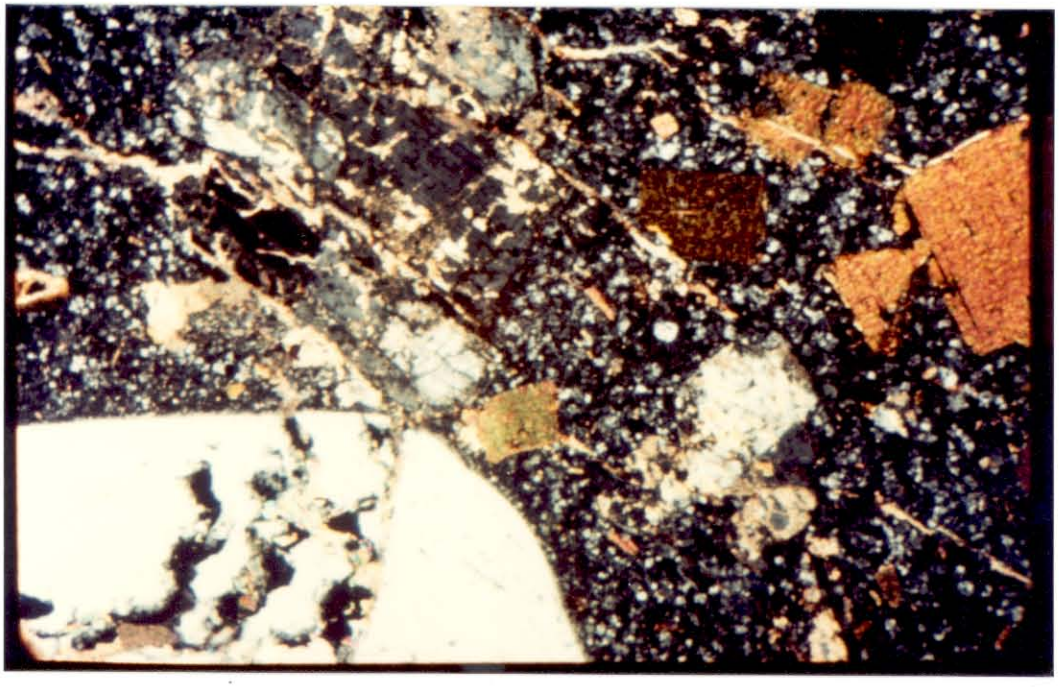

(16)

0.5 mm

PHOTO 17. Chip specimens illustrating alteration zones.

PROPYLITIC: Dacite porphyry of the weak argillic-propylitic zone. Surface sample, 700m northeast of EMH-10.

ARGILLIC: (a): Quartz porphyry. "Bughole" texture due to rapid weathering of argillized plagioclase. Note fresh K-feldspar. Surface sample, 640m east-northeast of Mount Hope summit.

(b): Mount Hope Tuff. EMH-14, 104m.

POTASSIC-PHYLLIC: Quartz porphyry. Note sheeted quartz veinlets and pale green-gray selvage containing quartz and sericite at upper right. K-feldspar stained yellow. Surface sample, 198m south of EMH-8.

PHOTO 18. Chip specimens illustrating alteration zones.

POTASSIC: Quartz porphyry. Note "ceramic" appearance of whitish groundmass, and thin white K-feldspar selvage along thickest quartz vein. EMH-6, 183m.

HIGH-SILICA (a): Quartz porphyry. EMH-9, 367m.
(b): Vinini hornfels. Note nebulous gray patches of silica flood. EMH-20, 425m.

BIOTITE: Coarse-grained quartz porphyry. Note distinct mafic sites, fresh K-feldspar phenocrysts, and pale green sericite-clay after plagioclase and in groundmass. EMH-5, 762m.

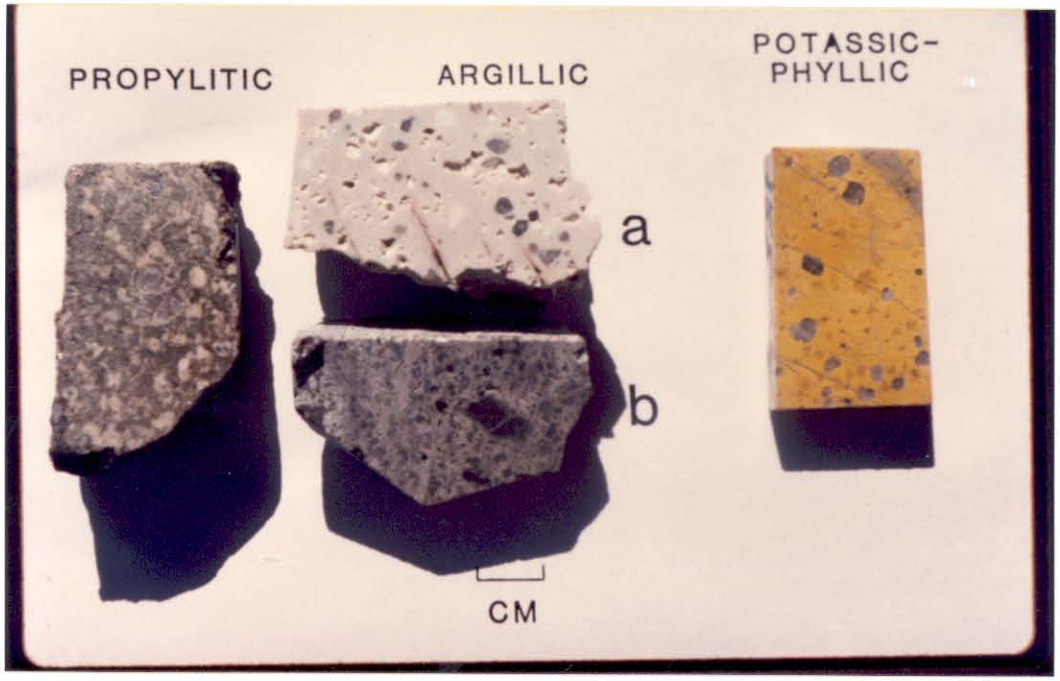
PROPYLITIC
ARGILLIC
POTASSIC-
PHYLLIC
a
b
CM

(17)

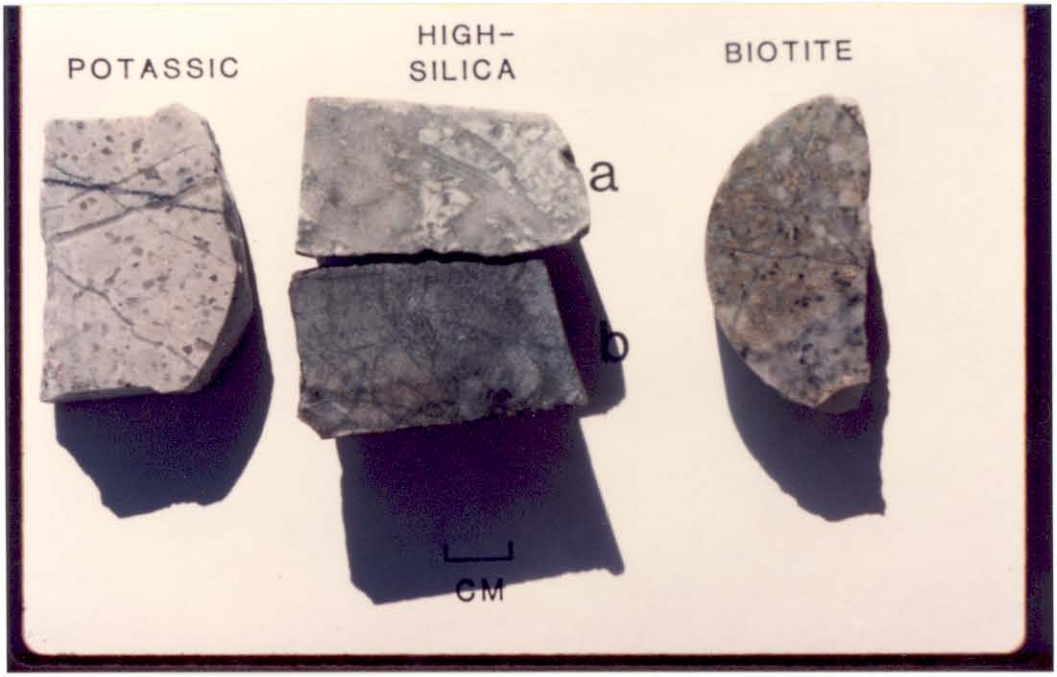
POTASSIC
HIGH-
SILICA
BIOTITE
a
b
CM

(18)

PHOTO 19. Photomicrograph of propylitized dacite porphyry of the weak argillic-propylitic zone. Clay and supergene sericite after plagioclase (right); lenses of chlorite in biotite (center). Surface sample, 700m northeast of EMH-10. Crossed nicols.

PHOTO 20. Photomicrograph of argillized quartz porphyry. Fresh K-feldspar (left); clay and supergene sericite replacing plagioclase (right). Surface sample, 640m east-northeast of Mount Hope summit. Crossed nicols.

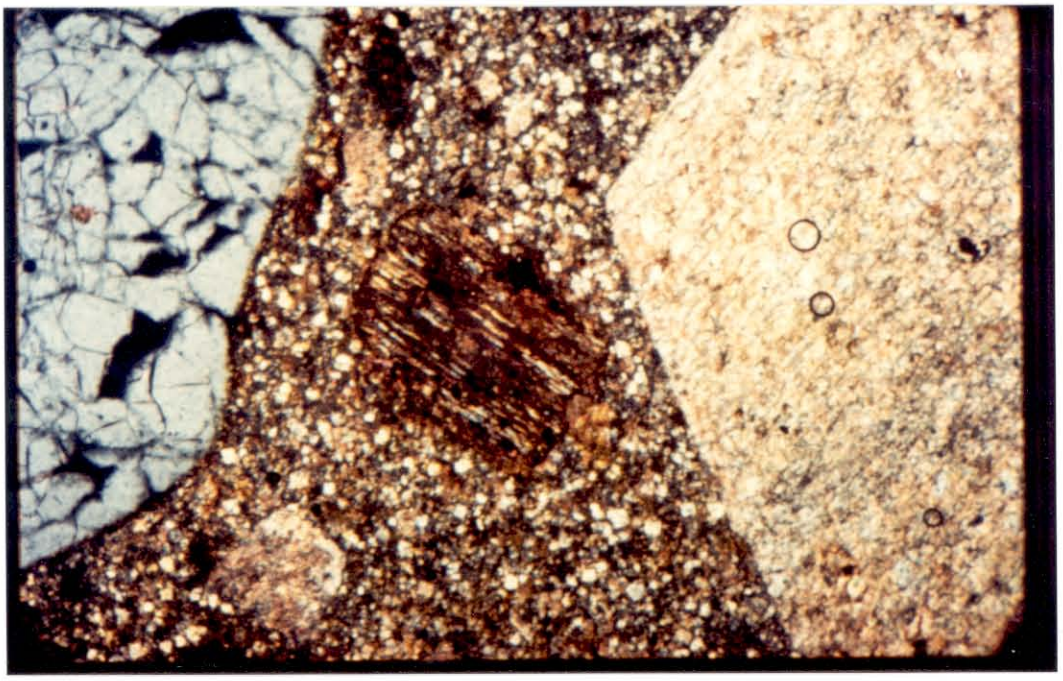

(19)

0.5 mm

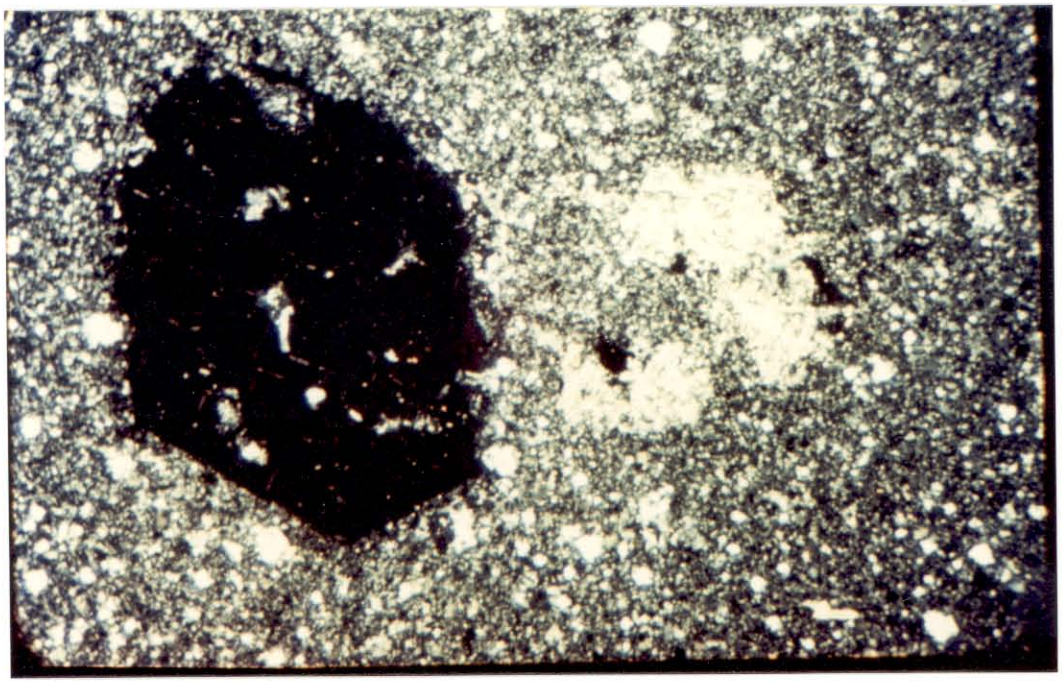

(20)

0.5 mm

PHOTO 21. Orbicular alteration aggregates in argillized Mount Hope Tuff. Orbicles consist of clays, carbonates, minor sericite, with pyrrhotite and sphalerite. EMH-5, 164m.

PHOTO 22. Photomicrograph of zoned orbicular alteration aggregate in Mount Hope Tuff. Rim of orbicle contains carbonates, sulfides, minor clay, and relict quartz phenocrysts. In core of orbicle (far left), sulfides are more abundant and primary rock texture is destroyed. EMH-14, 51m. Crossed nicols.

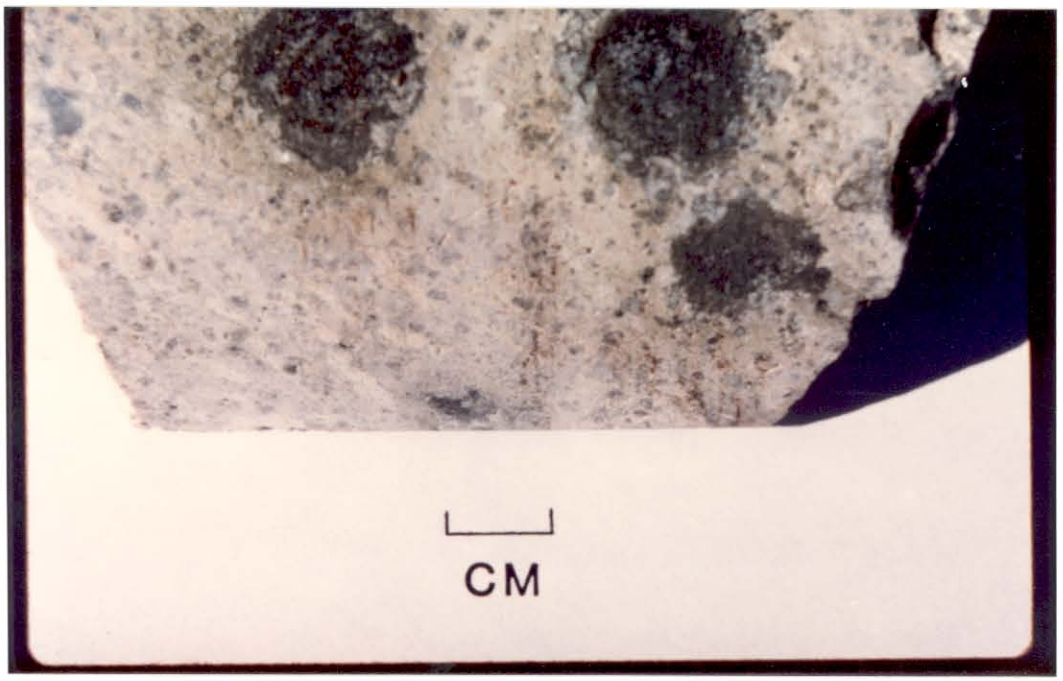

(21)

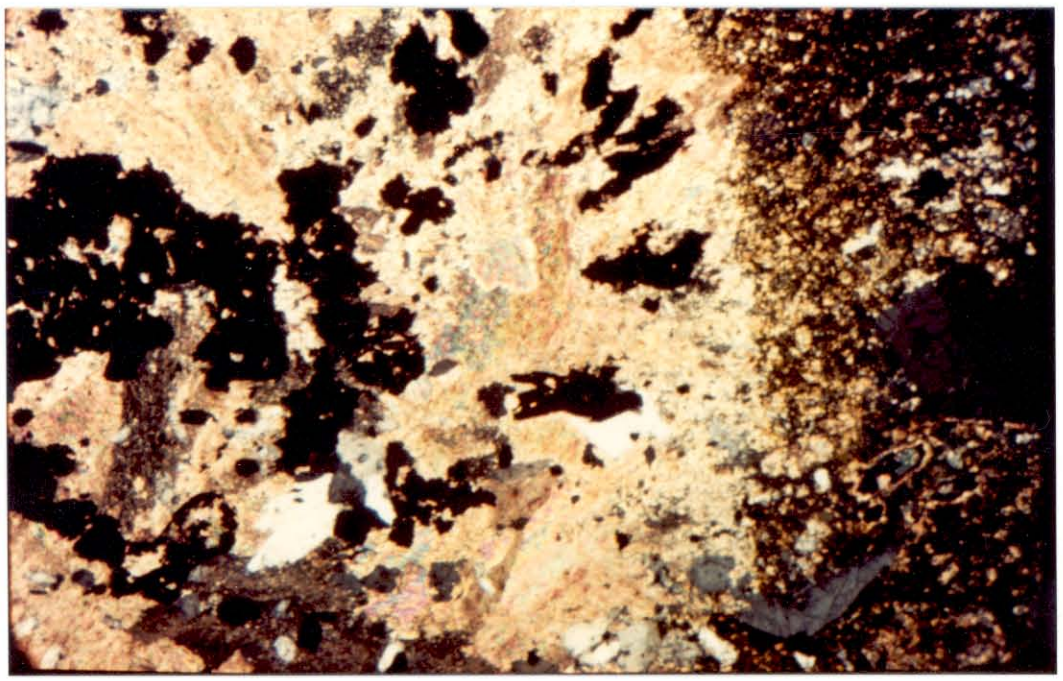

(22)

PHOTO 23. Photomicrograph of potassic-phyllic alteration in Vinini hornfels. Inner sericite selvage and outer biotite-rich selvage surround quartz veinlet. Surface sample, 150m southwest of EMH-8. Crossed nicols.

PHOTO 24. Photomicrograph of potassic-phyllic alteration in Mount Hope Tuff. Sheeted quartz-fluorite+K-feldspar veinlets surrounded by quartz-sericite selvages. Surface sample, 410m northeast of Mount Hope summit. Crossed nicols.

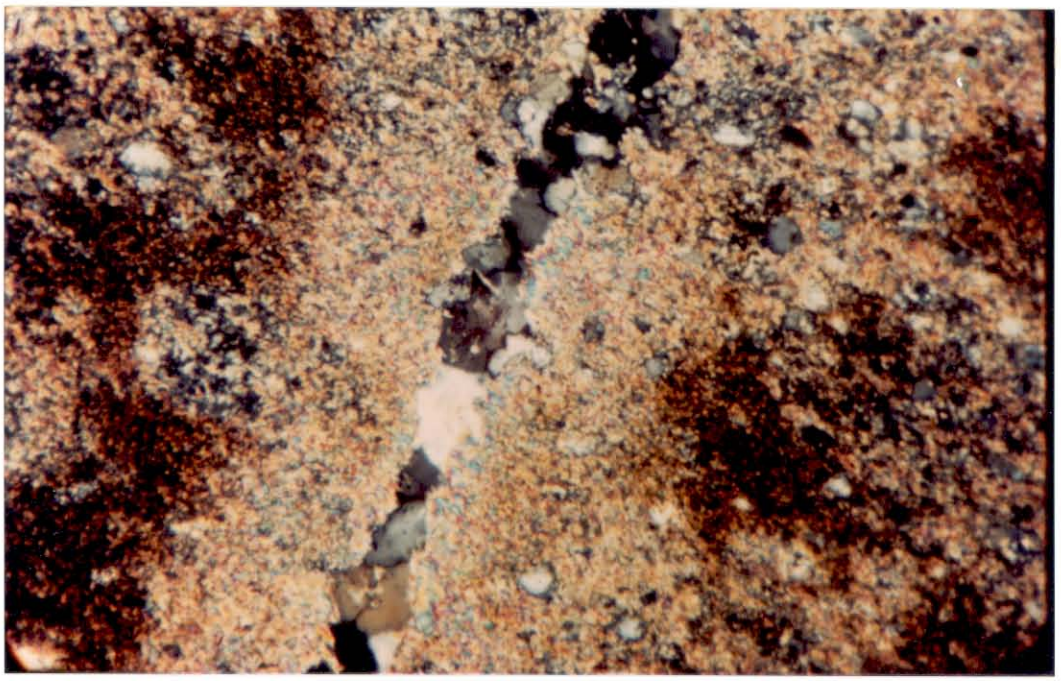

(23)

0.1 mm

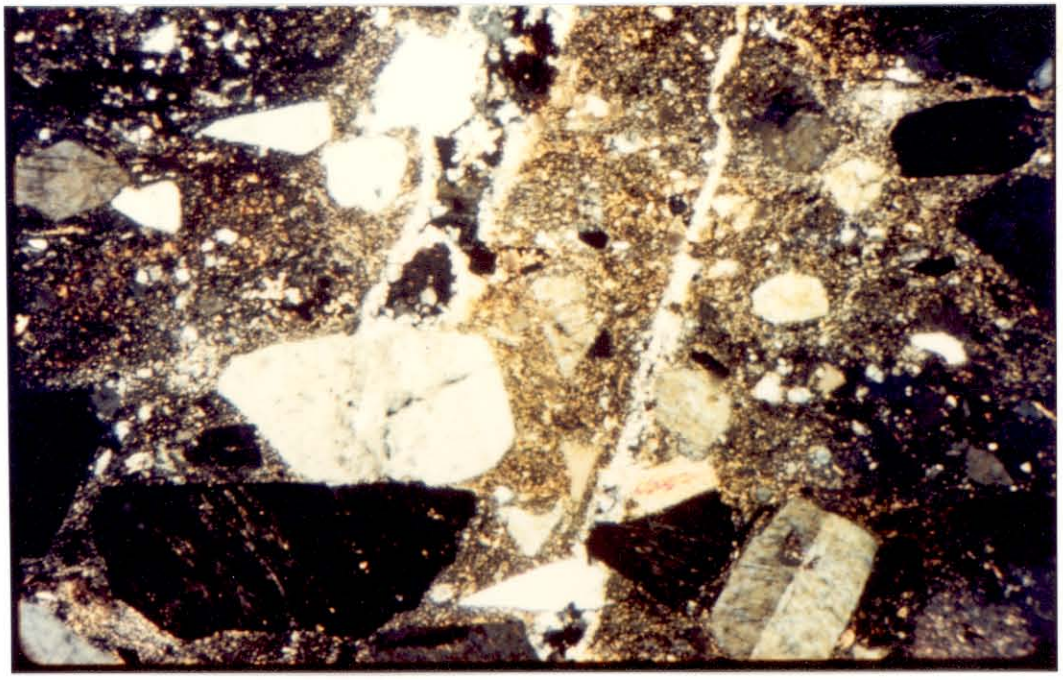

(24)

0.5 mm

PHOTO 25. Photomicrograph of weak potassic alteration in quartz porphyry. Secondary K-feldspar replacing plagioclase phenocryst in selvage along quartz veinlet. K-feldspar also rims portions of the phenocryst. Clay and sericite dust the core of the plagioclase crystal. EMH-22, 352m. Crossed nicols.

PHOTO 26. Photomicrograph of potassic alteration in quartz porphyry. Quartz-K-feldspar veinlet cuts sanidine phenocryst; secondary K-feldspar in veinlet crystallized in optical continuity with adjacent phenocryst, creating the illusion that the phenocryst truncates the veinlet. Note, however, slight offset of phenocryst along veinlet. EMH-6, 123m. Crossed nicols.

(25)

0.5 mm

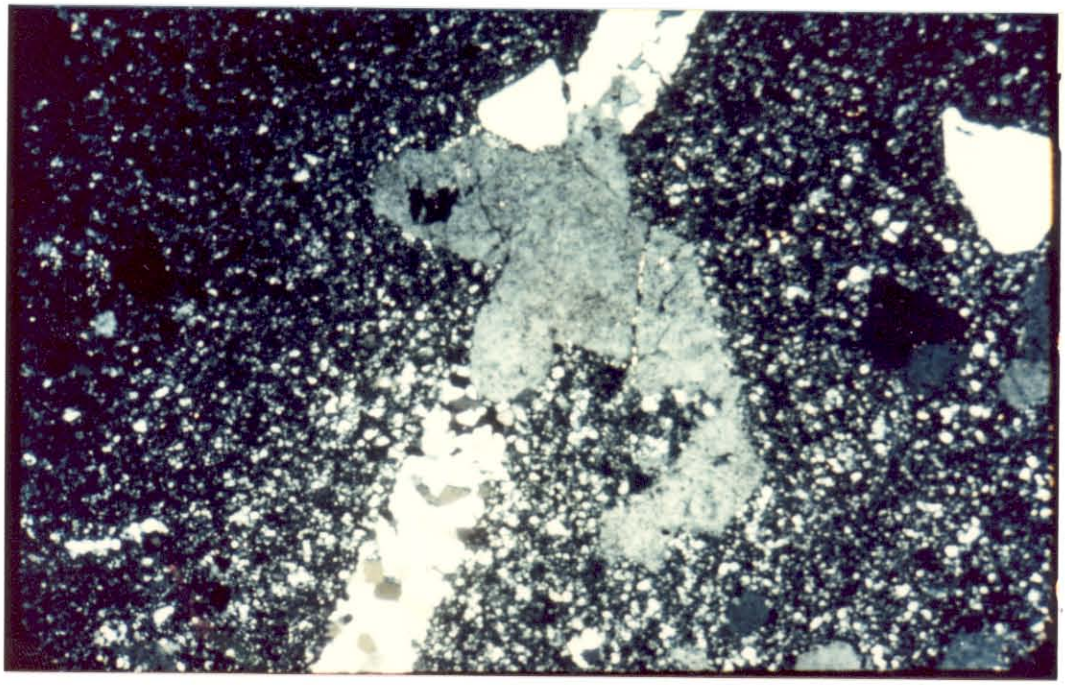

(26)

0.5 mm

PHOTO 27. Photomicrograph of potassic alteration in Vinini quartz-K-feldspar-biotite hornfels. Vuggy quartz-fluorite veinlet cuts quartz-molybdenite veinlet with dark gray K-feldspar selvage. EMH-17, 244m. Crossed nicols.

PHOTO 28. Photomicrograph of high-silica alteration in Vinini hornfels. Typical irregular, anastomosing quartz veinlet and patch of silica flood. EMH-20, 410m. Crossed nicols.

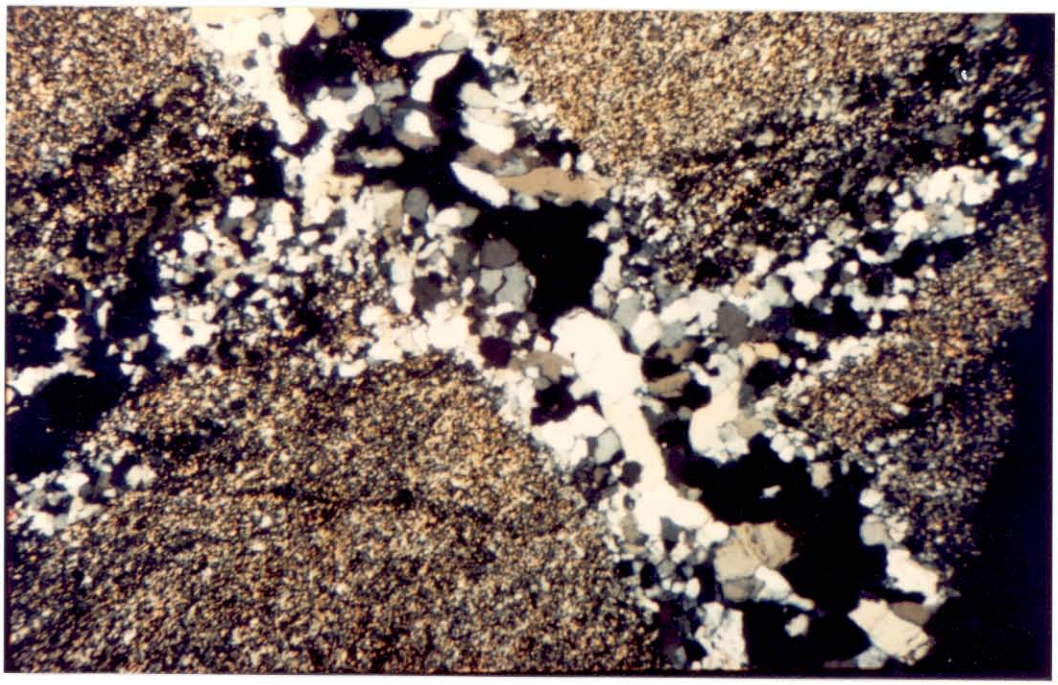

(27)

0.5 mm

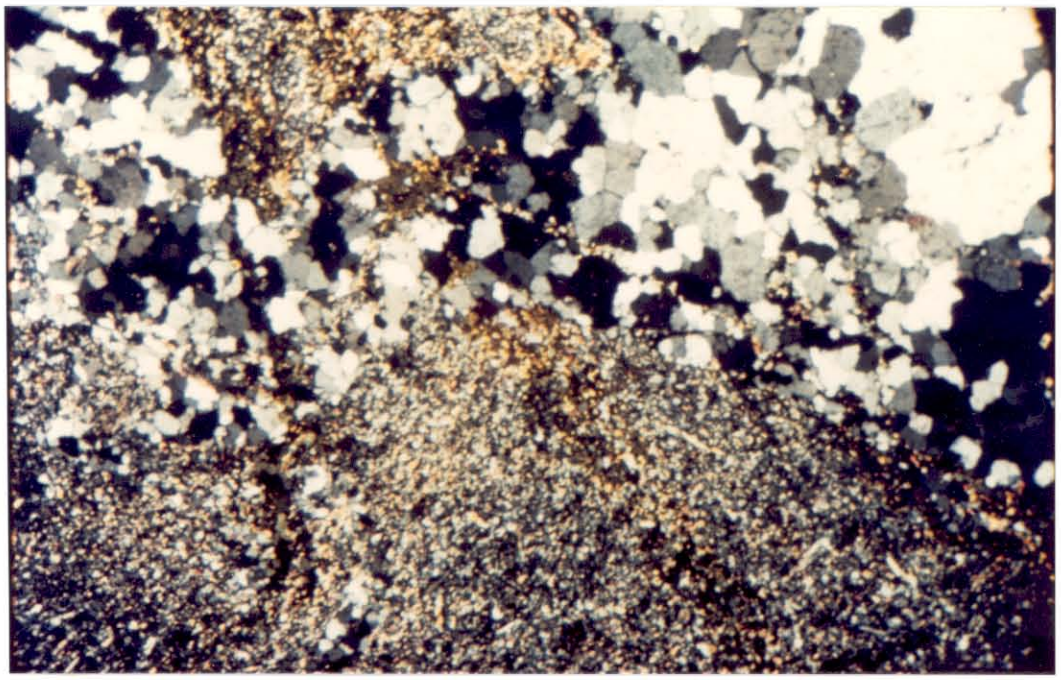

(28)

0.5 mm

PHOTO 29. Photomicrograph of incipient silica flooding in quartz porphyry. Note similarity in texture between mosaic quartz phenocryst at right and silica flood at left. EMH-14, 632m. Crossed nicols.

PHOTO 30. Photomicrograph of high-silica alteration in quartz porphyry. Silica replaces rock texture at left and bottom center. Late sericite and clay replace feldspar phenocryst at top center. EMH-5, 671m. Crossed nicols.

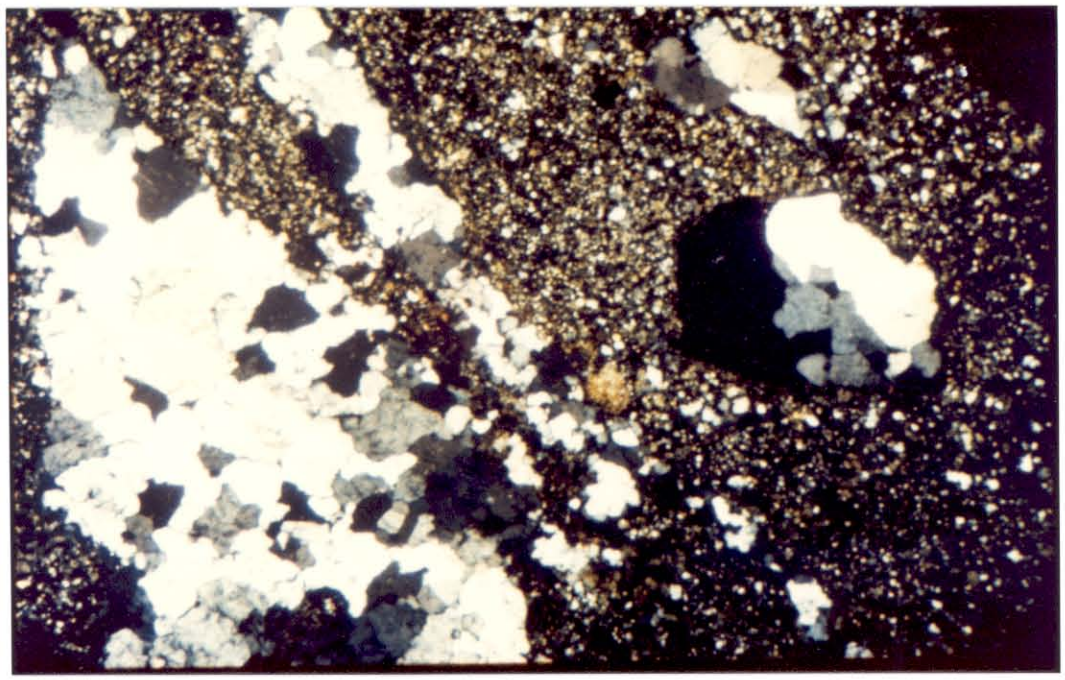

(29)

0.5 mm

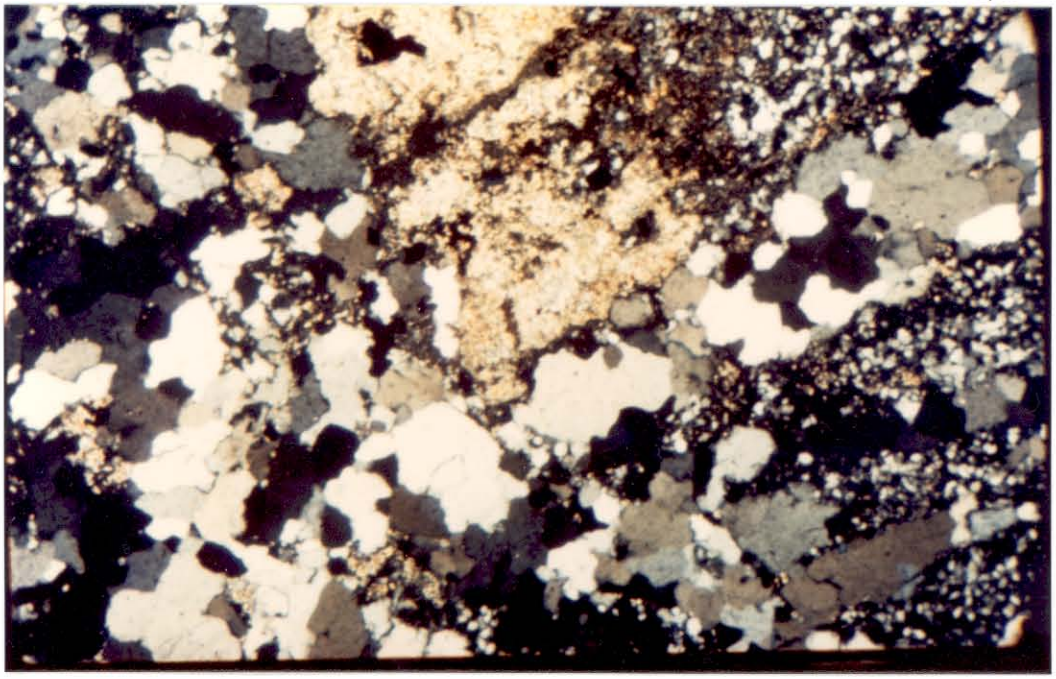

(30)

0.5 mm

PHOTO 31. Photomicrograph of biotite alteration in coarse-grained quartz porphyry. Chlorite rims biotite (right center); clay and sericite replace plagioclase (upper right and lower left). K-feldspar (upper left) is nearly fresh. EMH-5, 853m. Crossed nicols.

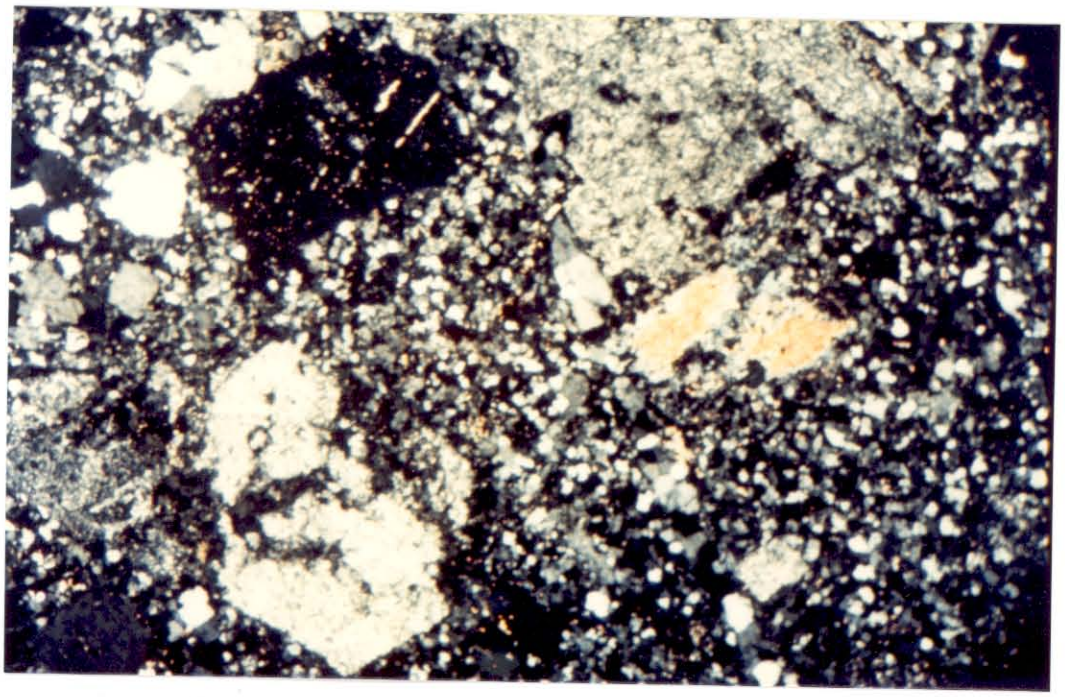

(31)

0.5 mm

PHOTO 32. Types of molybdenite mineralization in the Mount Hope deposit.

(a) Typical quartz-molybdenite veinlets. Quartz porphyry, EMH-3, 544m.

(b) Blue quartz veins. Vinini hornfels, EMH-14, 503m.

(c) Molybdenite paint. Vinini hornfels, EMH-12, 279m.

(d) Gaudy quartz-molybdenite veins. Vinini hornfels, EMH-12, 295m.

(32)

PHOTO 33. Blue quartz vein (diagonally from upper left to lower right) offsetting thinner quartz-molybdenite veinlet (right), which in turn cuts barren quartz veinlets with K-feldspar haloes. Quartz porphyry, EMH-14, 318m.

PHOTO 34. Silica flood cuts a quartz-molybdenite veinlet. Quartz porphyry, EMH-16, 289m.

(33)

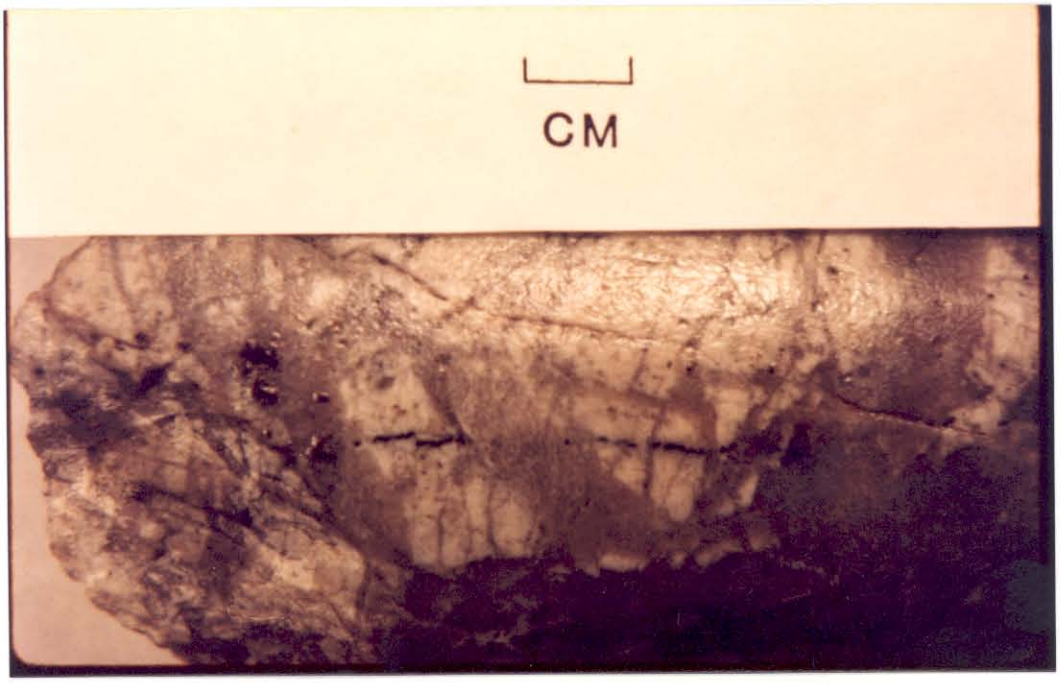

(34)

PHOTO 35. Photomicrograph showing a pyrite-fluorite veinlet (right center) offsetting a quartz-K-feldspar-molybdenite veinlet (upper left to lower right). Sericite selvage surrounding pyrite-fluorite veinlet is truncated because sericite cannot replace vein quartz. Quartz-K-feldspar-molybdenite veinlet in turn cuts a barren quartz veinlet (left center). Quartz porphyry, EMH-21, 173m. Crossed nicols.

PHOTO 36. Photomicrograph of coarse-grained quartz porphyry (lower three-quarters of photo) cutting silica flood (upper right) in quartz porphyry. EMH-11, 581m. Crossed nicols.

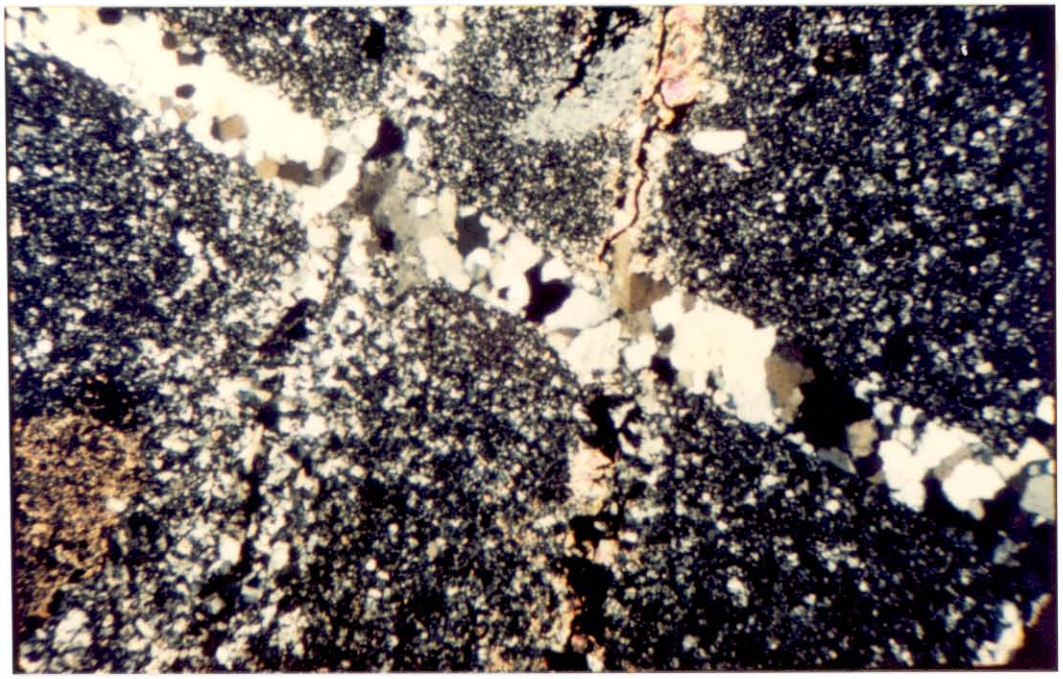

(35)

0.5 mm

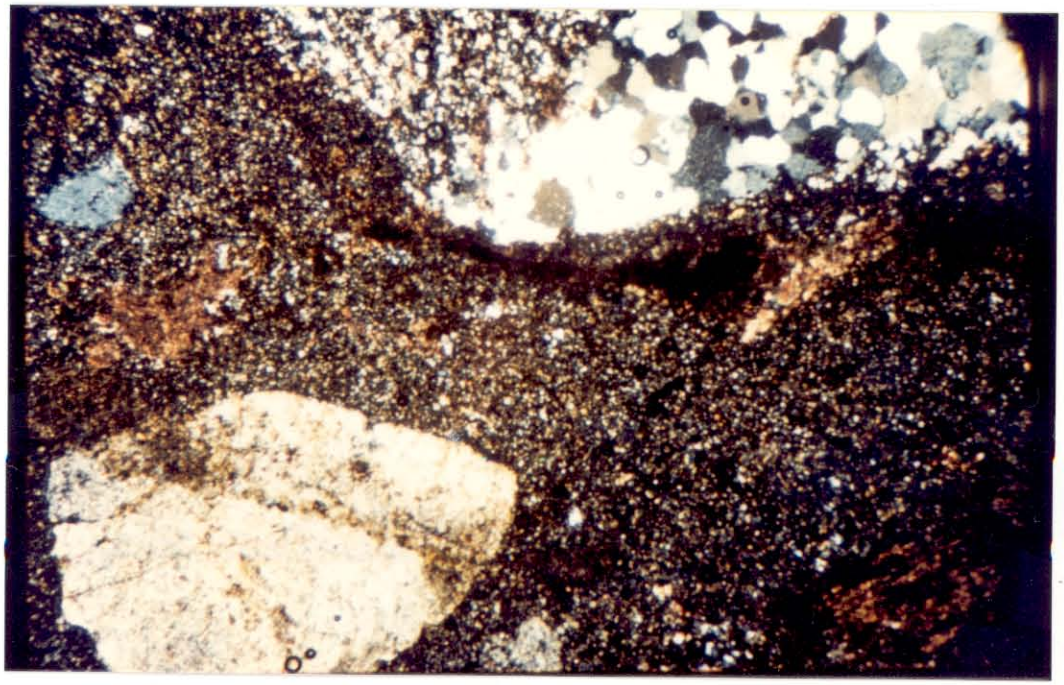

(36)

0.5 mm

PHOTO 37. Photomicrograph showing micrographic intergrowths of quartz and K-feldspar in groundmass of aplitic quartz porphyry. EMH-2, 704m. Crossed nicols.

PHOTO 38. Photomicrograph of crenulate banding in aplitic quartz porphyry. Coarse-grained bands consist of quartz only; fine-grained bands consist of quenched porphyry groundmass (compare grain size with top and bottom of photo). EMH-19, 557m. Crossed nicols.

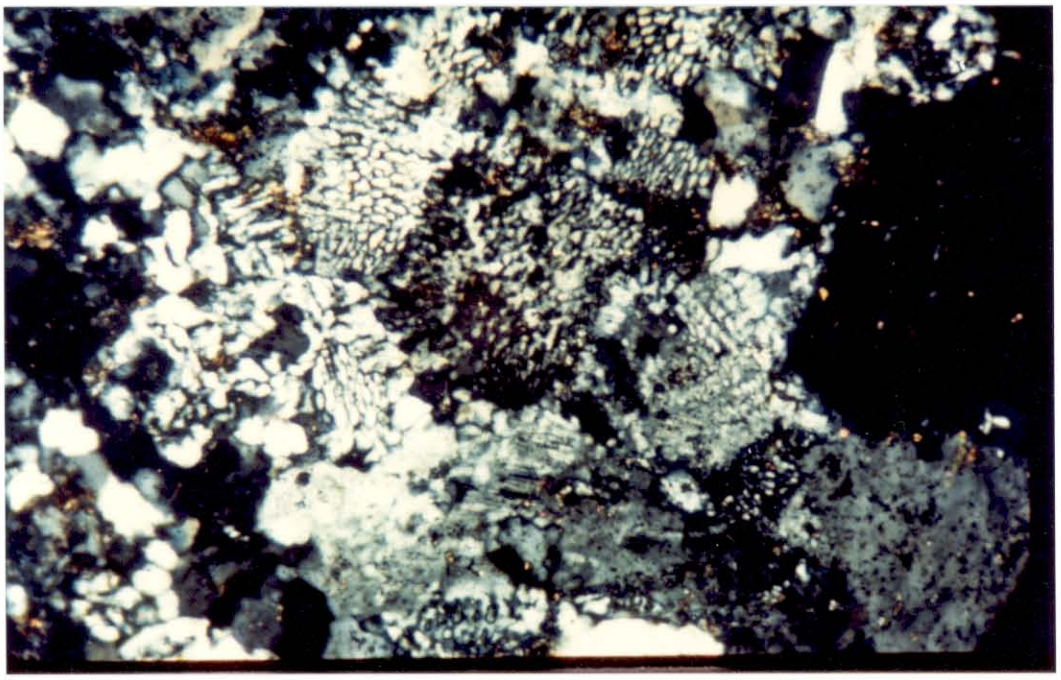

(37)

0.1 mm

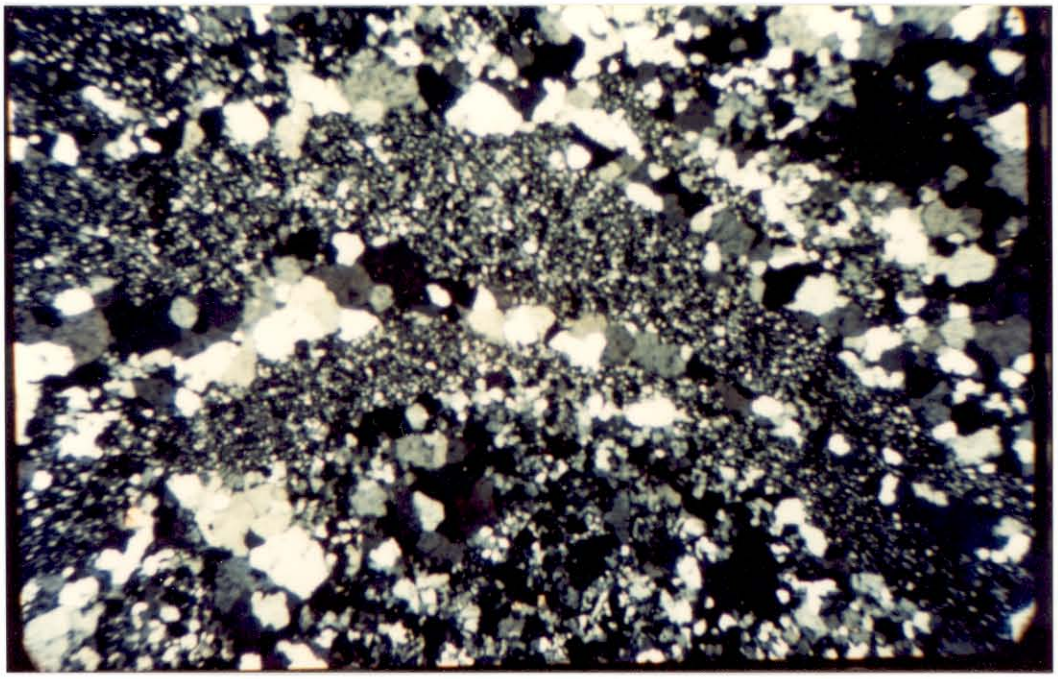

(38)

0.5 mm

PHOTO 39. Rhyolite vent breccia containing an autolith of early quartz porphyry cut by sheeted quartz veinlets. Surface sample, 245m east of EPMH-15.

PHOTO 40. Photomicrograph of sanidine phenocryst containing micrographic quartz intergrowths. Quartz porphyry border phase, EMH-12, 103m. Crossed nicols.

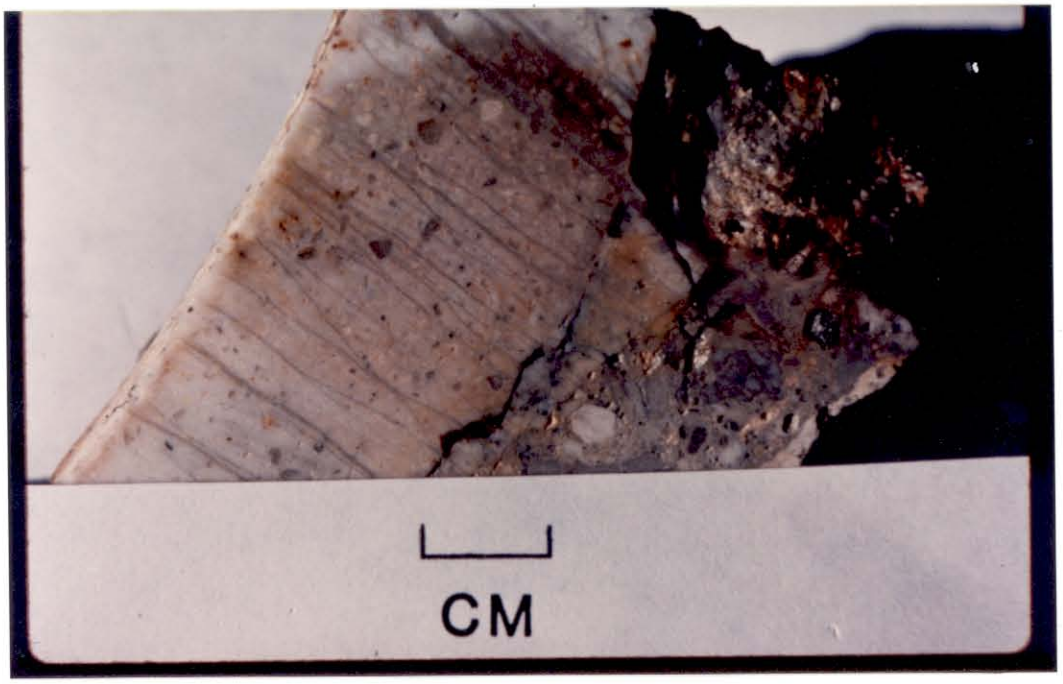

(39)

(40)

PROJECT MT. HOPE
HOLE No. EMH-1

COMPOSITE DOWNHOLE GEOCHEMISTRY

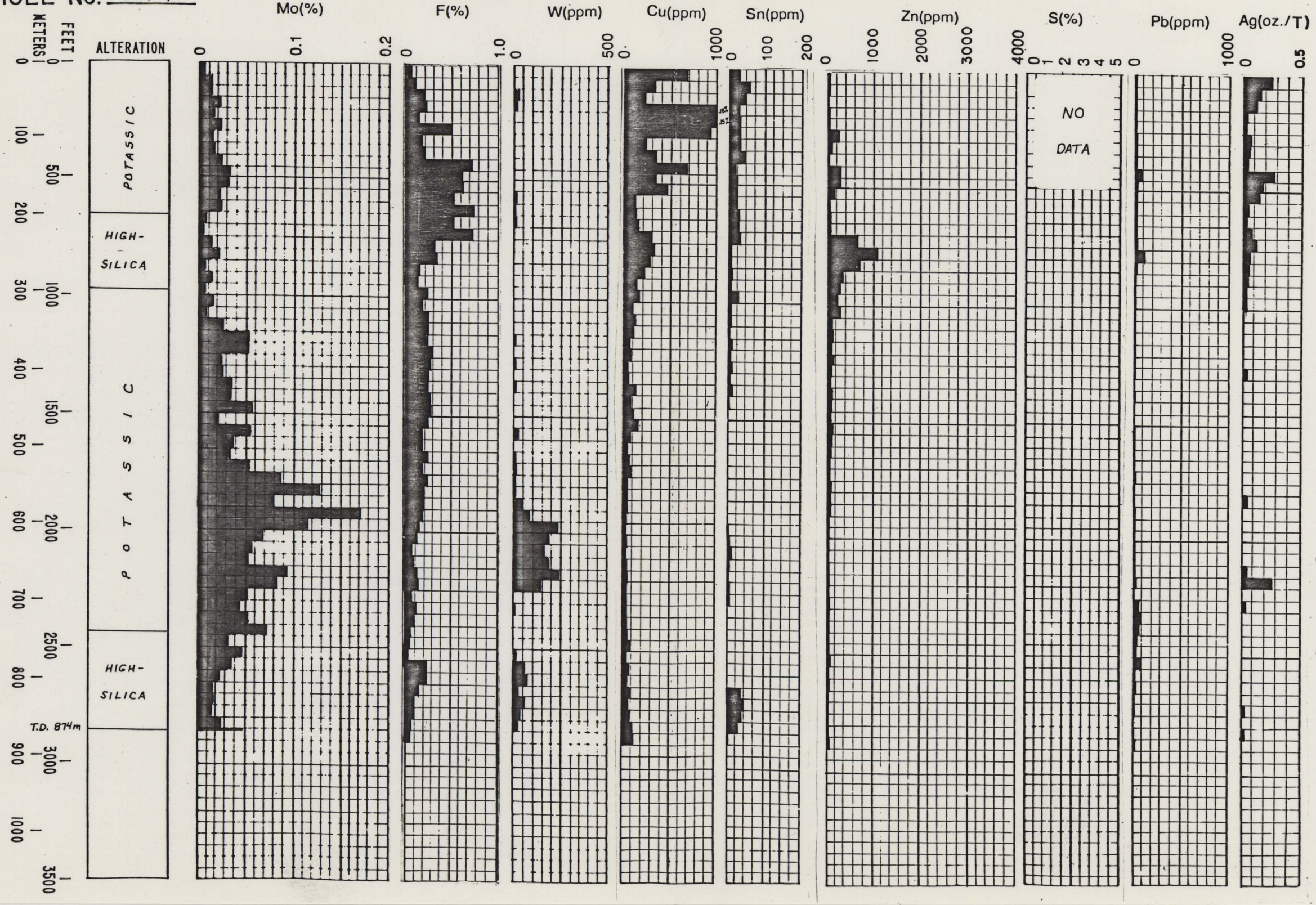

3820009

PROJECT MT. HOPE
HOLE No. EMH-2

COMPOSITE DOWNHOLE GEOCHEMISTRY

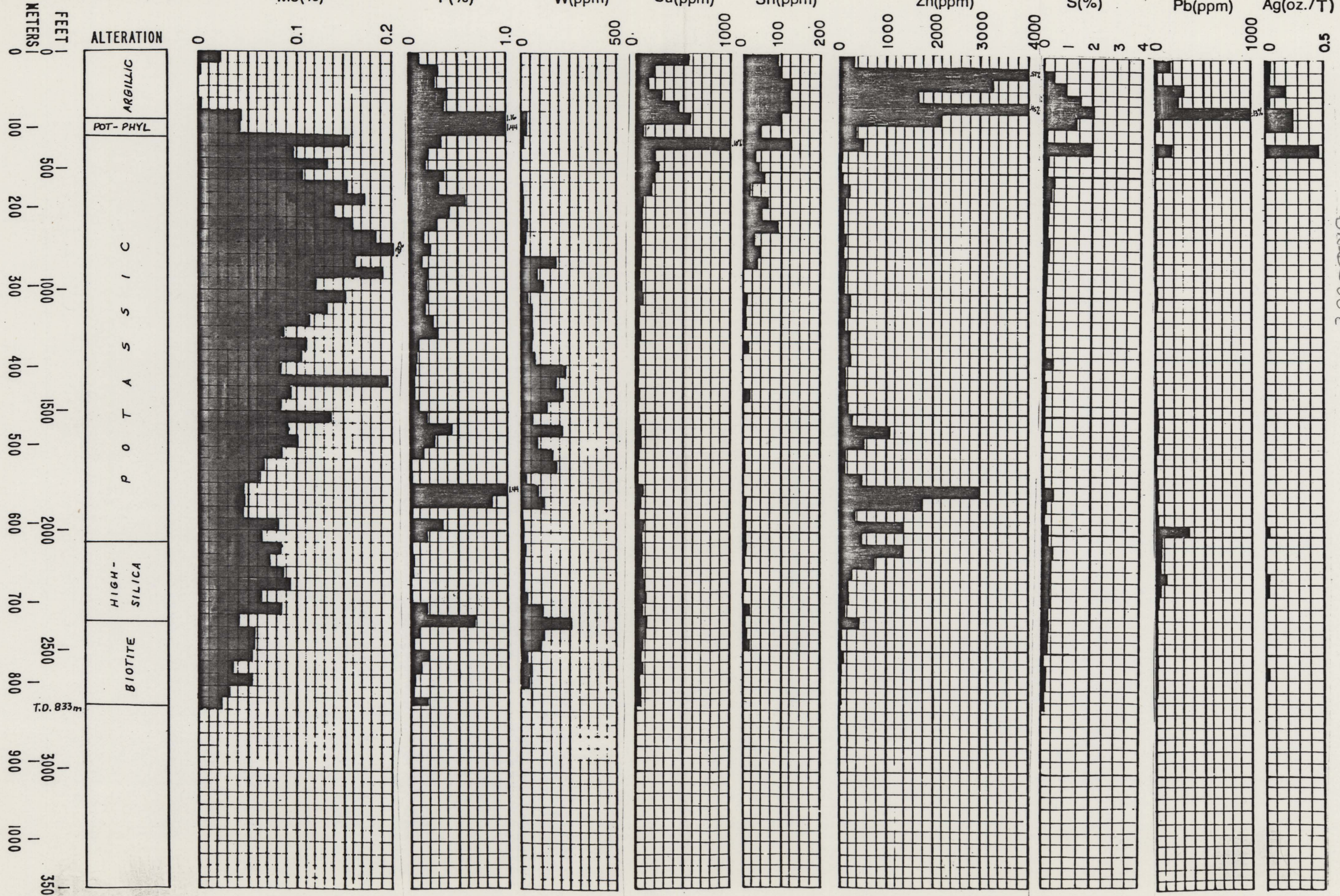

PROJECT MT. HOPE

HOLE No. EMH-20

COMPOSITE DOWNHOLE GEOCHEMISTRY

METERS 0 100 200 300 400 500 600

FEET 0 500 1000 1500 2000 2500 3000 3500

ALTERATION

POTASSIC-PHYLLIC

POTASSIC

HIGH-SILICA

T.D. 636 m

Mo(%) 0 0.1 0.2

F(%) 0 1.0

W(ppm) 0 500

Cu(ppm) 0 1000

Sn(ppm) 0 100 200

Zn(ppm) 0 1000 2000 3000 4000

S(%) 0 1 2 3 4 5

Pb(ppm) 0 1000

Ag(oz./T) 0 0.5

3220019

PROJECT MT. HOPE
HOLE No. EMH-19

COMPOSITE DOWNHOLE GEOCHEMISTRY

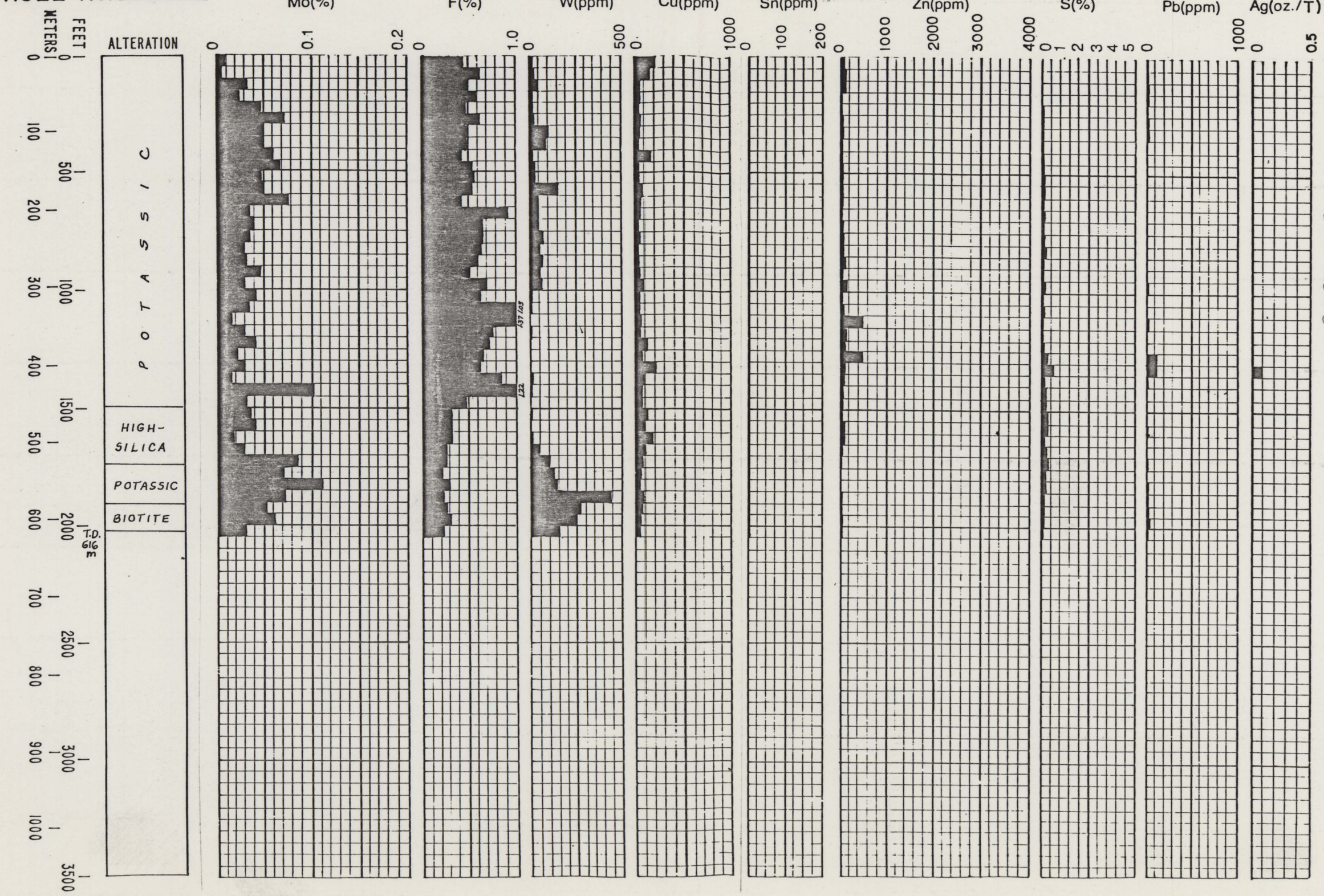

3220019

PROJECT MT. HOPE
HOLE No. EMH-18

COMPOSITE DOWNHOLE GEOCHEMISTRY

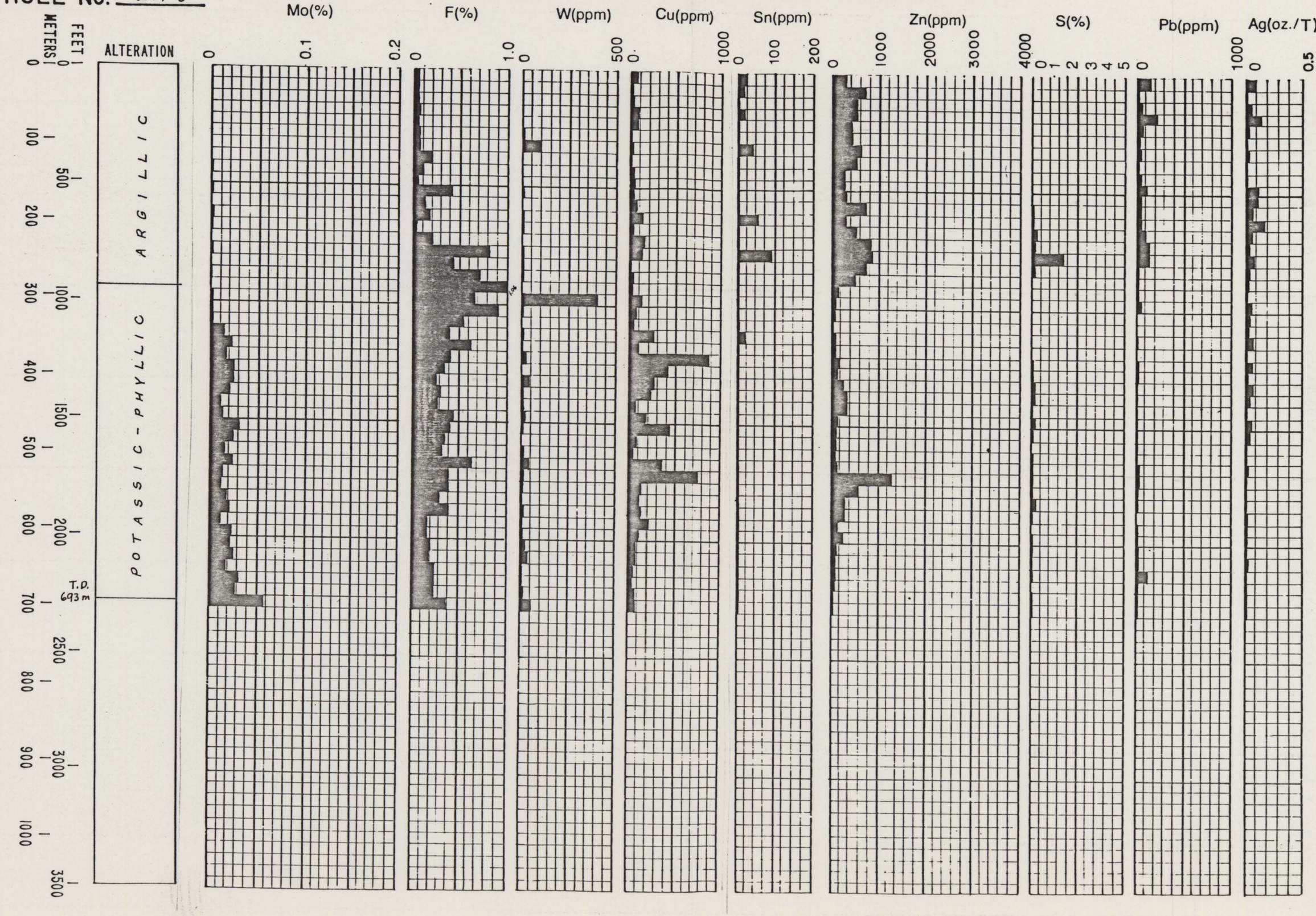

33200019

PROJECT MT. HOPE

HOLE No. EMH-17

COMPOSITE DOWNHOLE GEOCHEMISTRY

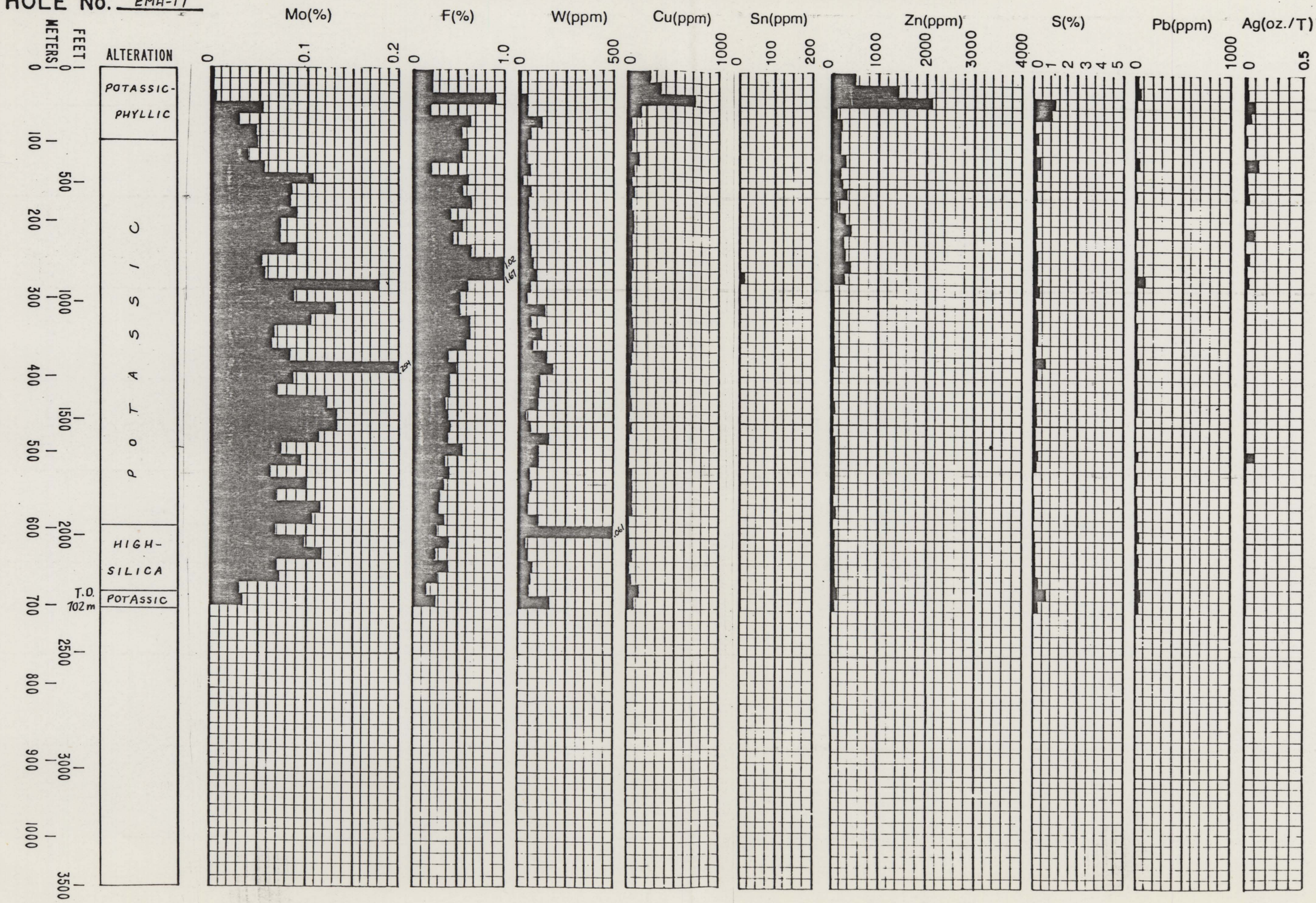

3200019

PROJECT MT. HOPE

HOLE No. EMH-16

COMPOSITE DOWNHOLE GEOCHEMISTRY

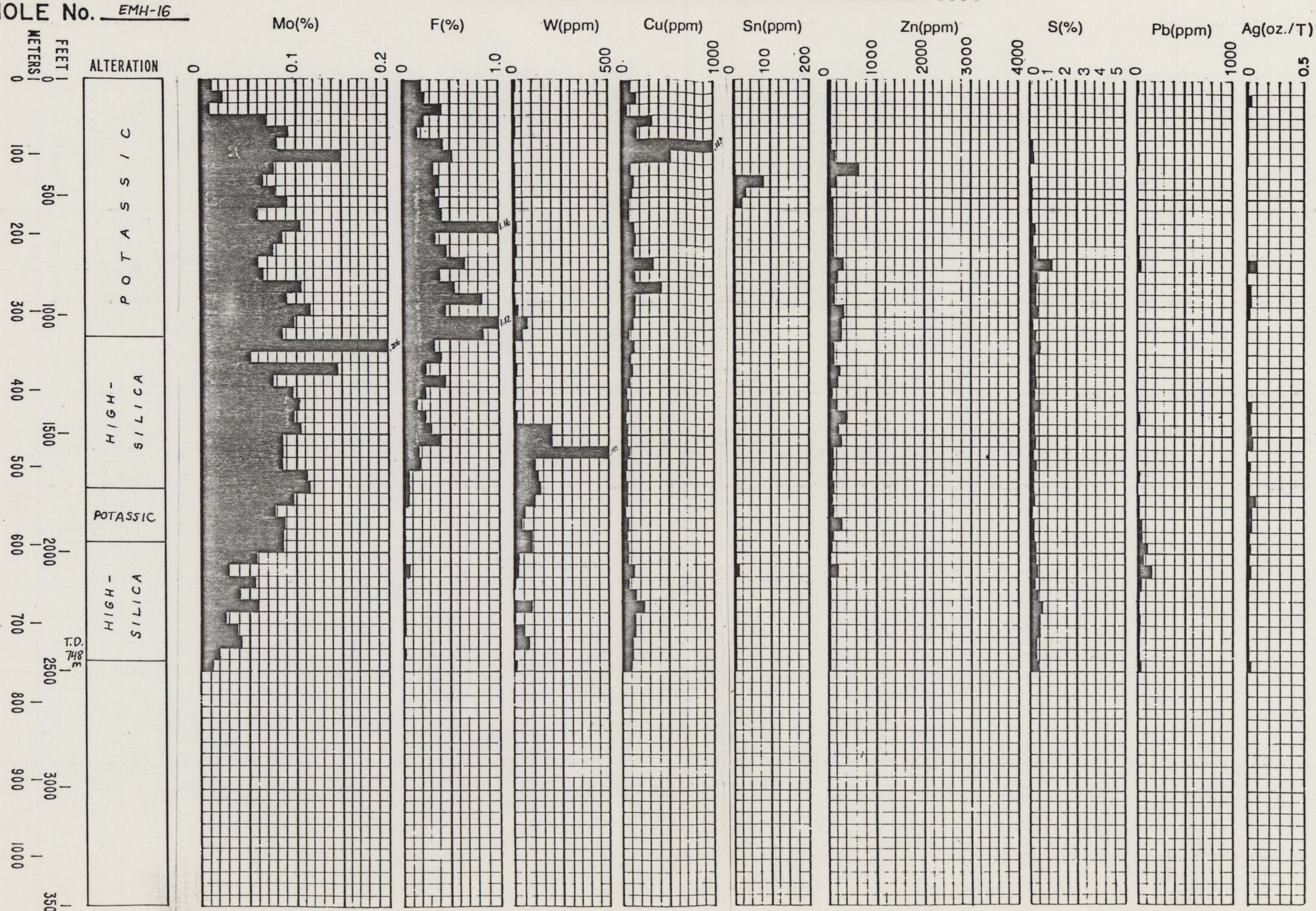

-3200019

PROJECT MT. HOPE
HOLE No. EPMH-15

COMPOSITE DOWNHOLE GEOCHEMISTRY

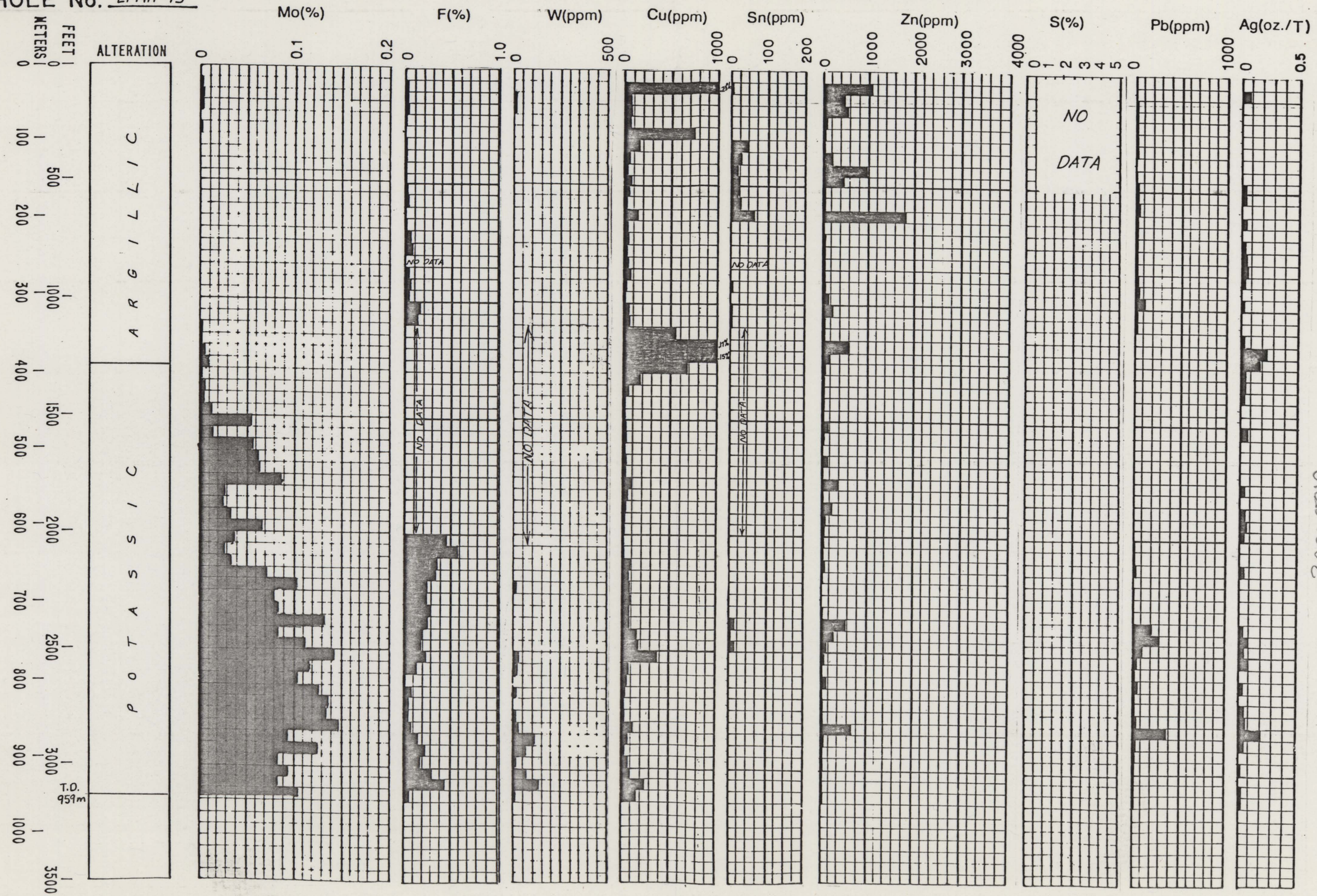

PROJECT MT. HOPE
HOLE No. EMH-14

COMPOSITE DOWNHOLE GEOCHEMISTRY

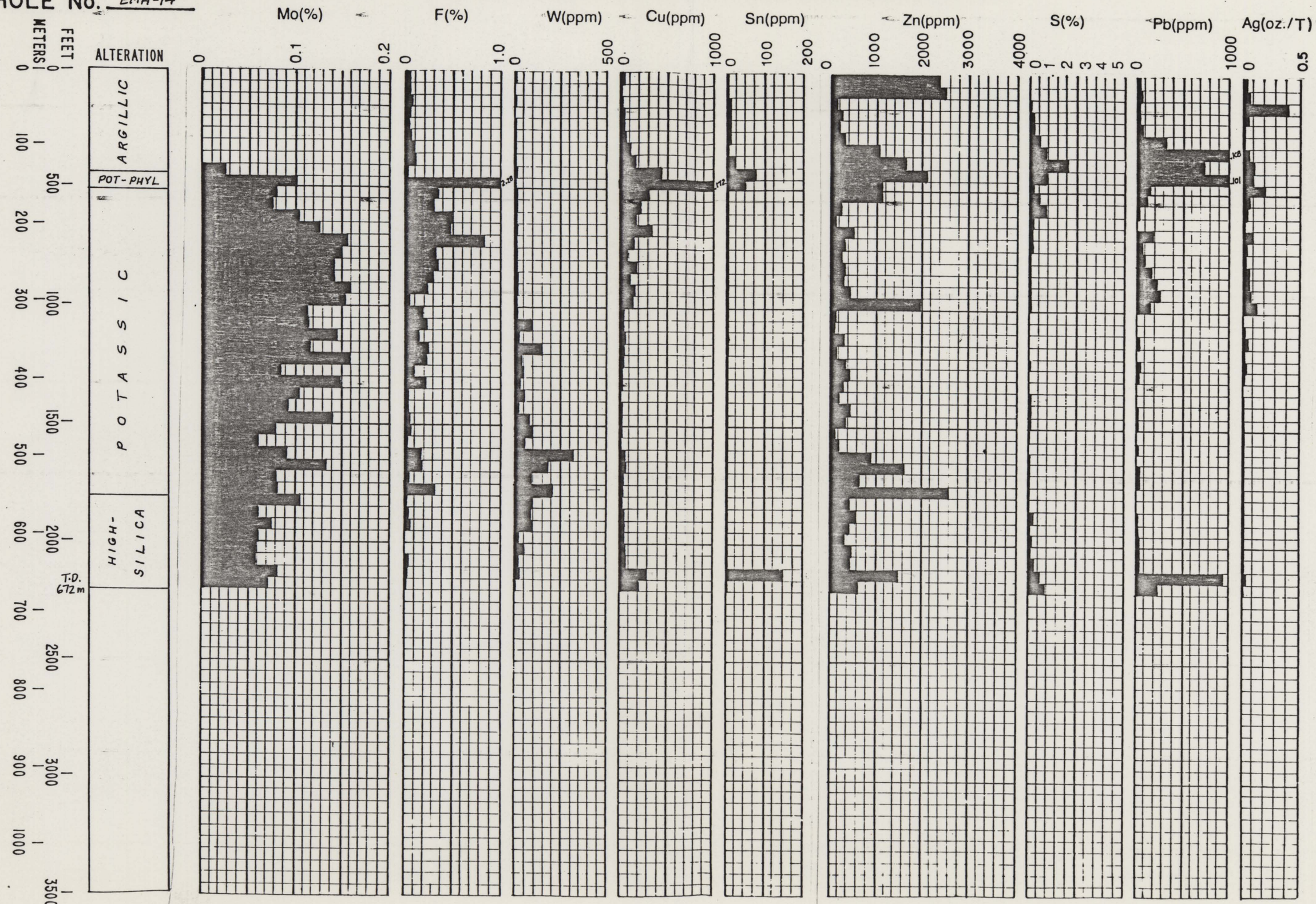

3390016

PROJECT MT. HOPE

HOLE No. EMH-13

COMPOSITE DOWNHOLE GEOCHEMISTRY

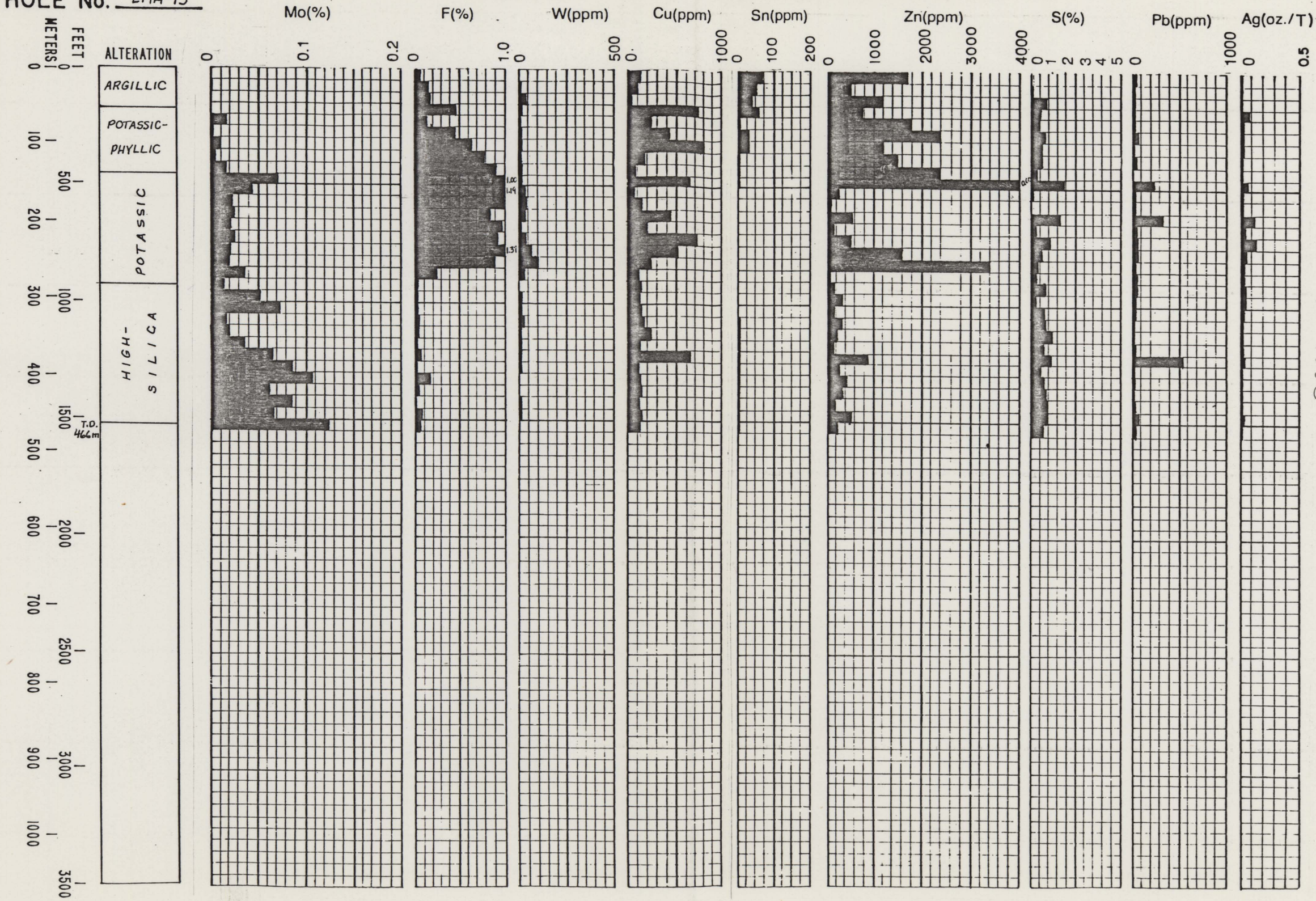

32200019

PROJECT MT. HOPE
HOLE No. EMH-12

COMPOSITE DOWNHOLE GEOCHEMISTRY

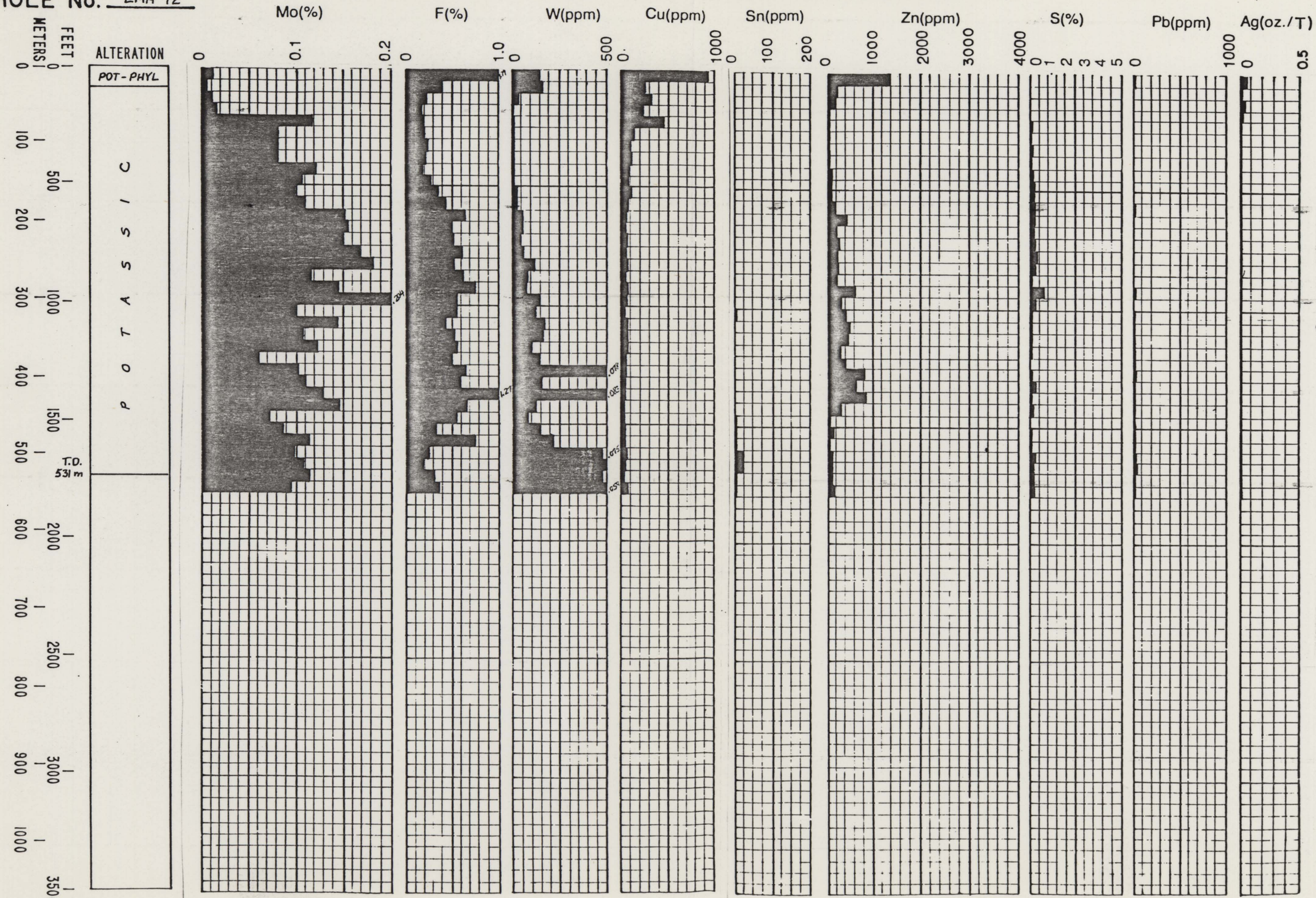

3300019

PROJECT MT. HOPE

HOLE No. EMH-II

COMPOSITE DOWNHOLE GEOCHEMISTRY

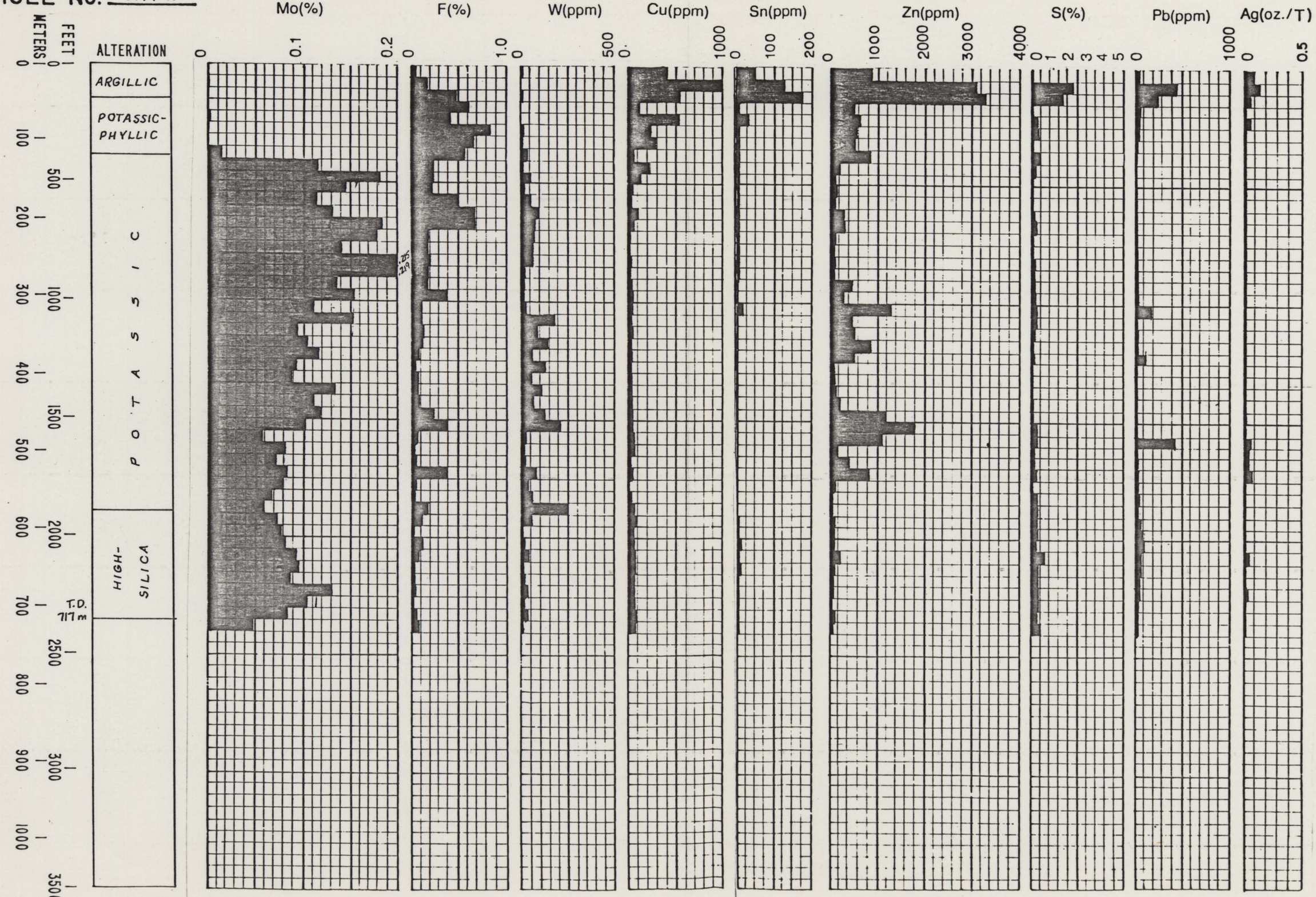

3000 ODG

PROJECT MT. HOPE

HOLE No. EMH-10

COMPOSITE DOWNHOLE GEOCHEMISTRY

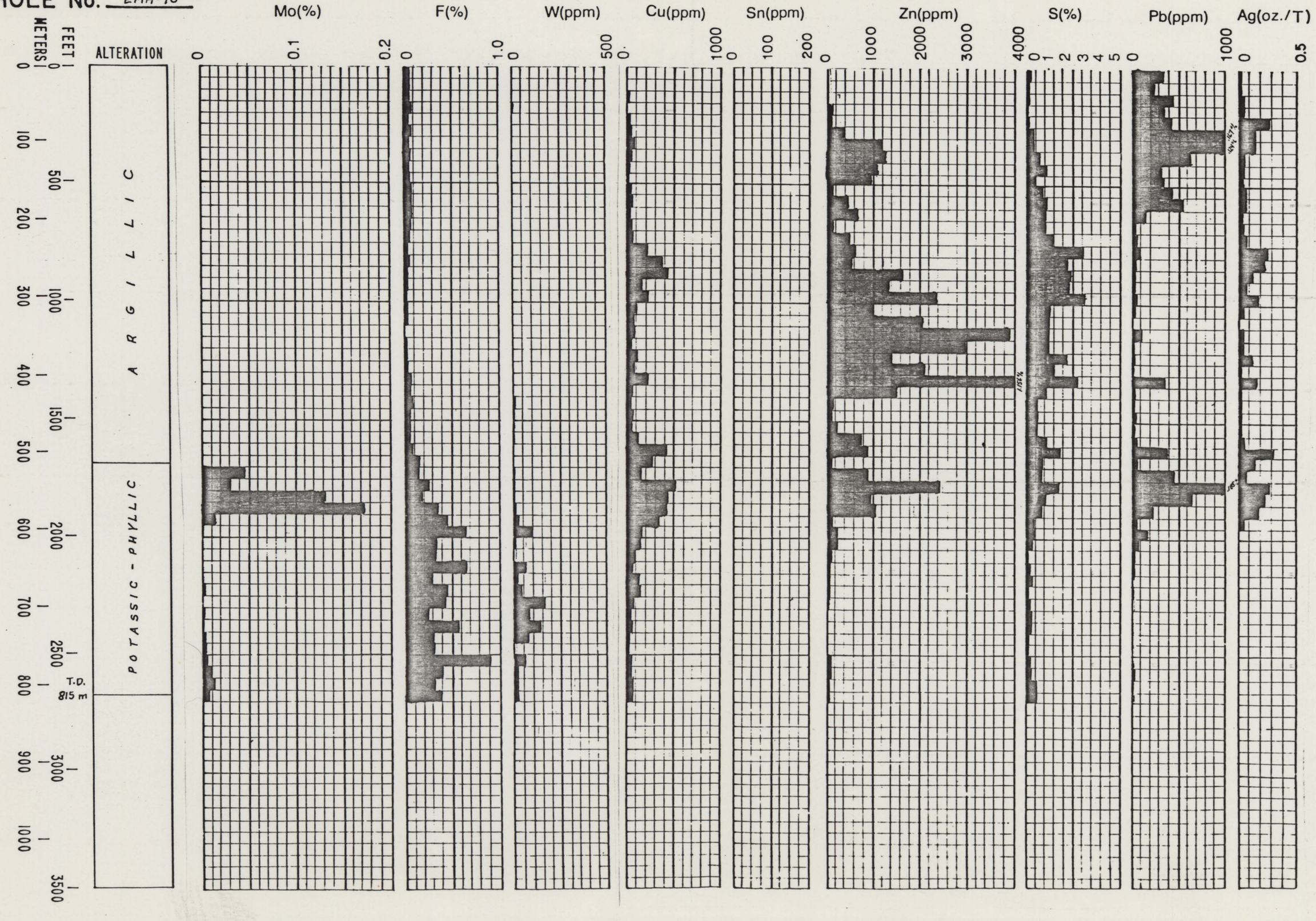

3200 CD19

PROJECT MT. HOPE
HOLE No. EMH-9

COMPOSITE DOWNHOLE GEOCHEMISTRY

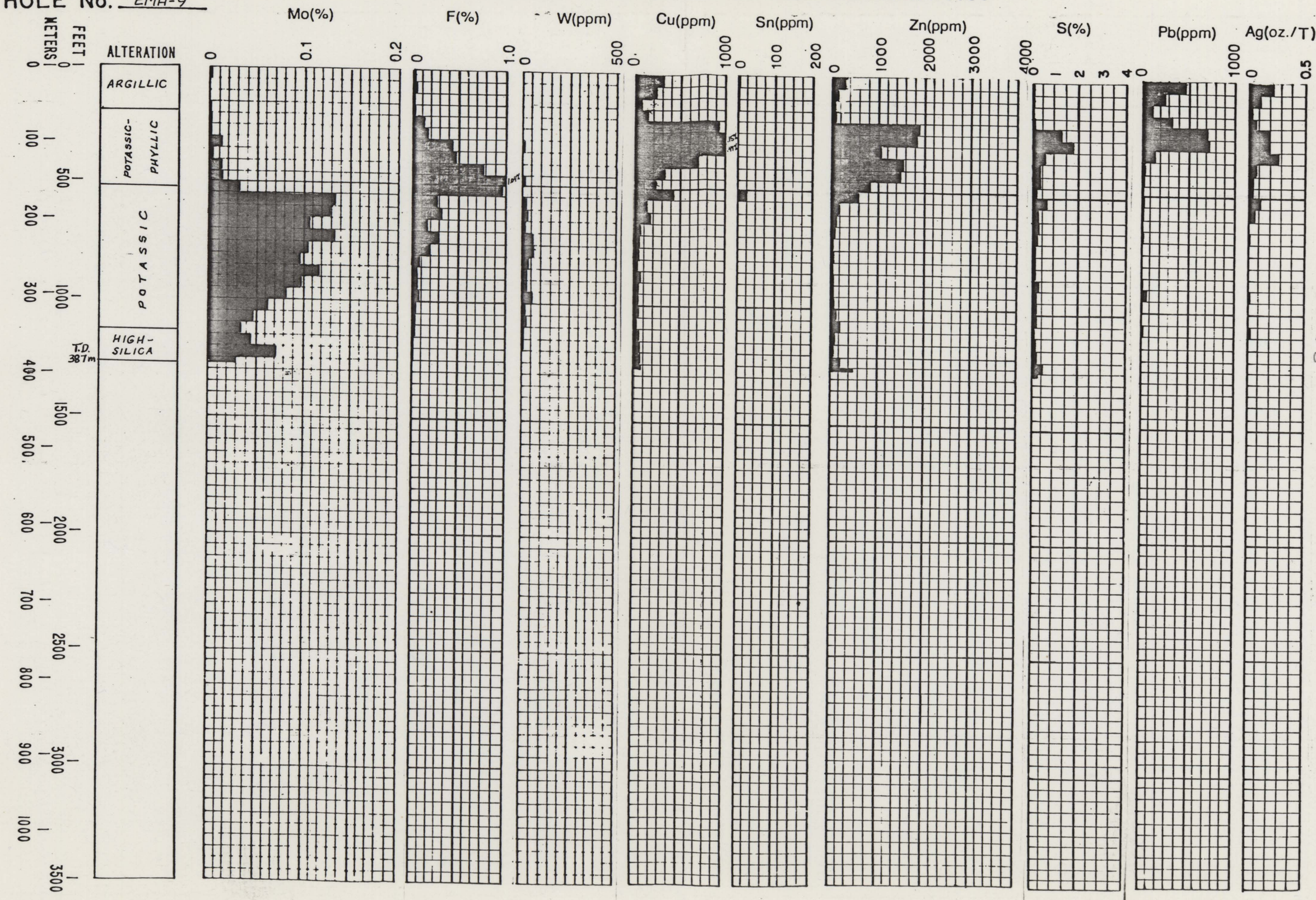

3200019

PROJECT MT. HOPE
HOLE No. EMH-8

COMPOSITE DOWNHOLE GEOCHEMISTRY

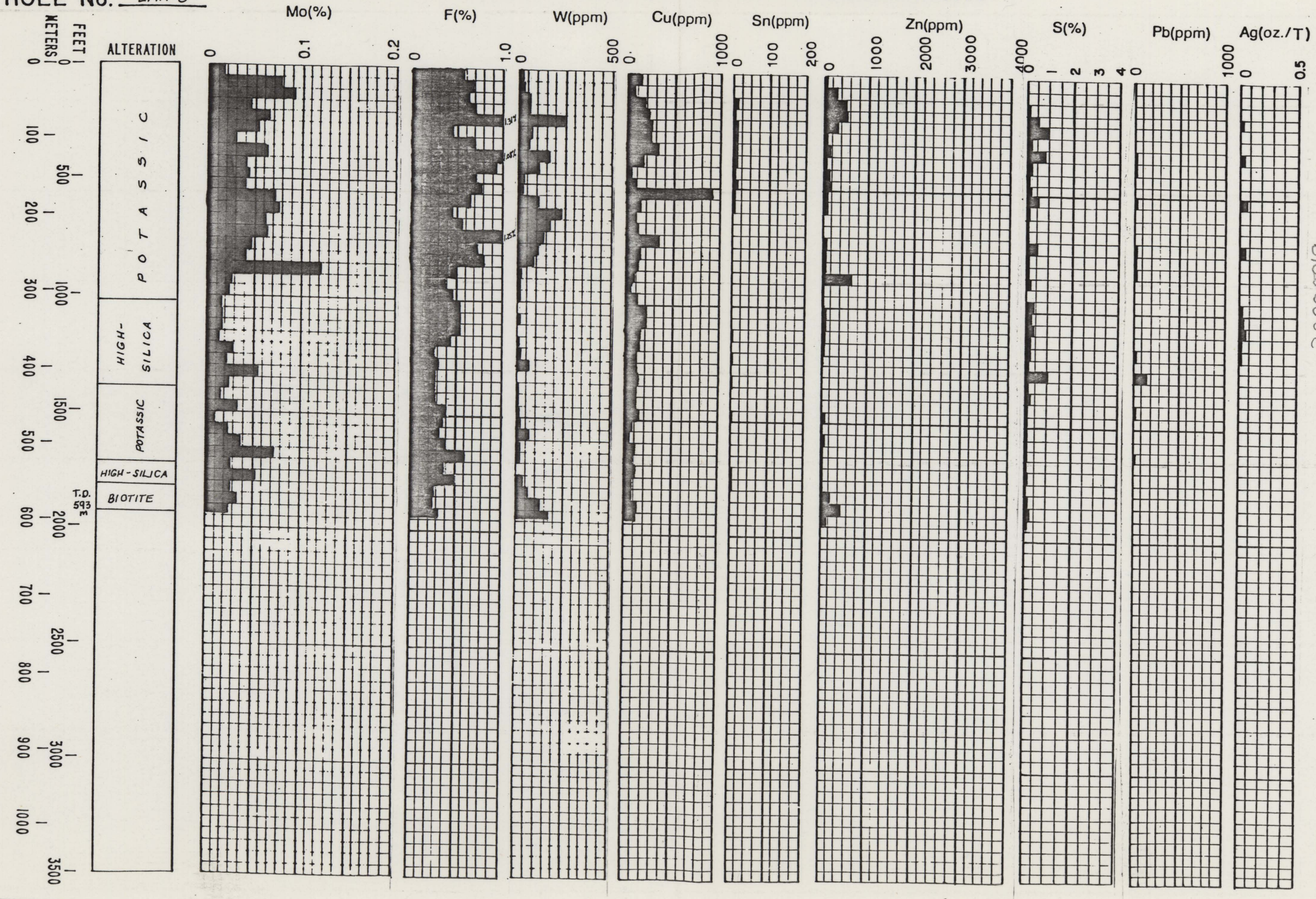

3220019

PROJECT MT. HOPE
HOLE No. EMH-7

COMPOSITE DOWNHOLE GEOCHEMISTRY

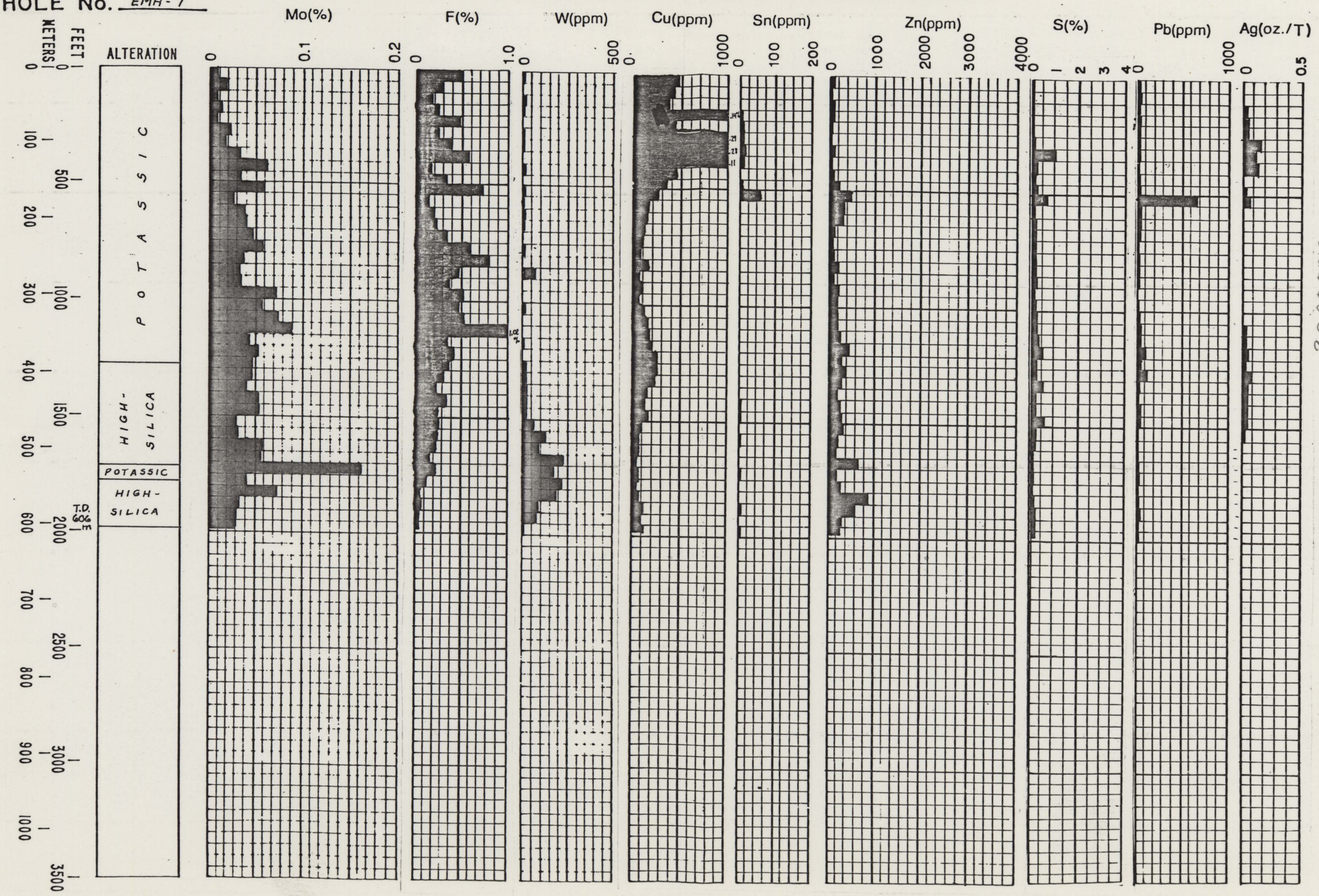

3200019

PROJECT MT. HOPE
HOLE No. EMH-6

COMPOSITE DOWNHOLE GEOCHEMISTRY

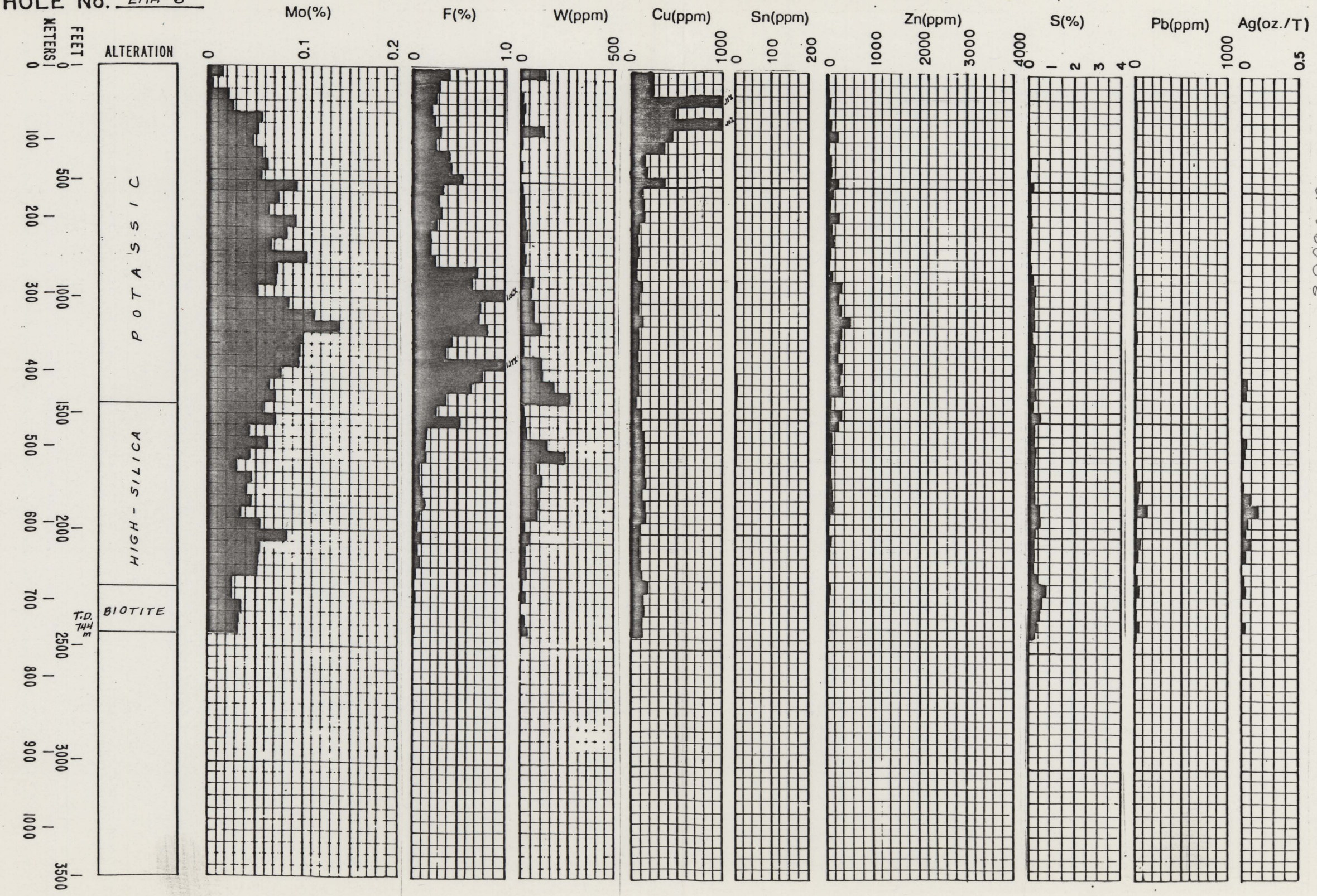

3800019

PROJECT MT. HOPE

HOLE No. EMH-5

COMPOSITE DOWNHOLE GEOCHEMISTRY

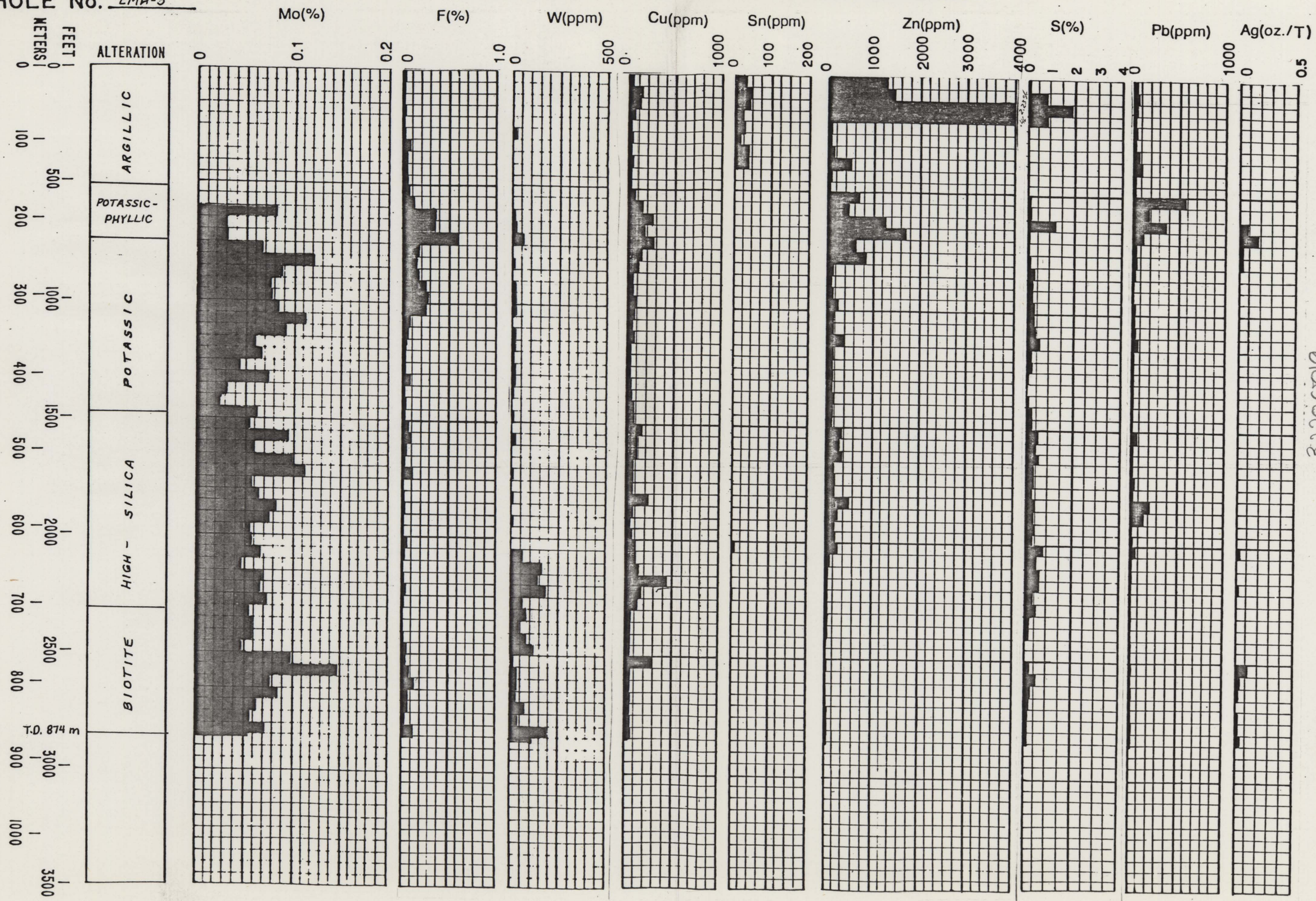

PROJECT MT. HOPE
HOLE No. EMH-4

COMPOSITE DOWNHOLE GEOCHEMISTRY

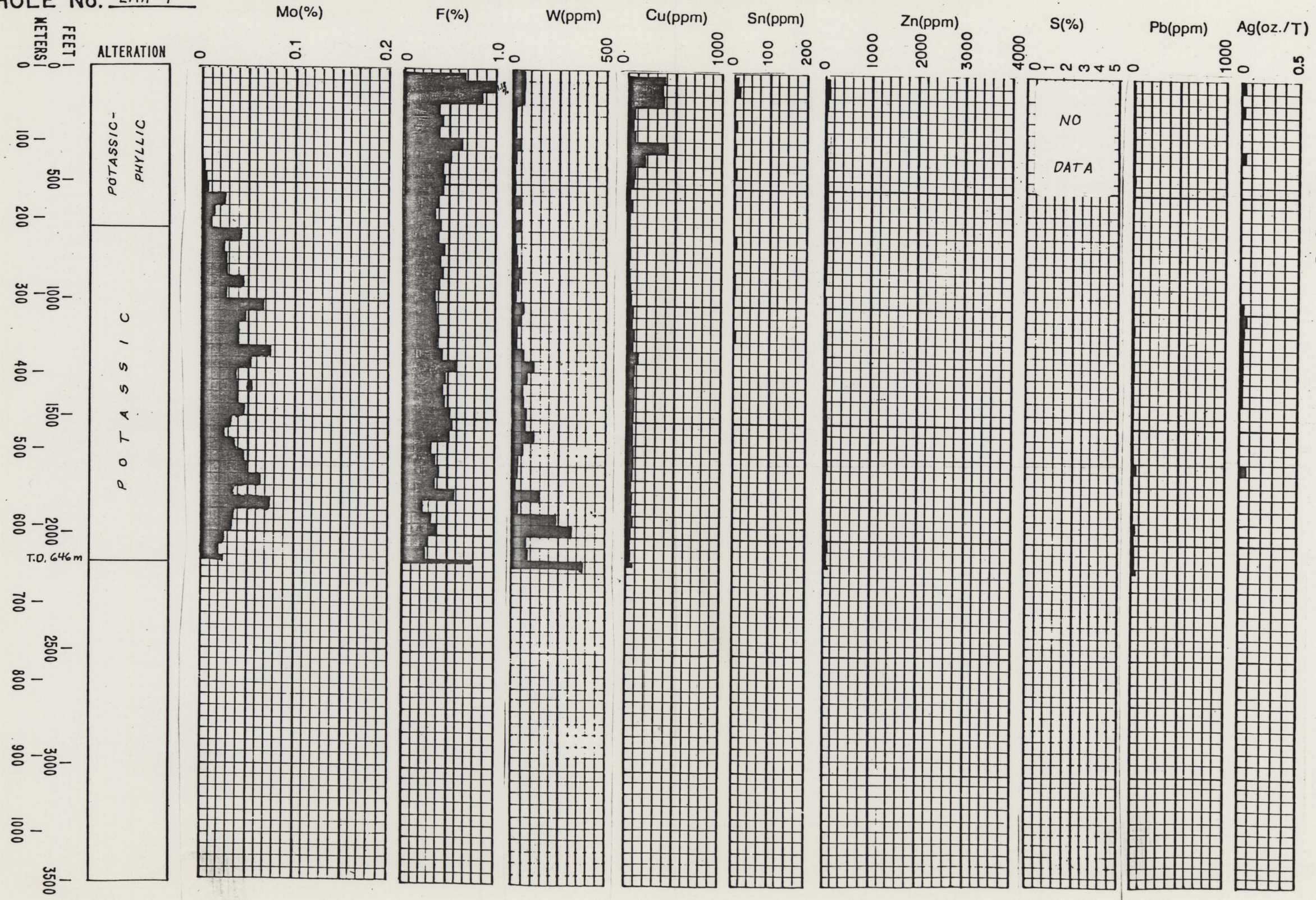

PROJECT MT. HOPE
HOLE No. EMH-3

COMPOSITE DOWNHOLE GEOCHEMISTRY

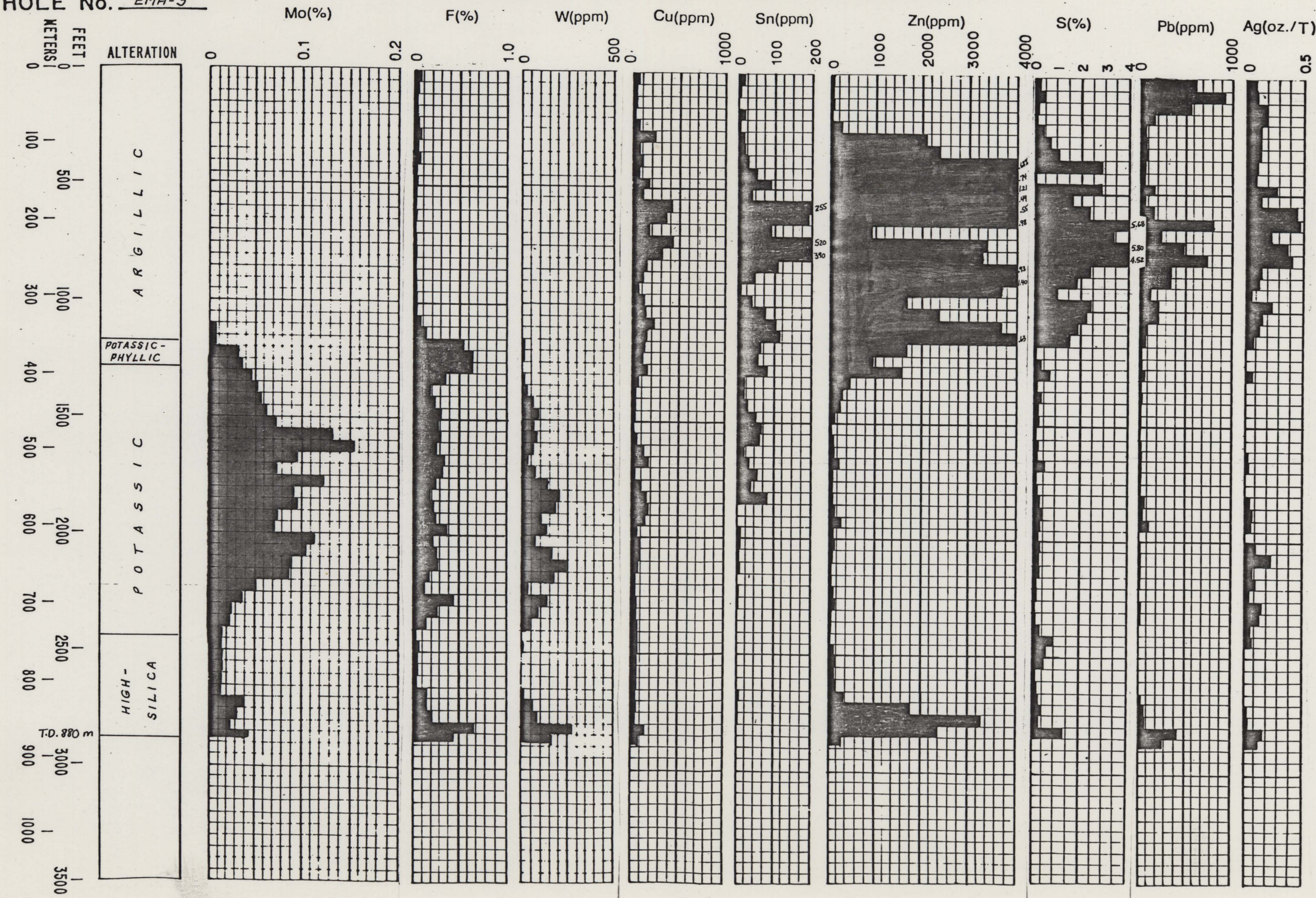

3220019

PROJECT SULPHUR SPRINGS
HOLE No. ESS-1

COMPOSITE DOWNHOLE GEOCHEMISTRY

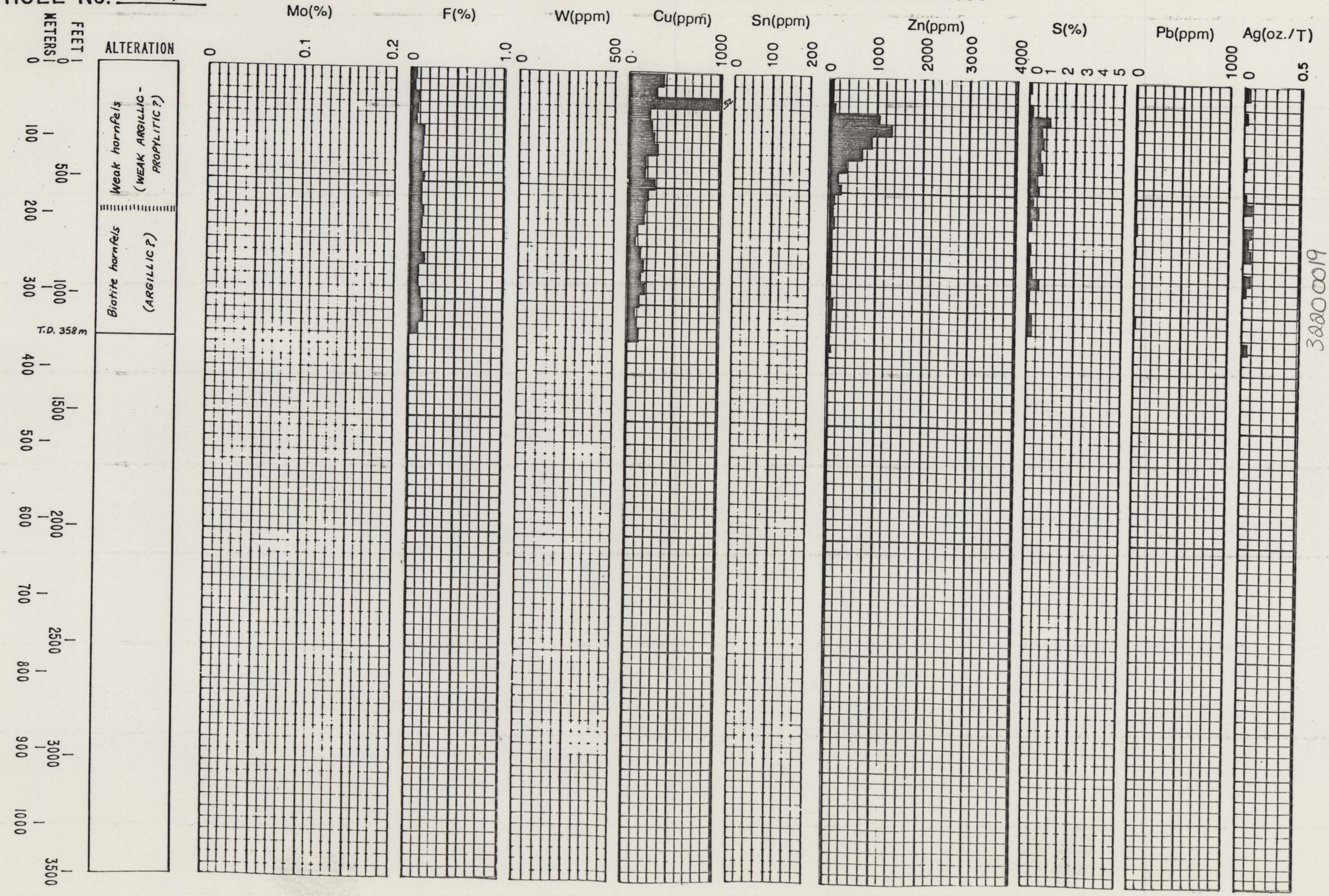

3220019

PROJECT MT. HOPE

HOLE No. EMH-22

COMPOSITE DOWNHOLE GEOCHEMISTRY

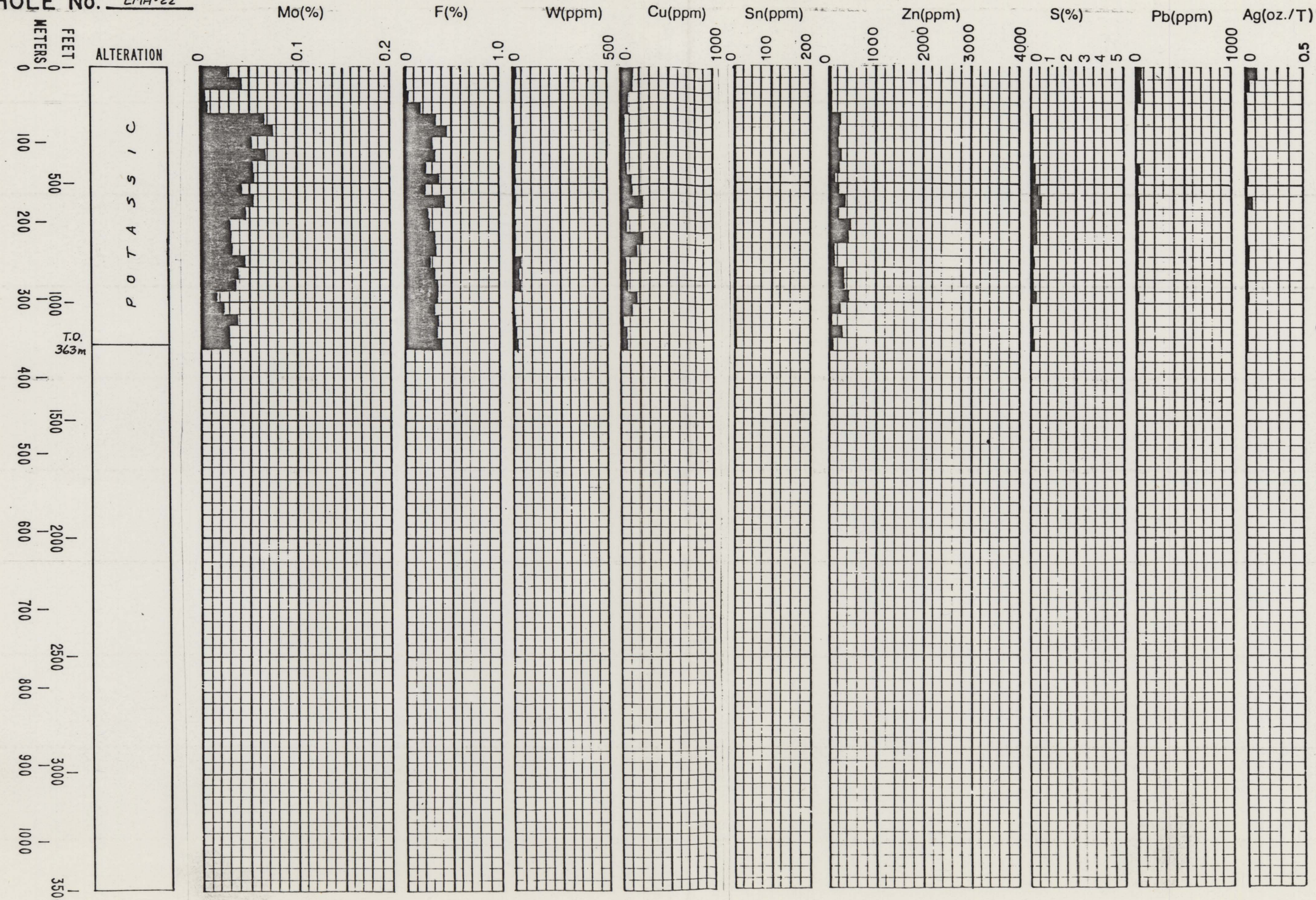

3000019

PROJECT MT. HOPE

HOLE No. EMH-21

COMPOSITE DOWNHOLE GEOCHEMISTRY

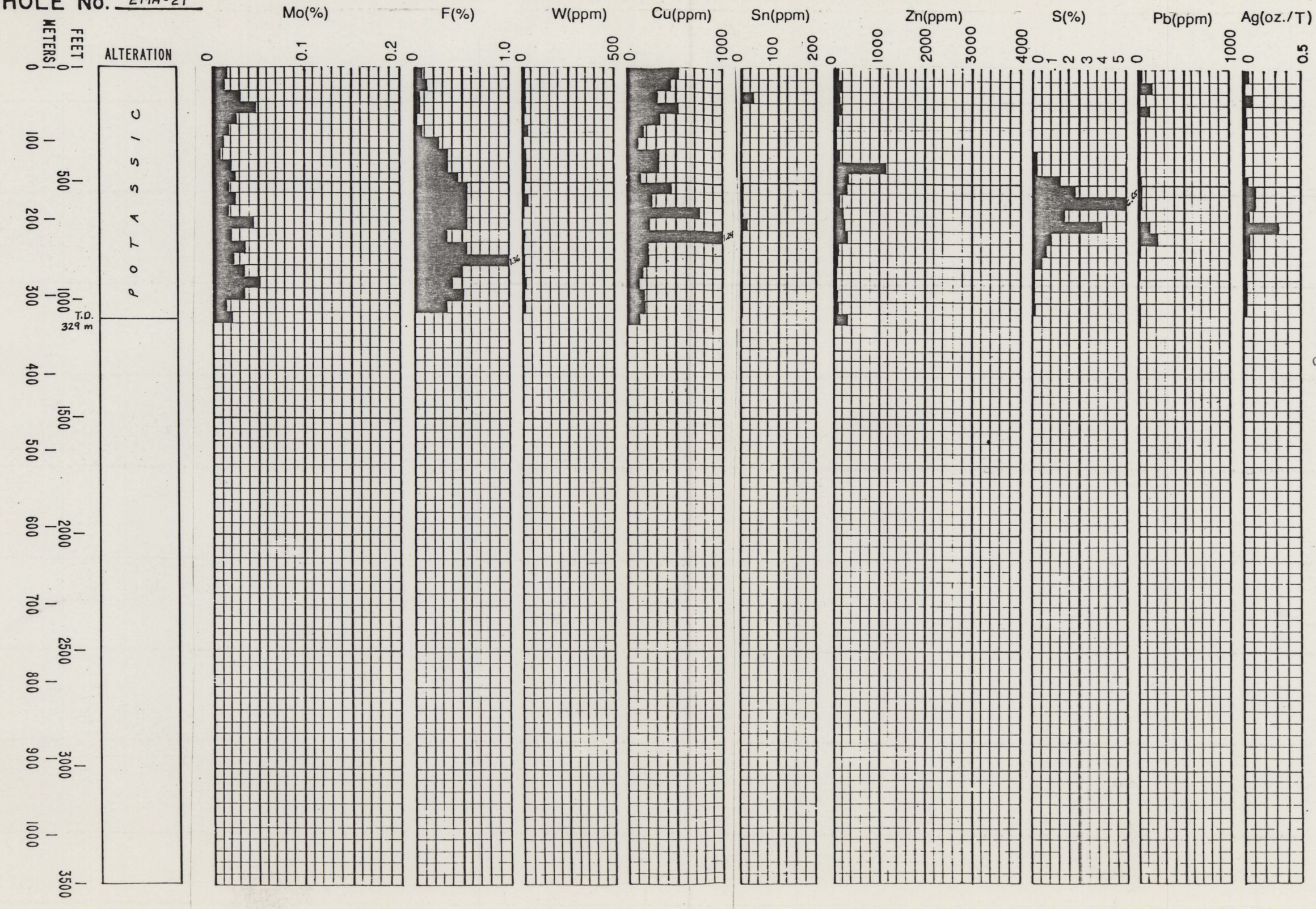

3200019

PLATES 1 - 9

PLATE 1. Generalized geologic map of the Mount Hope region. Compiled from Exxon mapping, Roberts and others (1967), and Murphy and others (1978).

PLATE 1A. Overlay showing molybdenum target areas, peripheral drill holes, and extent of Exxon and Mount Hope Mines, Inc. claim blocks.

PLATE 2. Detailed geologic map of the Mount Hope complex and vicinity.

PLATE 2A. Overlay showing surface extent of zones of hydrothermal alteration and sulfides.

PLATE 2B. Overlay showing distribution of molybdenum in surface rock and soil samples. Adapted from Westra (1980, Plate 1C).

PLATE 2C. Overlay showing location of Exxon Exploration drill holes, selected Asarco and Phillips Petroleum holes, and location of cross-sections in Plates 3 and 4.

PLATE 2D. Overlay showing surface projections of shallow molybdenum ore shells.

PLATES 3 and 4. Cross-sections through the Mount Hope complex and deposit; locations shown on Plate 2C. Rock units as on Plate 2.

PLATES 3A and 4A. Overlays showing subsurface extents of zones of hydrothermal alteration.

PLATES 3B and 4B. Overlays showing distribution of molybdenum mineralization.

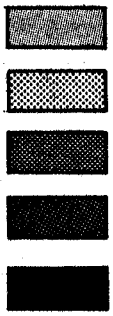

0.03 - 0.06% Mo

0.06 - 0.09% Mo

0.09 - 0.12% Mo

0.12 - 0.18% Mo

$\geqslant$ 0.18% Mo

PLATES 3C and 4C. Overlays showing extent of +100 ppm tungsten.

PLATES 5 - 9. Geologic plan maps through the Mount Hope complex and deposit at the 2195m, 2073m, 1951m, 1829m, and 1707m elevations. Rock units as on Plate 2.

Extent of high-silica alteration zone

PLATES 5A - 9A. Overlays showing distribution of molybdenum mineralization:

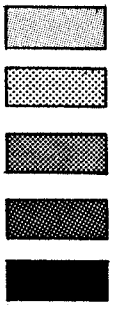

0.03 - 0.06% Mo

0.06 - 0.09% Mo

0.09 - 0.12% Mo

0.12 - 0.18% Mo

$\geq$ 0.18% Mo

Plate 3C

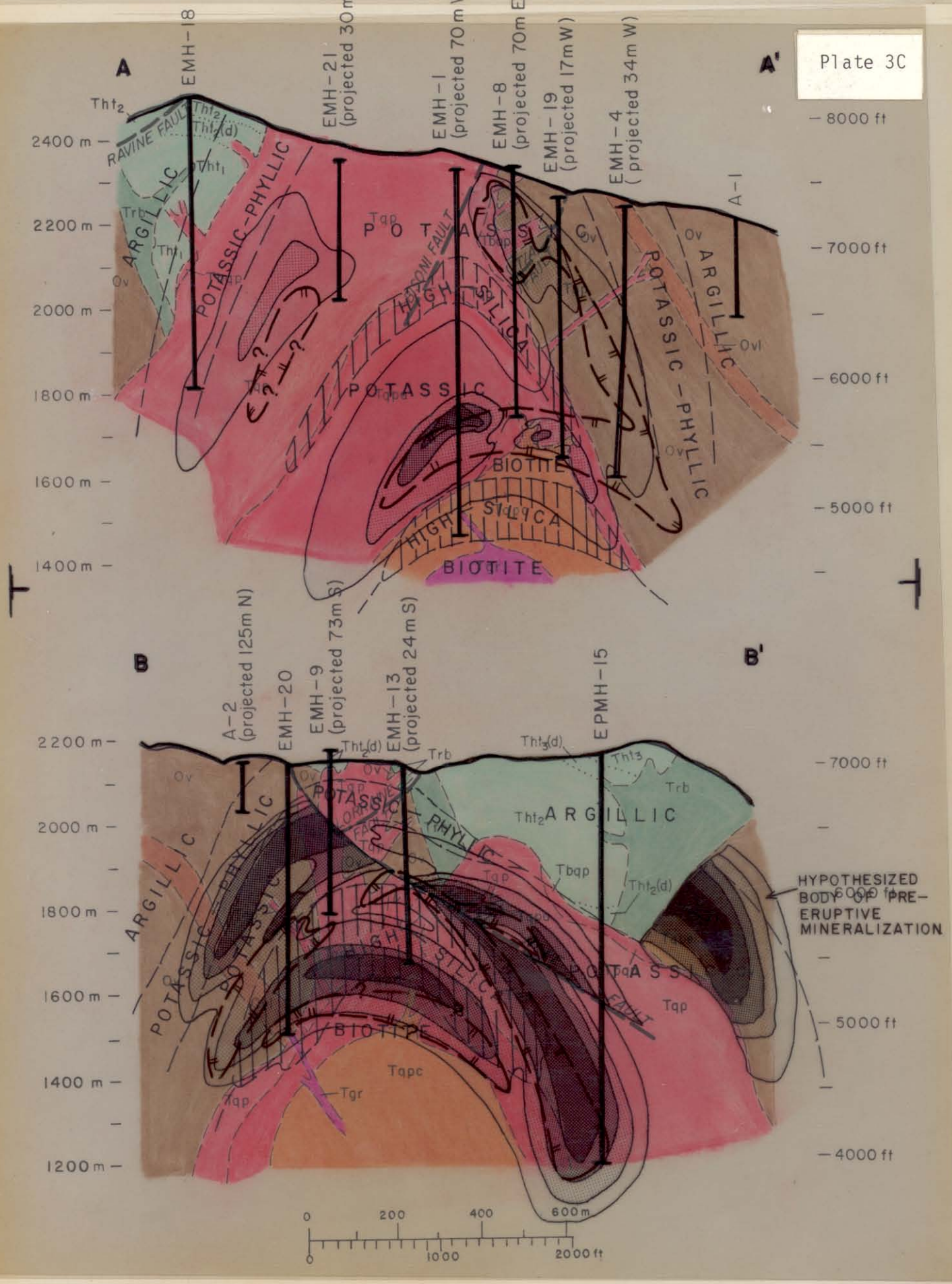
A
A'
EMH-18
EMH-21 (projected 30m W)
EMH-1 (projected 70m W)
EMH-8 (projected 70m E)
EMH-19 (projected 17m W)
EMH-4 (projected 34m W)
A-1
2400 m
2200 m
2000 m
1800 m
1600 m
1400 m
8000 ft
7000 ft
6000 ft
5000 ft
RAVINE FAULT
ARGILLIC
POTASSIC-PHYLLIC
POTASSIC
HIGH SILICA
BIOTITE
ARGILLIC
POTASSIC-PHYLLIC
B
B'
A-2 (projected 125m N)
EMH-20
EMH-9 (projected 73m S)
EMH-13 (projected 24m S)
EPMH-15
2200 m
2000 m
1800 m
1600 m
1400 m
1200 m
7000 ft
5000 ft
4000 ft
POTASSIC
PHYLLIC
ARGILLIC
HYPOTHESIZED BODY OF PRE-ERUPTIVE MINERALIZATION
BIOTITE
0
200
400
600m
1000
2000 ft

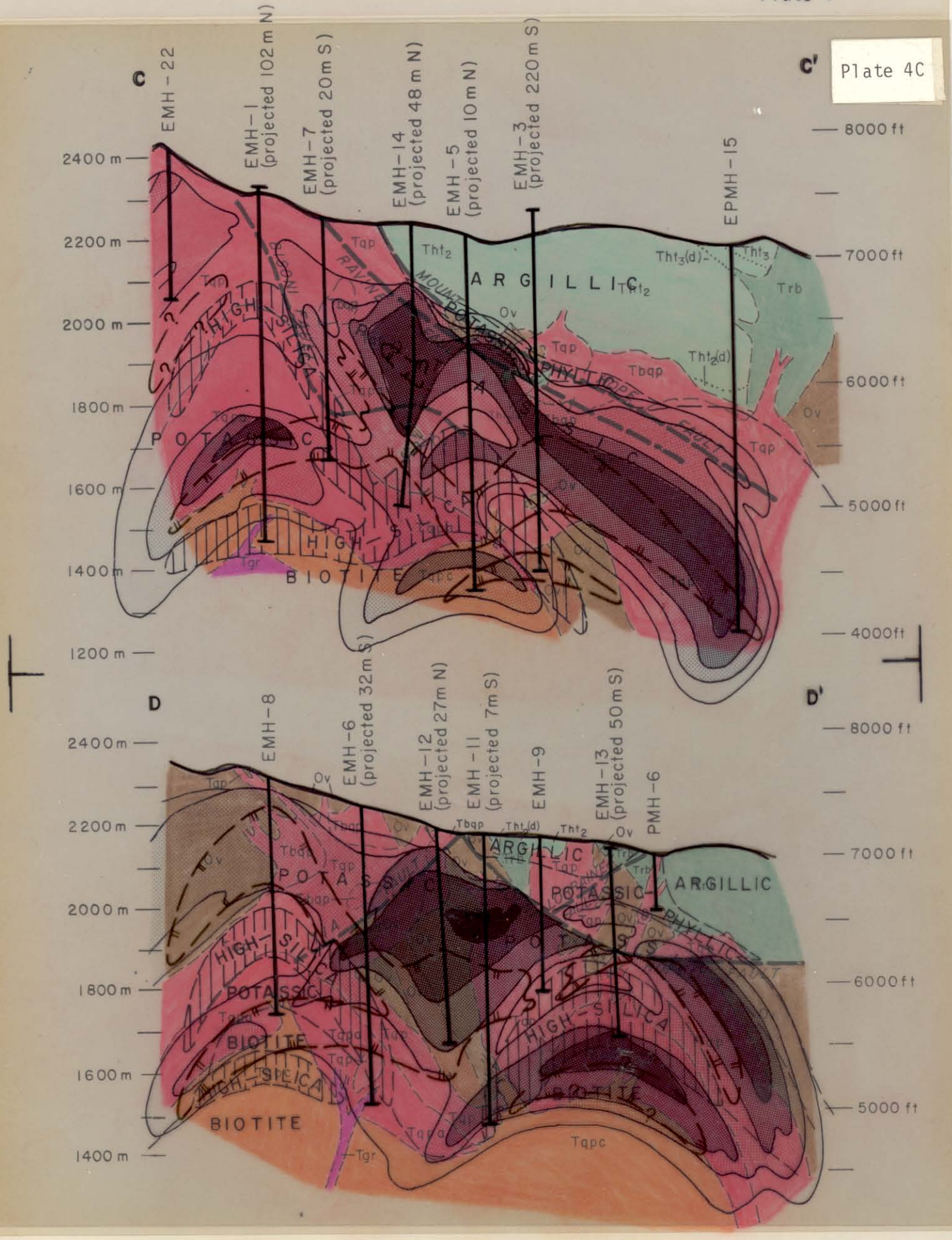
C
C'
Plate 4C
EMH-22
EMH-1 (projected 102 m N)
EMH-7 (projected 20m S)
EMH-14 (projected 48 m N)
EMH-5 (projected 10m N)
EMH-3 (projected 220m S)
EPMH-15
2400 m
2200 m
2000 m
1800m
1600 m
1400m
1200 m
8000 ft
7000 ft
6000 ft
5000 ft
4000ft
Tht2
Tht3(d)
Tht3
Tht2(d)
ARGILLIC
Trb
Ov
Tqp
Tbqp
Tgr
Tqpc
D
D'
EMH-8
EMH-6 (projected 32m S)
EMH-12 (projected 27m N)
EMH-11 (projected 7m S)
EMH-9
EMH-13 (projected 50m S)
PMH-6
2400m
2200 m
2000 m
1800 m
1600 m
1400 m
8000 ft
7000 ft
6000 ft
5000 ft
Tht(d)
Tht2
ARGILLIC
POTASSIC
HIGH-SILICA
BIOTITE
0
200
400
600 m
1000
2000 ft

Plate 5A

2195 m (7200 ft.) LEVEL

Plate 6A

2073 m (6800 ft.) LEVEL
N
103000 E
102500 E
102000 E
101500 E
101000 E
100500 E
561000 N
560500 N
560000 N
559500 N
559000 N
0
200
400
600 m
0
1000
2000 ft
Qal
Ov
Pg
Trb
Tap
Tbap
Tht3
Tht3(d)
Tht2
Tht1
MOUNT HOPE FAULT
LORRAINE FAULT
RAVINE FAULT
BISON FAULT
IAO FAULT
SOUTH

Plate 7A

1951 m (6400 ft.) LEVEL

Plate 8A

1829 m (6000 ft.) LEVEL
N
HYPOTHESIZED BODY OF PRE-ERUPTIVE MINERALIZATION
103000 E
102500 E
102000 E
101500 E
101000 E
100500 E
561000 N
560500 N
560000 N
559500 N
559000 N
Ov
Tqp
Trb
Th12
Th12(d)
Tbqp
Tqpa
Tqpa(d)
Tqm
TM
FAULT
RAVINE FAULT
BOWSER FAULT
SOUTH FAULT
HOPE FAULT
MOUNT
BIRD
0
200
400
600 m
1000
2000 ft

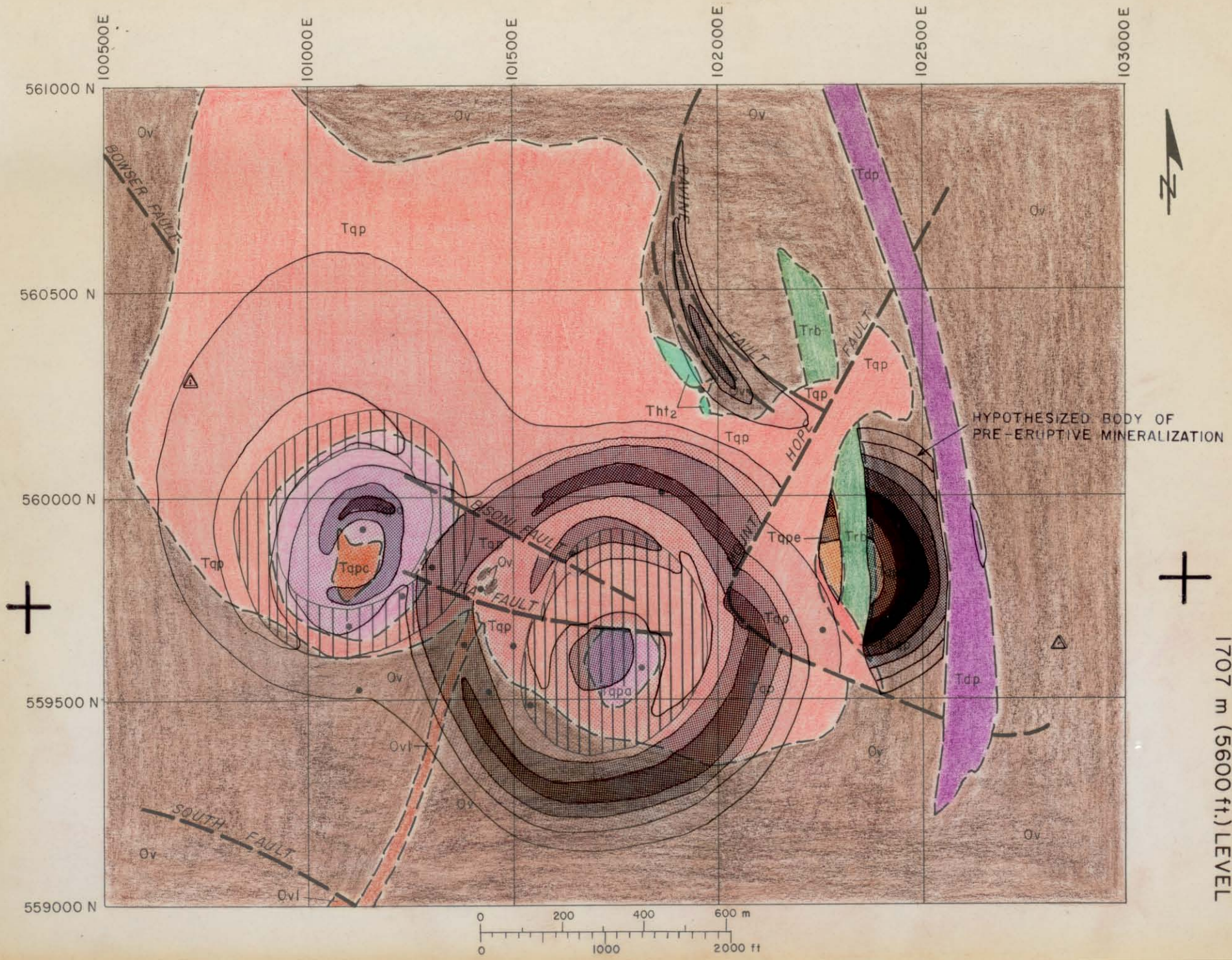

1707 m (5600 ft.) LEVEL

Plate 9A

Plate 2

EXPLANATION

LITHOLOGY

LAYERED ROCKS INTRUSIVE ROCKS

QUATERNARY

Qal ALLUVIUM

TERTIARY

30 – 33 m.y.

Tdp DACITE PORPHYRY

Tbx QUARTZ PORPHYRY BRECCIA (age uncertain)

Tgr FINE-GRAINED GRANITE

Tqpc COARSE-GRAINED QUARTZ PORPHYRY

Tqpa APLITIC QUARTZ PORPHYRY

Tqp QUARTZ PORPHYRY

Tbqp QUARTZ PORPHYRY BORDER PHASE

49 m.y.(?)

Tqt QUARTZ-EYE TUFF (age uncertain)

Trb RHYOLITE VENT BRECCIA

Tht Tht_3 $Tht_{2(d)}$ Tht_2 $Tht_{1(d)}$ Tht_1

MOUNT HOPE TUFF — cooling units designated Tht_1, Tht_2, and Tht_3, from oldest to youngest. Densely welded zones indicated by (d). Tht, undivided Mount Hope Tuff

Tqpe EARLY QUARTZ PORPHYRY (as presently known, occurs only as autoliths in Mount Hope Tuff and rhyolite vent breccias)

Tqmp BIOTITE QUARTZ MONZONITE PORPHYRY (age uncertain)

PERMIAN

Pg GARDEN VALLEY FORMATION

ORDOVICIAN

VININI FORMATION

Ov: chert, argillite, quartzite, minor limestone

Ovl: limestone, with subordinate clastic sediments

SYMBOLS

- Contact: mapped, approximate, inferred, showing dip
- Contact between cooling and welding unit in tuff
- Normal fault, showing displacement
- Strike and dip of beds
- Strike and dip of eutaxitic foliation
- Strike and dip of sheeted quartz vein set
- Adit
- Shaft

0 100 200 300 m

0 500 1000 ft

EXXON MINERALS COMPANY U.S.A.
SW OFFICE RENO TUCSON SILVER CITY

MOUNT HOPE

DETAILED GEOLOGY

Eureka Nevada

2608

K. BROCK RIEDELL 4-15-82

32200019

Plate 2A

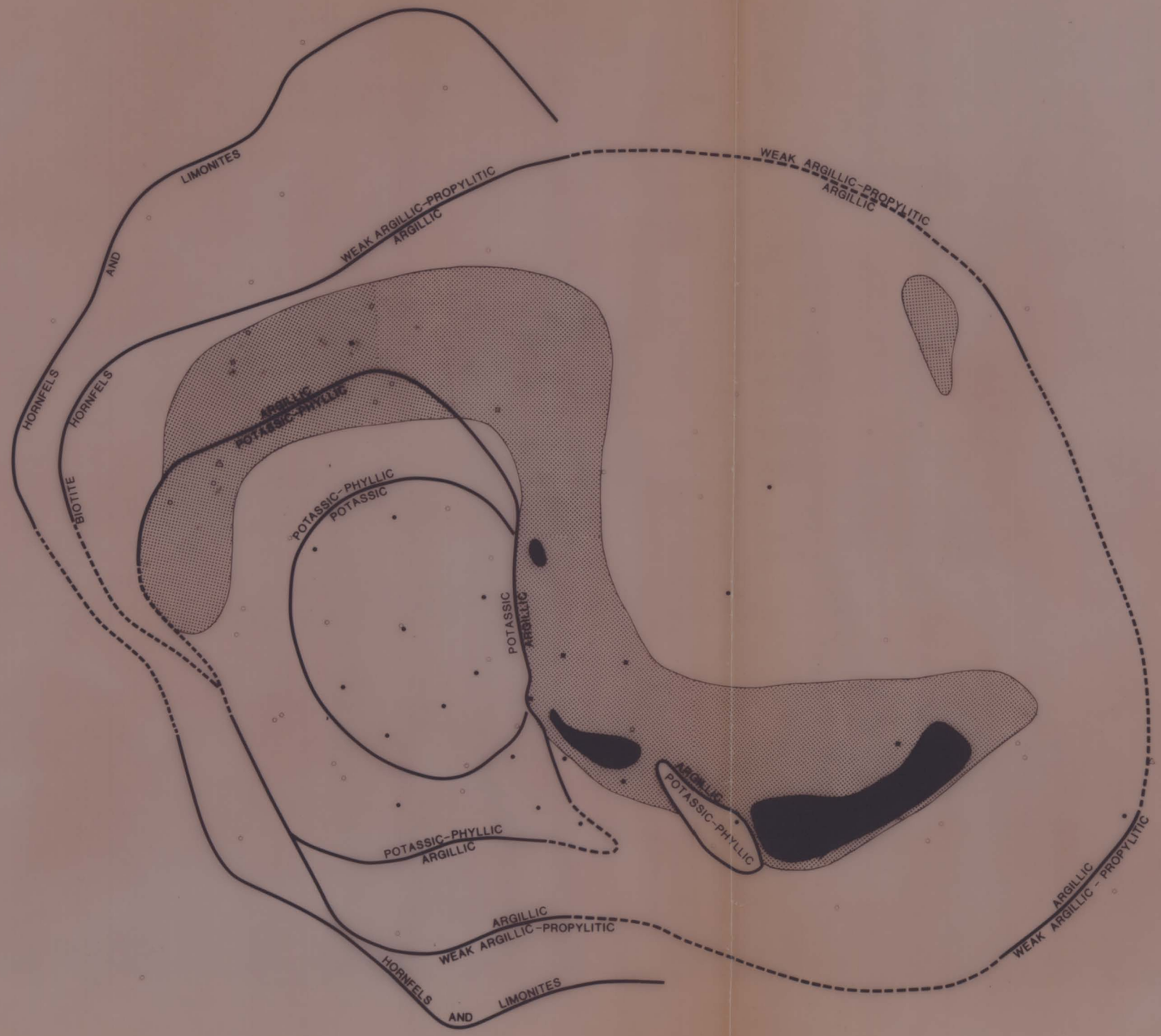

ALTERATION

- Thin section from surface outcrop
- Thin section from near collar of drill hole
- Extent of orbicular alteration aggregates
- Extent of abundant, large orbicular alteration aggregates

32200019

Plate 2B

SURFACE MOLYBDENUM DISTRIBUTION

• rock chip sample
o soil sample
Contours in ppm

Plate 2C

561000

560400

559800

559200

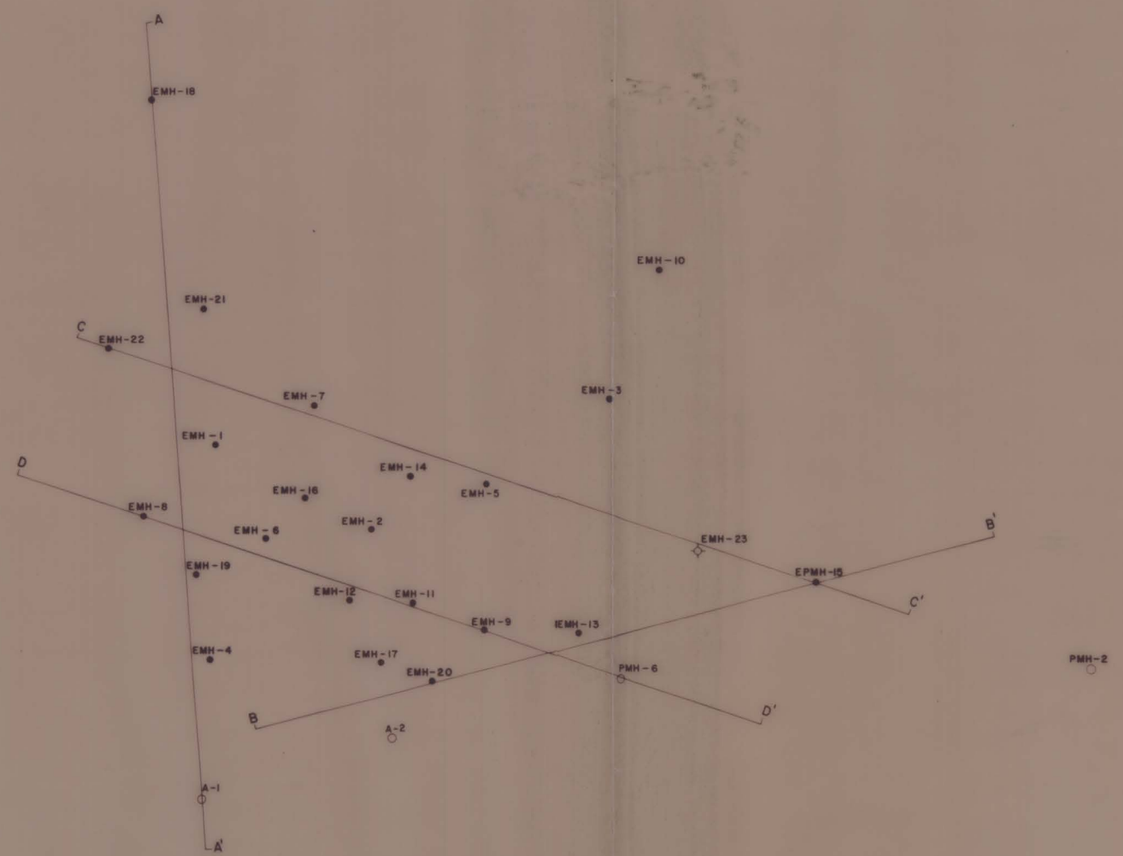

DRILLING

- ○ Phillips and Asarco holes
- • Exxon Exploration drilling 1978-1981
- ◇ Proposed Exploration drill hole
- A A' Line of cross section

32200019

Plate 2D

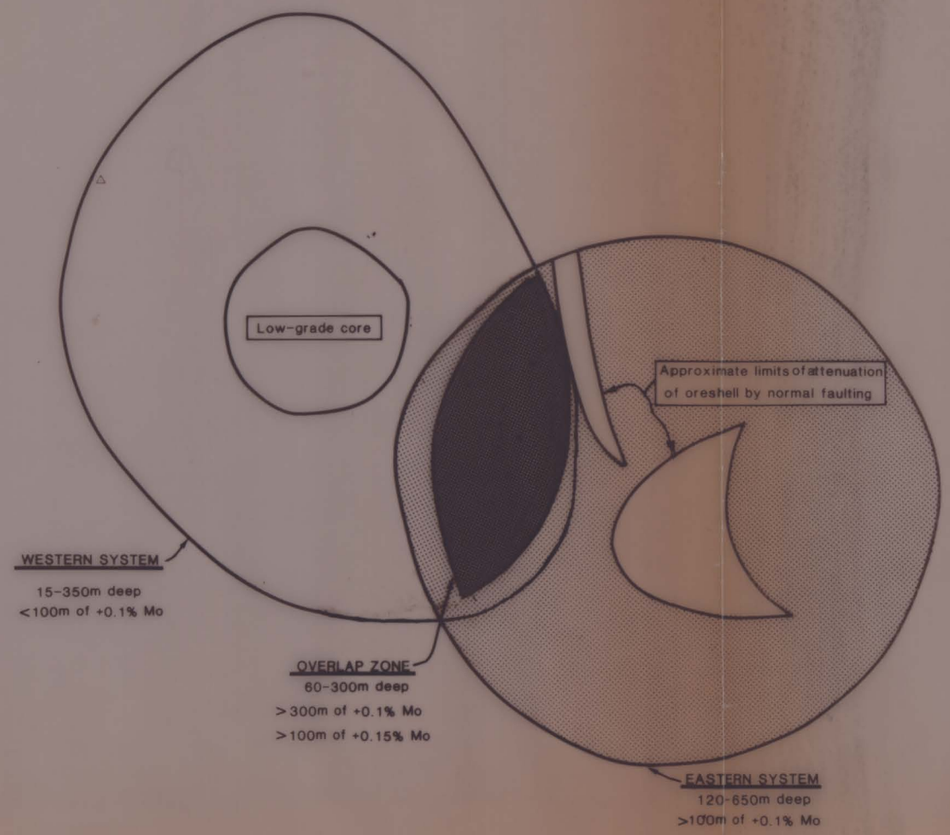

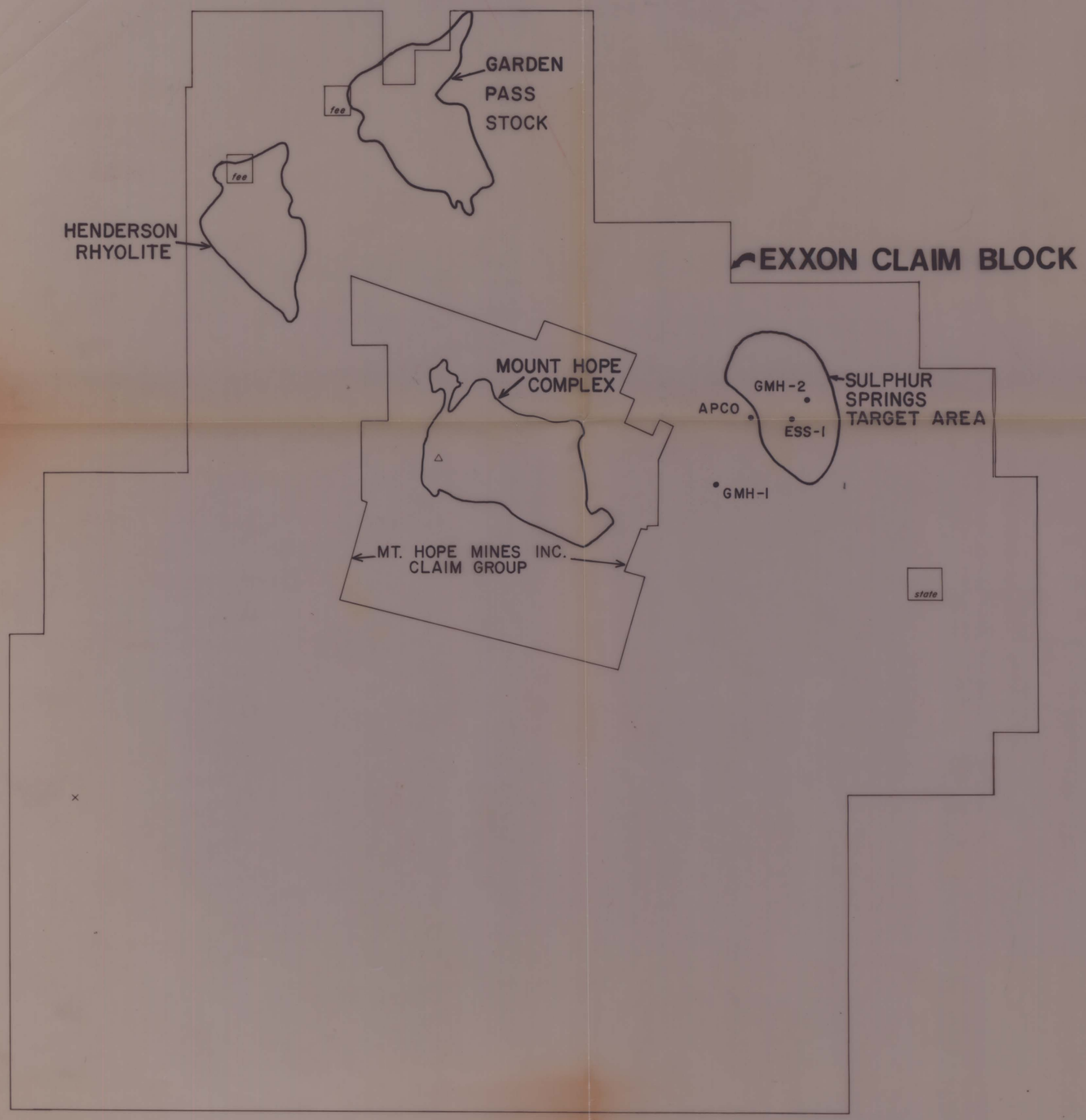

• drill holes outside the Mount Hope target area

Plate 1A

MT. HOPE

5-20-81

32200019

R 51 E

R 52 E

T 23 N

T 22 N

T 21 N

EXPLANATION

QUATERNARY

Qal ALLUVIUM

TERTIARY —

Tb BASALT FLOWS (14-19 m.y.)

Tdp DACITE PORPHYRY (30-33 m.y.)

Tqp QUARTZ PORPHYRIES

Trb RHYOLITE VENT BRECCIAS — 49 m.y.

Trt RHYOLITE ASH-FLOW TUFFS

PERMIAN —

Pg GARDEN VALLEY FORMATION - LIMESTONE, SANDSTONE, CONGLOMERATE

ORDOVICIAN TO DEVONIAN —

Pzc MIOGEOSYNCLINAL CARBONATES AND CLASTICS - INCLUDES EUREKA QUARTZITE, LONE MOUNTAIN AND NEVADA DOLOMITES, AND DEVILS GATE LIMESTONE

ORDOVICIAN —

Ov VININI FORMATION - CHERT, SILTSTONE, SHALE, LIMESTONE, SANDSTONE

SYMBOLS

contact

normal fault, showing displacement

thrust fault

N

RENO

ELY

LAS VEGAS

0 1000 2000 m

0 2000 4000 6000 ft.

Plate 1

EXXON MINERALS COMPANY U.S.A.
SW OFFICE RENO TUCSON SILVER CITY

MT. HOPE AREA GEOLOGY

EUREKA NEVADA

0 2000 4000 6000

2608

PREPARED BY: K B RIEDELL

DATE: 5-20-81

Revised 4/82

3220 0019